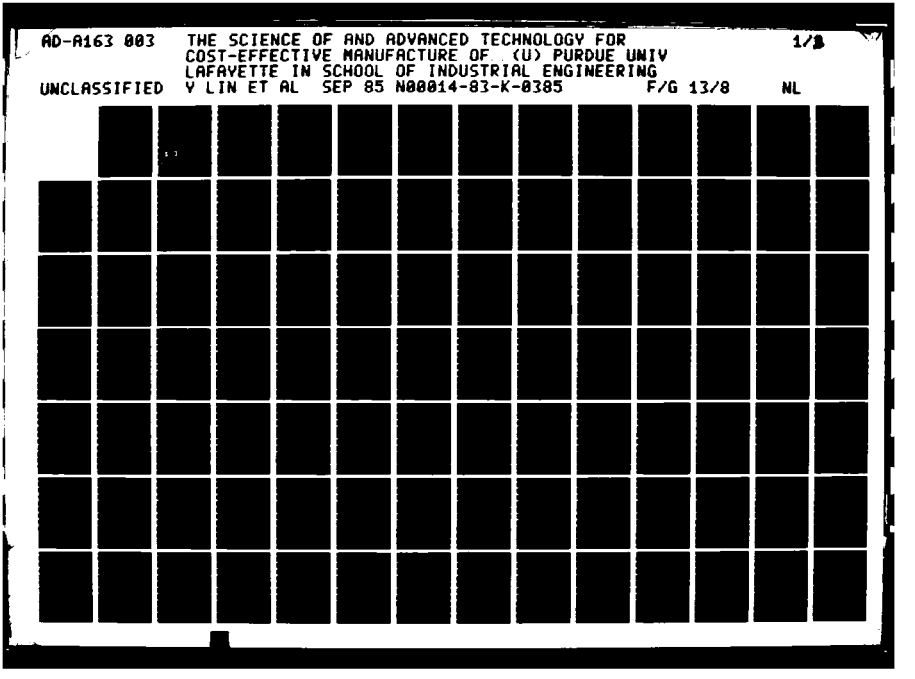
AD-A163 003 THE SCIENCE OF AND ADVANCED TECHNOLOGY FOR 1/2
COST-EFFECTIVE MANUFACTURE OF (U) PURDUE UNIV
LAFAYETTE IN SCHOOL OF INDUSTRIAL ENGINEERING
UNCLASSIFIED Y LIN ET AL SEP 85 N00014-83-K-0385 F/G 13/8 NL

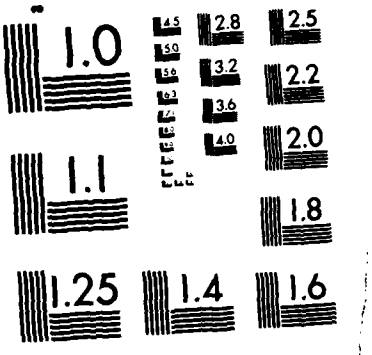

MICROCOPY RESOLUTION TEST CHART
NATIONAL BUREAU OF STANDARDS-1963-A

AD-A163 003

THE SCIENCE OF AND ADVANCED TECHNOLOGY FOR COST—EFFECTIVE MANUFACTURE OF HIGH PRECISION ENGINEERING PRODUCTS

ONR Contract No. 83K0385
FINAL REPORT
VOL. 3

GEOMETRIC ADAPTIVE CONTROL FOR ACCURACY AND STABILITY IN MACHINING CYLINDRICAL WORKPIECE

PREPARED BY
Yhu—Tin Lin and C. Richard Liu

SEPTEMBER 1985

This document has been approved for public release and sale; its distribution is unlimited

Schools of
Industrial, Electrical and Mechanical Engineering
Purdue University
West Lafayette, Indiana 47907

None
SECURITY CLASSIFICATION OF THIS PAGE

AD-A163003

REPORT DOCUMENTATION PAGE

1a. REPORT SECURITY CLASSIFICATION: None	1b. RESTRICTIVE MARKINGS: None
2a. SECURITY CLASSIFICATION AUTHORITY: None	3. DISTRIBUTION/AVAILABILITY OF REPORT
2b. DECLASSIFICATION/DOWNGRADING SCHEDULE: None	
4. PERFORMING ORGANIZATION REPORT NUMBER(S): Final Report Vol. 3	5. MONITORING ORGANIZATION REPORT NUMBER(S)
6a. NAME OF PERFORMING ORGANIZATION: PURDUE UNIVERSITY; 6b. OFFICE SYMBOL (If applicable)	7a. NAME OF MONITORING ORGANIZATION: Department of Defense, Office of Naval Research
6c. ADDRESS (City, State, and ZIP Code): School of Industrial Engineering, West Lafayette, Indiana 47907	7b. ADDRESS (City, State, and ZIP Code): Arlington, VA 22217-5000
8a. NAME OF FUNDING/SPONSORING ORGANIZATION; 8b. OFFICE SYMBOL (If applicable): 614A	9. PROCUREMENT INSTRUMENT IDENTIFICATION NUMBER: N00014-83-K-0385/12/12
8c. ADDRESS (City, State, and ZIP Code)	10. SOURCE OF FUNDING NUMBERS: PROGRAM ELEMENT NO: ONR: 433; PROJECT NO; TASK NO: SRO-153; WORK UNIT ACCESSION NO

11. TITLE (Include Security Classification)

GEOMETRIC ADAPTIVE CONTROL FOR ACCURACY AND STABILITY IN MACHINING CYLINDRICAL WORKPIECE

12. PERSONAL AUTHOR(S)
Lin, Yhu-Tin and C. Richard Liu

13a. TYPE OF REPORT	13b. TIME COVERED	14. DATE OF REPORT (Year, Month, Day)	15. PAGE COUNT
Final	FROM 1-1-83 TO 8-15-85	September 1985	192

16. SUPPLEMENTARY NOTATION

17. COSATI CODES			18. SUBJECT TERMS (Continue on reverse if necessary and identify by block number)
FIELD	GROUP	SUB-GROUP	Machining, machining errors, NC machines, roundness accuracy, metrology, geometric adaptive control.
13			

19. ABSTRACT (Continue on reverse if necessary and identify by block number)

A new geometric adaptive control (GAC) system has been developed for improving the accuracy and stability in machining cylindrical workpiece. The system takes into consideration error generation process, machine tool dynamics, and metrology. The new stochastic model constructed in this thesis provides not only insight into the nature of machining processes, but also a means for the systematic design of geometric adaptive controllers.

The adaptive control algorithms for the GAC system are derived by using the theory of self-tuning control (STC). The algorithms are simple, robust, and suitable for microprocessor implementation. Whitehouse's multiprobe measurement is modified for use in the control system for the first time. Interesting properties of this measurement in control are analyzed and predicted.

The results of simulation show that the GAC system can improve both the accuracy and the stability considerably. Through the theoretical analysis it was possible to resolve
(continued on reverse)

20. DISTRIBUTION/AVAILABILITY OF ABSTRACT: ☐ UNCLASSIFIED/UNLIMITED ☒ SAME AS RPT ☐ DTIC USERS	21. ABSTRACT SECURITY CLASSIFICATION: None
22a. NAME OF RESPONSIBLE INDIVIDUAL: Dr. David Mizell, Scientific Officer	22b. TELEPHONE (Include Area Code): 818-795-5971 x 56; 22c. OFFICE SYMBOL: 433

19. (continued)

the control problems imposed by multiprobe measurement, and to achieve near optimum control performance. A comparison with another GAC system which uses FCC technique is made to show that the proposed GAC system does have better performance than other existing GAC systems in precision machining.

THE SCIENCE OF AND ADVANCED TECHNOLOGY FOR COST-EFFECTIVE MANUFACTURE OF HIGH PRECISION ENGINEERING PRODUCTS

ONR Contract No. 83K0385
Final Report
Vol. 3

GEOMETRIC ADAPTIVE CONTROL FOR ACCURACY AND STABILITY IN MACHINING CYLINDRICAL WORKPIECE

Prepared by
Yhu-Tin Lin and C. Richard Liu

Accesion For
NTIS CRA&I
DTIC TAB
Unannounced
Justification
By
Distribution /
Availability Codes
Dist | Avail and / or Special
A-1

September 1985

Schools of
Industrial, Electrical and Mechanical Engineering
Purdue University
West Lafayette, Indiana 47907

QUALITY INSPECTED 3

This report represents, with minor changes, the thesis submitted by Mr. Yhu-Tin Lin to the Faculty of Purdue University for the award of the Degree of Doctor of Philosophy.

Research described in this report has been supported by the Office of Naval Research through Contract No. N83K0385 in the framework of the ONR Precision Engineering projects.

C. R. Liu served as Major Professor for the thesis; he is a member of the faculty of the School of Industrial Engineering at Purdue University.

Work on the Precision Engineering project at Purdue University greatly benefited from the use of the technical facilities of the Purdue Computer Integrated Design, Manufacturing and Automation Center (CIDMAC) and the advice of the CIDMAC member companies*.

Moshe M. Barash
Principal Investigator

C. Richard Liu
Principal Investigator

*Member companies of CIDMAC are:
Cincinnati Milacron; TRW; Ransburg Corporation; Cummins Engine Co.; Control Data Corporation; ALCOA which is gratefully acknowledged.

TABLE OF CONTENTS

	Page
LIST OF TABLES	v
LIST OF FIGURES	vi
ABSTRACT	ix
CHAPTER 1 - INTRODUCTION	1
1.1 Sources of Geometrical Errors	3
1.2 Methods for Error Reduction	4
1.3 GAC System and Related Problems	6
1.4 The Objective of the Research	8
CHAPTER 2 - METROLOGY AND DYNAMICS	11
2.1 Metrology	11
2.1.1 Workpiece Metrology	13
2.1.2 Machine Tool Metrology	22
2.1.3 In-process Metrology	26
2.2 Machine Tool Dynamics	28
2.2.1 Chatter and Cutting Dynamics	30
2.2.2 Methods for Chatter Reduction	38
CHAPTER 3 - SELF-TUNING CONTROL THEORY	40
3.1 Self-tuning Control (STC)	41
3.2 Self-tuning Techniques	42
3.2.1 Parameter Estimation	43
3.2.2 Control Criteria	45
3.3 Implementation Aspects	47
3.3.1 Identification Issues	47
3.3.2 Control Issues	49
3.3.2 General Issues	50

Page

CHAPTER 4 - THEORETICAL DEVELOPMENT 52

4.1 Model of the GAC System 54
4.2 STC Algorithm 57
4.3 Stability, Convergence, and Robustness 60
4.4 Multiprobe Measurement in GAC 64
4.4.1 Properties of Multiprobe Measurement 68
4.4.2 STC With Multiprobe Measurement 73

CHAPTER 5 - SIMULATION OF THE GAC SYSTEM 76

5.1 Simulation Model and Conditions 77
5.2 Simulation With Ideal Measurement 83
5.2.1 Deterministic Systems 84
5.2.2 Stochastic Systems 96
5.3 Simulation With Multiprobe Measurement 104
5.3.1 Configuration of Probes for Simulation 104
5.3.2 Test of Detuning Factor 105
5.3.3 Test of Invisible Harmonics 107
5.3.4 Test of Stochastic System and Stability 113
5.4 Summary of Discussions 116

CHAPTER 6 - A COMPARISON OF STC AND FCC 120

6.1 Theoretical Investigation 121
6.2 Digital Simulation 129
6.3 Analog Test 139
6.4 Summary 143

CHAPTER 7 - CONCLUSIONS AND RECOMMENDATIONS. 145

7.1 Conclusions 145
7.2 Recommendations 147

BIBLIOGRAPHY 148

APPENDICES

Appendix 1: Derivation of (4.1) 158
Appendix 2: STC With Weighted Minimum Variance Criterion 163
Appendix 3: The FORTRAN Program for Digital Simulation . 165
Appendix 4: Project Staff 1983-1984 178

LIST OF TABLES

Table		Page
5.1	Simulation Conditions	82
5.2	Simulation Results of Different Disturbance Levels and System Delays	98

LIST OF FIGURES

Figure		Page
1.1	Geometric Adaptive Control System	7
2.1	Isodiametrical Shapes	14
2.2	Configurations of V-block for Measuring Out-of-Roundness	14
2.3	Centerless Grinding	16
2.4	Absolute Methods of Measurement for Workpiece . . .	16
2.5	Determination of Minimum Zone Center (MZC)	18
2.6	Determination of Least Squares Center (LSC).	19
2.7	Limacon-shaped Polar Profile of Mis-centered Part .	21
2.8	Techniques of Machine Tool Metrology	24
2.9	Another Measurement Technique for Process of Rotating Tool Type	24
2.10	Typical Measurement of Spindle Radial Error Motion	25
2.11	Reversal Method for In-Process Measurement	27
2.12	Multi-Step Method for In-Process Measurement	27
2.13	Machine Tool Dynamics	29
2.14	Stability of a Milling Process	32
2.15	Machine Tool Dynamics in Control Block Diagram . . .	34
2.16	A Theoretical Stability Chart of Fig. 2.15	37
4.1	Structural Dynamics and Regenerative Effect of Plunge Cutting	55
4.2	Control Diagram of the GAC System	55
4.3	Multiprobe Measurement	65

Figure		Page
5.1	Plunge Cutting Process	78
5.2	Simulation Model	80
5.3	GAC System With Periodic Disturbance Only (Simulation I-1)	85
5.4	The Effect of Forgetting Factor on the Convergence of GAC System (Simulation I-2)	88
5.5	GAC System With Periodic Disturbance From Stiffness Variation of Chucked Workpiece (Simulation I-3) . .	90
5.6	GAC System With Insufficient Model Order for Two Periodic Disturbances (Simulation I-4)	92
5.7	GAC System With Sufficient Model Order for Two Periodic Disturbances (Simulation I-5)	93
5.8	Perturbation Input for GAC System With Large Time Delay (Simulation I-6)	95
5.9	GAC System With Both Periodic and Stochastic Disturbances (Simulation I-7)	97
5.10	GAC System for Unstable Machining Process (Simulation I-12)	100
5.11	GAC System for More Unstable Machining Process (Simulation I-13)	101
5.12	GAC Using General STC for Unstable System (Simulation I-14)	103
5.13	GAC System With Multiprobe Measurement and Periodic Disturbance (Simulation II-1)	106
5.14	The Effect of Detuning Factor in GAC System With Multiprobe Measurement (Simulation II-2)	108
5.15	GAC System for Once-Per-Revolution Harmonic Invisible to Multiprobe Measurement (Simulation II-3)	109
5.16	GAC System for Higher Harmonic Invisible to Multiprobe Measurement (Simulation II-4)	111
5.17	GAC System With Modified Configuration of Multiprobes (Simulation II-5)	112

Figure		Page
5.18	GAC System With Multiprobe Measurement, Periodic disturbance and Stochastic Disturbance (Simulation II-6)	114
5.19	GAC System With Multiprobe Measurement for Unstable Machining Process (Simulation II-7) . . .	115
5.20	GAC System With Multiprobe Measurement for More Unstable Machining Process (Simulation II-8) . . .	117
6.1	A SISO Control System	122
6.2	STC for Machining Process With Deterministic Disturbance Only	132
6.3	STC for Machining Process With Both Deterministic and Stochastic Disturbances	133
6.4	STC for Machining Process With Less Rigid Structure	134
6.5	FCC for Machining Process With Deterministic Disturbance Only	136
6.6	FCC for Machining Process With Both Deterministic and Stochastic Disturbances	137
6.7	FCC for Machining process With Less Rigid Structure	138
6.8	Experimental Setup for Analog Test	140
6.9	Electronic Circuit for Analog Test	141
6.10	Output of Uncontrolled System	141
6.11	Output of STC System	144
6.12	Output of FCC System	144

ABSTRACT

A new geometric adaptive control (GAC) system has been developed for improving the accuracy and stability in machining cylindrical workpiece. The system takes into consideration error generation process, machine tool dynamics, and metrology. The new stochastic model constructed in this thesis provides not only insight into the nature of machining processes, but also a means for the systematic design of geometric adaptive controllers.

The adaptive control algorithms for the GAC system are derived by using the theory of self-tuning control (STC). The algorithms are simple, robust, and suitable for microprocessor implementation. Whitehouse's multiprobe measurement is modified for use in the control system for the first time. Interesting properties of this measurement in control are analyzed and predicted.

The results of simulation show that the GAC system can improve both the accuracy and the stability considerably. Through the theoretical analysis it was possible to resolve the control problems imposed by multiprobe measurement, and to achieve near optimum control performance. A comparison with another GAC system which uses FCC technique is made to show that the proposed GAC system does have better performance than other existing GAC systems in precision machining.

CHAPTER 1

INTRODUCTION

The progress of machining accuracy has been accelerated by the requirement of high precision parts in space exploration, electronics miniaturization, and laser applications [70,93]. Not only do these technologies need precision hardware, which are usually produced by machining, to accomplish their extraordinary performance. In the traditional industries the pursuit for better accuracy never stops. Accurately machined parts can assure assembly efficiency in mass production systems, reduce noise and vibration for improving the quality of the product, and simplify product design [18].

It can be seen that cylindrical machined parts exist in most, if not all, of the products. This is particularly true for those having rotary motions. Dimensional accuracy, roundness, and finish are the three most important aspects of the accuracy of cylindrical parts. Dimensional accuracy refers to the bias error of the effective diameter of the machined part from the specified diameter in the part drawing. It determines the clearance or tightness in the assembly of a hole and a shaft. Dimensional accuracy is usually specified in the design stage as tolerance to allow for the machining errors.

It has been shown by Moore [70] that roundness becomes proportionally more critical as tolerances become tighter.

Roundness, or more precisely out-of-roundness, refers to the deviation of the cross-section of a cylindrical workpiece from an ideal circle. Depending on the types of applications, out-of-roundness may result in various kinds of problems, such as leakage, stress concentration, noise and vibration, and so on [34]. Most of the time, out-of-roundness is regarded as the form error of low frequency undulations on the part surface.

Unlike dimensional accuracy and roundness, finish is a microscopic description of the part surface. The machined part usually has many random and high frequency undulations on the surface in addition to out-of-roundness. The qualitative interpretation of these small undulations through human sensors, vision and touch, is finish. Its effects on the performance of the product are also of microscopic nature, such as friction, wear, erosion, and reflectability.

According to the above descriptions, it is understandable that the development in cylindrical machining has always been the most rewarding in the history of machine tools. Lathes and drilling machines are used for machining basic cylindrical surfaces. Other machine tools such as boring, reaming, grinding, and honing are devised to trim excessive dimensions, to true round shapes, or to polish surfaces. However, the higher the precision the process can achieve, the higher the unpredictability it has, and the higher the skill it needs [53]. Some automatic control systems for geometrical accuracy are needed to overcome this barrier. For setting up effective control systems, it would be helpful to identify the

sources of and the processes generating geometrical inaccuracies or errors on the machined part in advance.

1.1 Sources of Geometrical Errors

The sources of geometrical errors can be categorized as follows:

i. Structural inaccuracies and deformation - All members of the machine tool are produced by using various production processes. Consequently they are subject to manufacturing errors. And because of the finite rigidity of the members, structural deformation is induced whenever there are forces of cutting, clamping, gravity, or heat expansion. These errors are copied to the machined surfaces through tne machining processes.

ii. Vibrations - Vibration is the most annoying problem for the machine tool builders and operators. It can be from anywhere, unbalanced rotating parts, loose objects, or the floor of machine base. The most detrimental vibration is from the cutting process itself, called chatter. Vibration not only reduces the accuracies of the machined part but also shortens the lives of the tool and the machine.

iii. Machining processes - Besides the process related chatter, the tool may leave unwanted marks on the machined surfaces as it moves relative to the workpiece. Also the wear of the tool affects finish and dimensional accuracy.

iv. Microstructural changes - This involves the rupture or the plastic deformation of the metallic grains of workpiece caused

by the cutting forces and the effect of friction on the tool-workpiece interface.

Roughly speaking, the first two categories contribute to dimensional error and out-of-roundness. And the last two categories have major effects on surface finish. It is not wise to consider all the error sources in developing an automatic control system for geometrical accuracy. Some error sources are of minor importance, and can be neglected. Some of them may never be good for automatic compensation. Therefore, it is a good practice to learn about the available techniques of error reduction. Then we can determine the error sources which should be considered in the control system.

1.2 Methods for Error Reduction

According to Blaedel [15], the methods for error reduction can be divided into:

(a) error avoidance

*eliminating the error sources

*altering the processes of error generation

(b) error compensation

*precalibrated

*active

The methods of error avoidance prevail in most of the machine tool builders. They typically need painstaking trials and tests in order to identify the true error sources or error generation processes. Then, one can reduce errors by redesigning, modifying, or carefully manufacturing the critical members of the machine tool. For cutting process related errors, sometimes, it is necessary to limit cutting

conditions at the expense of productivity. In general, error avoidance applies to those error sources which are steady or which can be eradicated once for all.

Error compensation, on the other hand, is suitable for dynamic errors. It attempts to model the process of error generation from the measured variables and then to predict the control inputs for compensation. If the measurement is performed before or after the cutting operations and then the errors are compensated for, it is called precalibrated error compensation. The principle of precalibrated compensation is based on the existence of systematic errors for modeling. The off-line measurement simplifies the system of precalibrated compensation. However, certain nonrepeatable or dynamic errors, chatter, for instance, will never be sensed and corrected. Production time is also wasted in measurement for calibration.

Active error compensation, with in-process measurement, therefore, emerges as the most promising method for reducing unpredictable errors [47,48,77,78]. One type of in-process measurement is to measure the error motions of certain critical members of the machine by attaching external masters to those members. The other type is to measure the geometrical profile of the machined surface directly. Although sometimes the latter type of active compensation has accessibility problems in setting up the instruments, its performance is more effective than that of the former type because of the direct assessment of geometrical errors.

The modeling of the process in active compensation, as shown in Fig. 1.1, is quite complex. The unpredictable properties of the system can be resolved by devising an adaptive model for the compensator or controller according to in-process measurement, compensation input, and appropriate control criteria. This has been termed "geometrical adaptive control" (GAC) [77,48,47].

1.3 GAC System and Related Problems

Basically, a GAC system should consist of in-process measurement, on-line modeling or system identification, and real time control. It is best for the applications in fine turning, honing, and cylindrical grinding processes. Like its companions in machining, adaptive control for optimization (ACO) and adaptive control for constraint (ACC) [99], the development of GAC has been relatively slow. Until now, only a handful of recent research papers can be seen [50,84,55,68,69,87,102]. Most of these research work still fail to fully resolve the following problems:

A. Problems in measurement - Apart from the problems of the accessibility and reliability of sensors in harsh production environments, a major concern in GAC is the separation problem. That is, with the workpiece attached to the rotating spindle, any in-process measurement of the surface geometry will be contaminated by the spindle error motions, which are difficult to be separated. The external masters used in [84,55] can measure and compensate for the spindle error motion only.

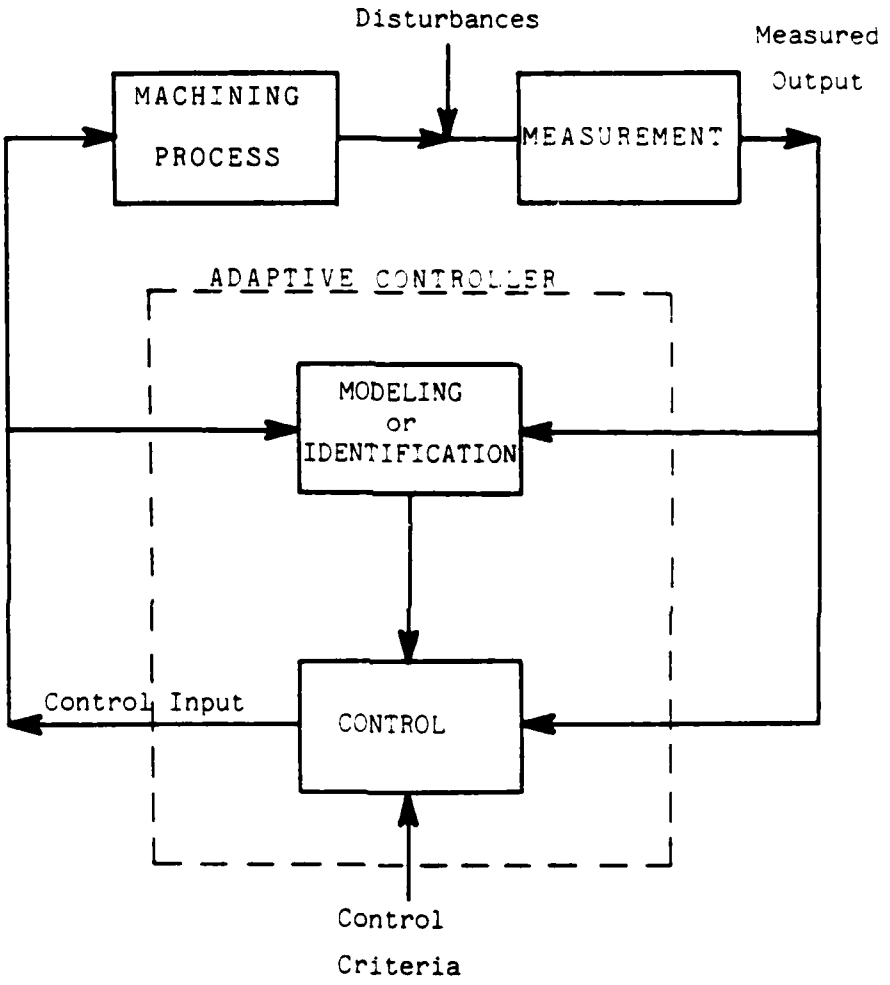

Figure 1.1 Geometric Adaptive Control System

B. Problems in system modeling - A thorough understanding of machining processes has been elusive for the inconsistencies of experimental findings caused by different cutting conditions, tool geometries, and work materials. Traditional models are deficient in handling the nonlinear, nonstationary, and stochastic nature of machining processes. On the other hand, the stochastic time series model used by Wu and his coworkers [84,55,68,69] bears little physical meaning.

C. Problems in adaptive control - In the absence of appropriate models for machining processes, most of the adaptive control techniques of GAC are quite crude and inadequate in assuring the stability of the GAC system. A systematic approach for the design of adaptive controller is still lacking.

1.4 The Objective of the Research

The objective of this thesis is to propose a new GAC system which can improve the precision of today's cylindrical machining processes by at least an order of magnitude. To realize this objective the above problems should be tackled more rigorously.

In Chapter 2, we investigate in detail the nature of the problems in measurement and modeling. The basic principles and characteristics of metrology are studied to help develop a suitable technique of in-process measurement. For the purpose of modeling, we review machine tool dynamics and try to find the most significant nature of machining processes for developing a generic but physically meaningful model of the GAC system.

In Chapter 3, the general theory of self-tuning control is introduced. It is applicable to our GAC system for its ability to control time varying and stochastic systems. Also, it satisfies the requirement for a systematic design of adaptive controllers. In general, self-tuning control consists of two parts, identification and control. There are many algorithms for parameter identification and controller design. To develop an effective self-tuning controller, some practical issues have to be considered cautiously in the construction of algorithms.

Mathematical models of the GAC system and the corresponding adaptive control algorithms in discrete forms for digital computation are presented in Chapter 4. The derivations are based on the investigations in Chapters 2 and 3. The stability and convergence properties of the control algorithms are analyzed. In addition, special properties of multiprobe measurement, a method of in-process measurement, in the GAC system are studied.

To evaluate the performance of the developed algorithms in Chapter 4, simulation is carried out and the results are presented and discussed in Chapter 5. The determination of some important factors associated with the practical issues in self-tuning control can be observed through the simulation results. The geometrical accuracies and the increase in stability are the measures of the performance of the GAC system. The simulation also accomplishes the interesting studies of multiprobe measurement.

In Chapter 6 comparisons with Forecasting Compensatory Control (FCC), which has been used for roundness control [84,55], are given to show that the GAC system we developed here does have significant improvement in performance, accuracy and stability over other existing techniques. We make the comparison in theoretical analysis, digital simulation, and analog test.

Chapter 7 concludes the work we have done and suggests future work which will support the success of this new development.

CHAPTER 2

METROLOGY AND DYNAMICS

The development of GAC systems involves the consideration of metrology, machine tool dynamics, and control theory. In this chapter the discussion will be focussed on metrology and dynamics. The control theory will be presented in next chapter.

2.1 Metrology

"Metrology is the science of measurement, which determines a dimension through the use of some type of calibrated device that permits the magnitude of the dimension to be determined, directly and indirectly, in scalar units" [31]. The evolution of metrology in manufacturing, since the early nineteenth century, has gone through three stages: passive, active, and dynamic [80]. In the first stage, passive metrology only served to reduce assembly work and to guarantee interchangeability by checking the dimensional parameters after manufacturing. In the next stage, active metrology was introduced in order to achieve quality and interchangeability more economically. The measurement is brought nearer to the manufacturing process so that inaccuracies can be actively corrected by a certain precalibrated compensation technique as mentioned in Chapter 1. In the third stage, starting from 1960's, dynamic metrology emerged as an essential part of the integrated manufacturing system for a

continuous and in-process measurement. The measurement can be used not only to correct the inaccuracies but also to optimize the production system by the feedback or feedforward control action. When correction of the geometrical inaccuracies is the major function, the integrated system is the GAC system as defined in Chapter 1; otherwise, it can be an ACC or ACO system.

In parallel with the above evolution, the instrument for metrology has also developed from James Watt's micrometer to today's highly sophisticated and precise laser interferometers [44]. Meanwhile, the advent of electronics and digital computers in metrology have made the measurement more consistent and efficient. In addition, metrology also extends from simple distance measurement to surface profile assessment. More metrological parameters are needed to quantify the functions or performances of a manufactured part. Standards, such as ANSI, BS, and ISO, have various documents on metrology [42]. They are used to justify the measurement of the metrological parameters.

Metrology in manufacturing, in general, can be categorized into three types: workpiece metrology, machine tool metrology, and in-process metrology. Although, for the GAC system, we are interested in in-process metrology, measuring workpiece during machining operation, the basic metrology principles and instrumentation of the other two types are presented here to help in identifying and solving problems in in-process metrology or measurement. Since we are proposing a GAC system for cylindrical machining processes, most of the discussion will be confined to cylindrical machined parts and the associated machine tools.

2.1.1 Workpiece Metrology

Workpiece metrology is the easiest to conduct, as the workpiece can be placed in an ideal metrology room and measured carefully. For a cylindrical workpiece, we are most interested in the measurement of roundness. The methods of measuring roundness can be divided into production type and absolute type [70]. The methods of production type are:

(i) diametral

(ii) circumferential confining gage

(iii) rotating on centers

(iv) V-block

(v) three-point probe

These methods are relatively inexpensive, easy to operate, and rugged in use. The disadvantage, however, is that the relative measurement of roundness can only be used for passing or rejecting the part in production line. The method of rotating on centers is even susceptible to errors from both the measuring setup and the part itself.

The major criticism of the diametral method and the V-block method is their inability to detect, for example, the iso-diametrical out-of-roundness as shown in Fig. 2.1. From the configurations in Fig. 2.2, the out-of-roundness is determined by the magnification factor [90].

$$F_n = 1 + \frac{\cos n\beta}{\sin(\alpha/2)} \tag{2.1}$$

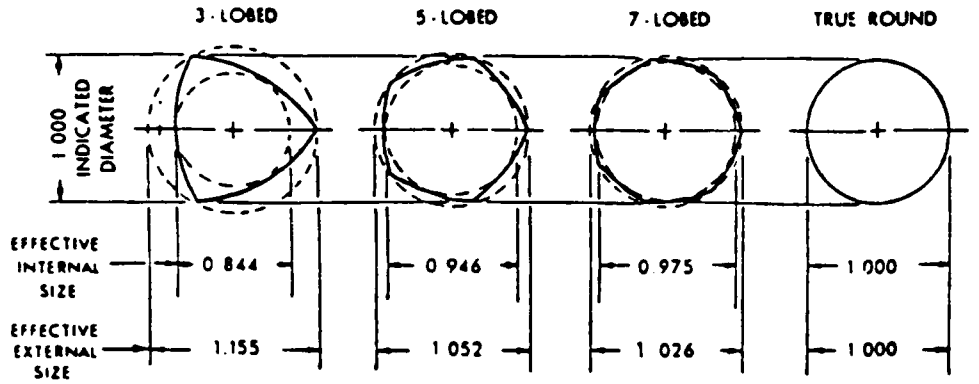

Figure 2.1 Isodiametrical Shapes [1]

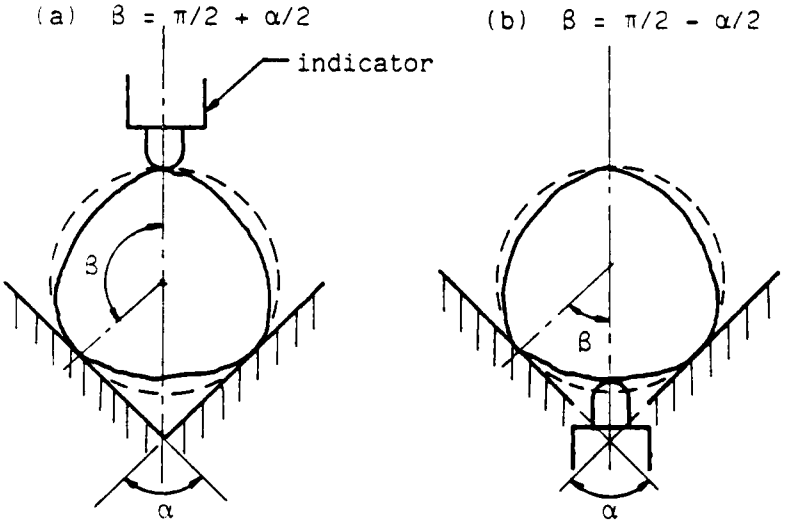

Figure 2.2 Configurations of V-block for Measuring Out-of-Roundness

where α is the angle of V-block and n is the number of lobes distributed on the part surface uniformly. F_n equal to zero means that the out-of-roundness will not be detected for an n-lobed part. It can be shown, from (2.1), that the diametral gage, equivalent to a 180° V-block, is unable to detect the out-of-roundness of the part with odd-numbered lobes. And 60° V-block is not good for 5, 7-lobed parts; 90° V-block not for 7, 9-lobed parts [70]. More specifically, the V-block of Fig. 2.2(a) can not detect the out-of-roundness of the n^*-lobed part, where

$$n^* = 2\pi k/\beta \pm 1 \qquad (2.2)$$

and k is any positive integer making n^* integer. The same property can also be found in the multiprobe measurement of Chapter 4.

The configuration of V-block method is also analogous to that of centerless grinding. As shown in Fig. 2.3, the edges of V-block correspond to the grinding wheel and the control wheel, and the indicator above the V-block corresponds to the workplate of the grinding machine. Therefore, (2.1) or (2.2) explains why the ground workpiece usually has odd-numbered lobes, and the out-of-roundness diminishes as the workplate raises to a higher position.

The absolute method means that the roundness is assessed directly from the surface profile measured in a roundness measuring machine which has an extrinsic datum [34]. The measuring machine can be either with overhead spindle or with rotating table as shown in Fig. 2.4. The overhead spindle type, such as Moore Universal

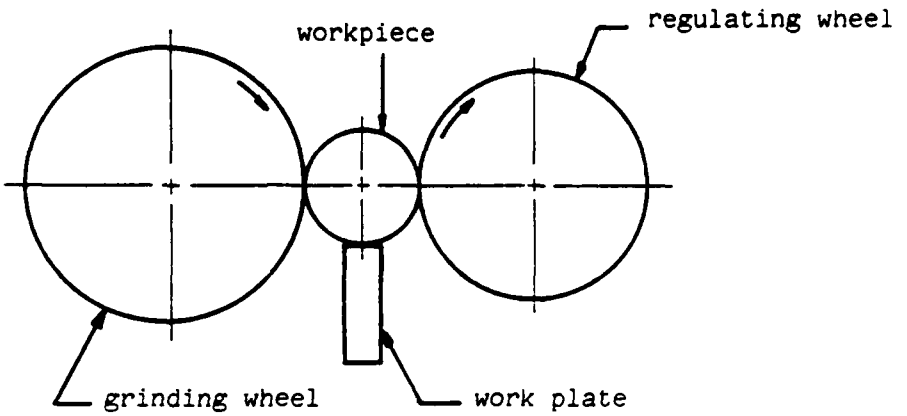

Figure 2.3 Centerless Grinding

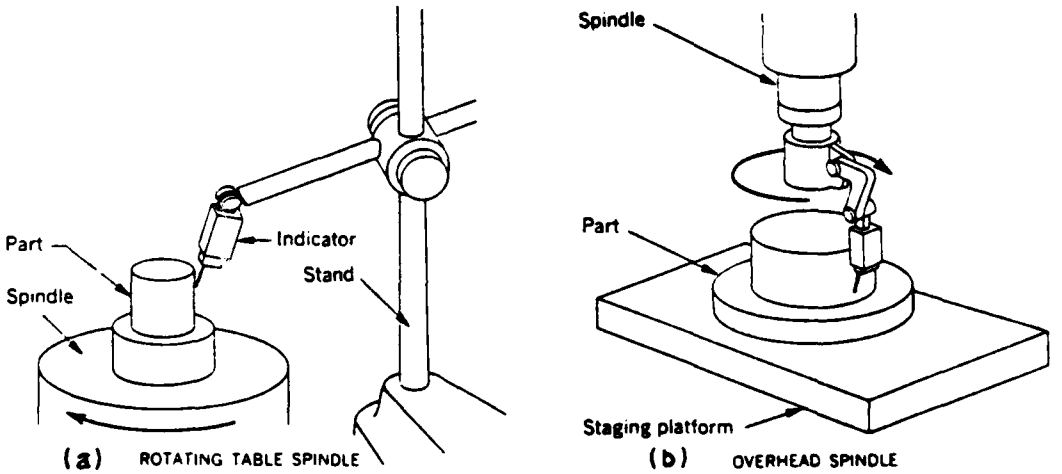

Figure 2.4 Absolute Methods of Measurement for Workpiece [70]

Measuring Machine, has a stylus tracing around the cylindrical part on a fixed flat table. It is good for heavy and short parts. The rotating table type, such as Talyrond, on the other hand, is good for light parts. The stylus assembly positioned on a fixed stand can be adjusted freely. Specifications on stylus tip radius, stylus static force, cycles per revolution, and other operational information can be found in British Standard [17] and ANSI Standard [1].

The movement of the stylus is amplified and plotted on a circular chart. The two most popular methods for evaluating the out-of-roundness are: minimum zone center (MZC) and least squares center (LSC) [17]. The MZC method, as shown in Fig. 2.5, needs several graphical trials done manually to determine the two concentric circles having the minimum radial difference. This radial difference is defined as out-of-roundness. Recently, Murthy and Abdin [72] devised the simplex search for finding the MZC in a more systematic way.

The LSC method, as shown in Fig. 2.6, computes and finds the center and the radius of the least squares circle by

$$a = \frac{2\ \Sigma x_i}{N}$$

$$b = \frac{2\ \Sigma y_i}{N} \qquad (2.3)$$

$$R = \frac{\Sigma r_i}{N}$$

The out-of-roundness is the summation of the largest outward

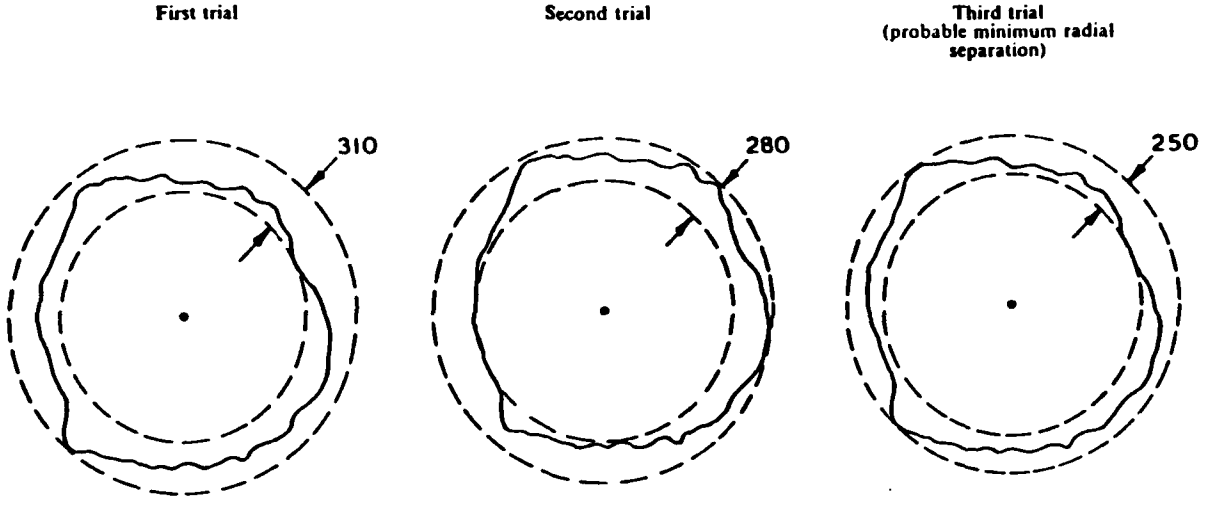

Figure 2.5 Determination of Minimum Zone Center (MZC)[17]

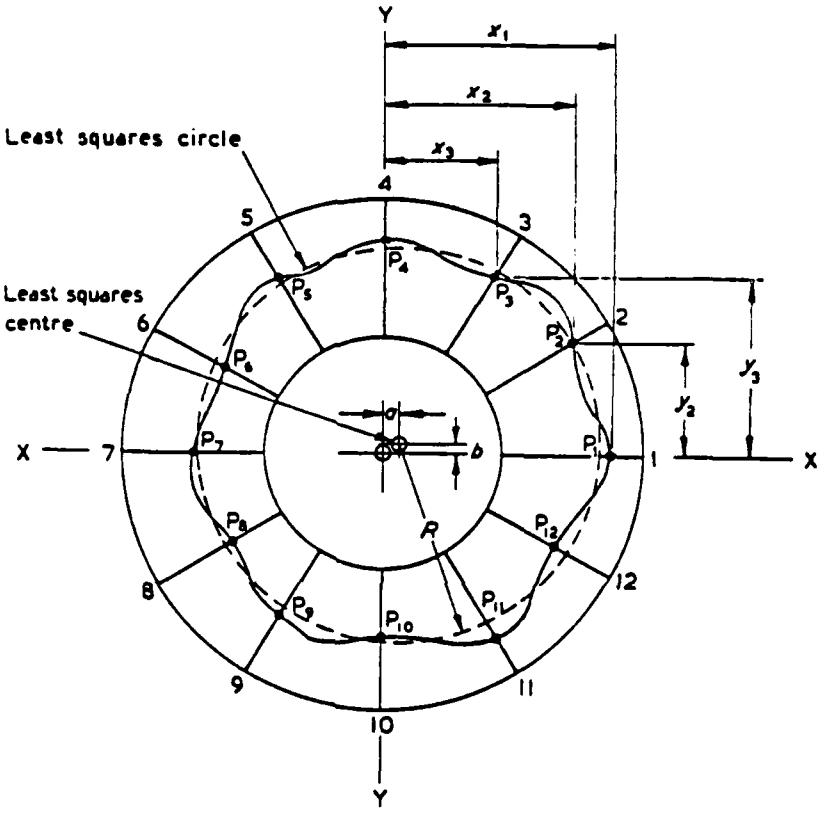

Figure 2.6 Determination of Least Squares Center (LSC)[17]

deviation of the polar profile from the LS circle and the largest inward deviation. Since the LS circle can be determined uniquely, this method is more suitable for computer controlled measuring machines.

Special care should be taken in assessing out-of-roundness when the cylindrical part is miscentered with respect to the axis of rotation of the measuring machine. Fig. 2.7 shows that a perfect round part will have a limacon-shaped polar graph provided that eccentricity exists. The reason for this kind of distortion is the suppressed radius used in plotting the polar graph [110]. The suppressed radius is the preset distance between the stylus tip and the axis of rotation. It should be as close to the mean diameter of the part as possible so that the undulation of the part surface can be distinguished by a high amplification factor.

Therefore, the above descriptions on assessing out-of-roundness are just approximately true if the eccentricity ratio is less than 15% [95,1]. Whitehouse [110], Chetwynd [22], and McCool [63] proposed a more accurate approach for numerical assessment. This approach uses the following regression equation:

$$r_i = R + a \cos \theta_i + b \sin \theta_i + e_i$$

$$i = 1,2,\ldots,N \qquad (2.4)$$

By the least squares method, the estimated values for R, a, and b are the same as those in (2.3), and

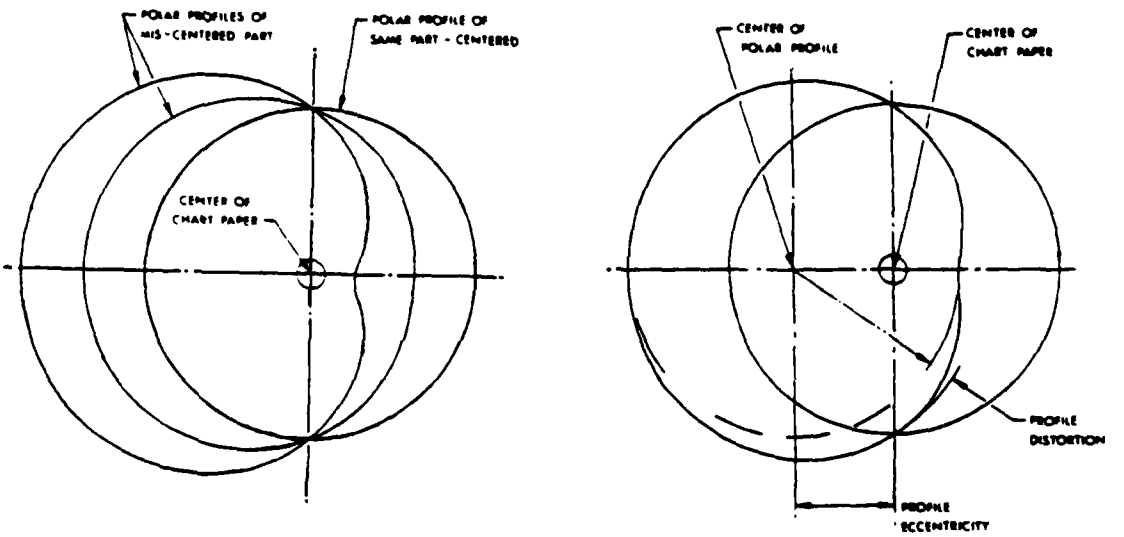

Figure 2.7 Limacon-shaped Polar Profile of Mis-centered Part [1]

$$\rho(\theta_i) = R + a \cos \theta_i + b \sin \theta_i$$

represents the limacon graph of the LS circle of a mis-centered part. The residual error e_i is the quantity used for assessing roundness. As defined in the British Standard, the LSC out-of-roundness is the maximum peak-to-peak error of e_i. Besides the improved accuracy, the limit on maximum allowable eccentricity is less restrictive for this technique. It simplifies the centering operation during measurement.

Also, (2.4) shows that the limacon consists of the constant and the first harmonic of the Fourier series, and e_i is the sum of all higher harmonics. Hence, the removal of limacon from the polar graph is equivalent to using a high-pass filter in signal processing. This technique is frequently used in machine tool metrology.

2.1.2 Machine Tool Metrology

Basically machine tool metrology is the same as workpiece metrology with the absolute method, except that the part to be sensed is a perfect round master attached to the spindle of the machine tool. Any measured movement can be attributed to the spindle error motion, which may generate uneven surface profile on the machined part [20,86]. Since the position of the sensor is where the tool resides normally, the spindle error motion in the radial direction relative to the sensor is particularly important in producing the geometrical inaccuracies of dimensional error, out-of-roundness, and roughness.

Unlike the absolute method of workpiece metrology, the setup for machine tool metrology is determined by the machining processes. For turning and most grinding operations, the setup for measurement involves the replacement of the stationary cutting tool by a noncontact sensor and the rotating workpiece by a spherical master, as shown in Fig. 2.8(a). For the boring process with rotating tool, Fig. 2.8(b) shows the setup with two perpendicular probes for measuring the error motion at the angular position of the tool. The setup in Fig. 2.9, an alternative for the setup in Fig. 2.8(b), is more convenient for using single probe [49]. Other methods related to the above two cases can be seen in the survey by Bryan and Vanherck [20] and Murthy et al. [73].

Because of the nonrepetitive nature of the spindle error motion, the measurement is normally made of readings for several revolutions as shown in Fig. 2.10; it is defined as the total error motion polar plot. The mean contour of the total error motion polar plot is termed as the average error motion polar plot, and the difference between the total error motion polar plot and the average error motion polar plot is called the random error motion [101]. Using the LSC method, the eccentricity can be located in the average error motion polar plot.

Since the spindle runs normally at the operating speed during measurement, the induced once-per-revolution unbalanced motion may mix with the misalignment of the master. One of the approaches for removing the misalignment effect from the measurement is to take a second measurement at a fairly low spindle speed to get a new average

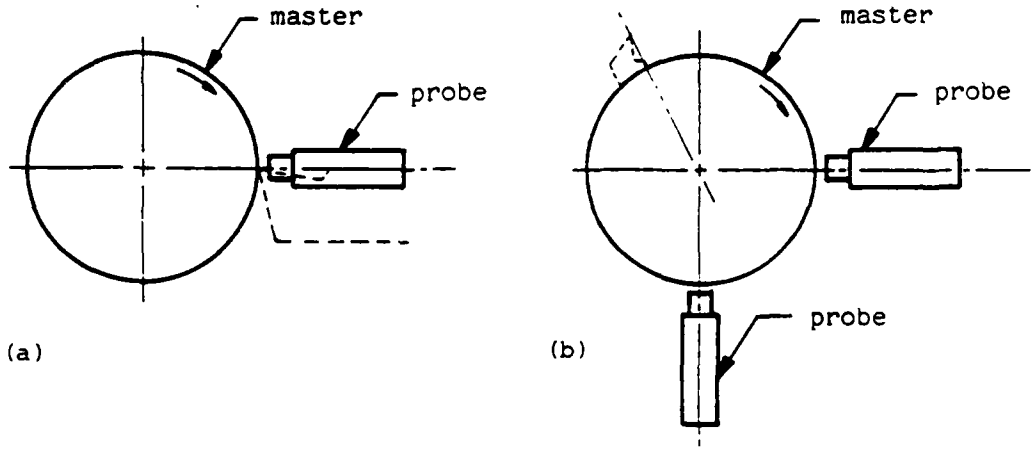

Figure 2.8 Techniques of Machine Tool Metrology
(a) Stationary Tool Type
(b) Rotary Tool Type

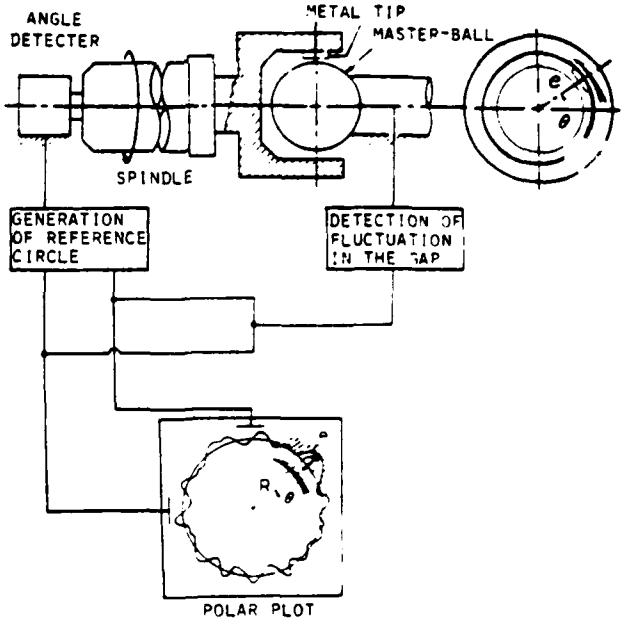

Figure 2.9 Another Measurement Technique for Process of Rotating Tool Type [49]

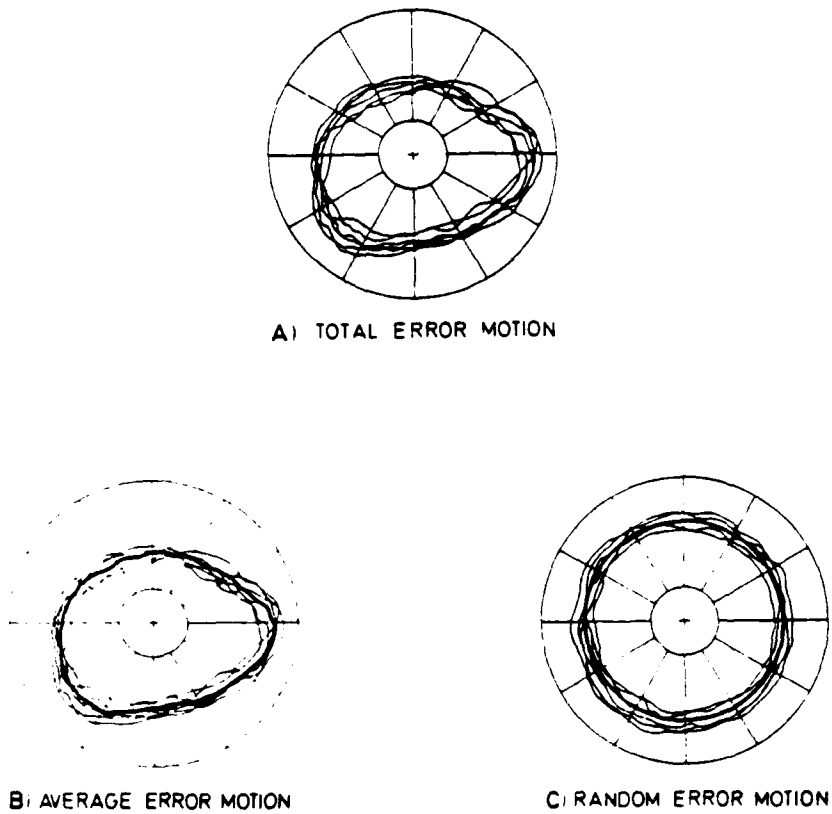

Figure 2.10 Typical Measurement of Spindle Radial Error Motion [101]

motion, then to find the eccentricity purely caused by misalignment. The digital technique we mentioned is good for this type of signal processing.

2.1.3 In-process Metrology

For very precise measurement, we can no longer assume perfect spindle in workpiece metrology or perfect master in machine tool metrology. This situation corresponds to in-process metrology which involves the measurements of both the workpiece geometry and the spindle error motion. The reversal method [32,1], as shown in Fig. 2.11, separates the spindle error motion $e(\theta)$ and the surface profile $s(\theta)$ by

$$e(\theta) = (v_1(\theta) - v_2(\theta))/2$$

$$s(\theta) = (v_1(\theta) + v_2(\theta))/2$$

where $v_1(\theta)$ is the measurement taken at position 1 and $v_2(\theta)$ at position 2. Whitehouse [111] devised the multi-step method as shown in Fig. 2.12. In step i, the measurement is

$$v_i(\theta) = s(\theta + \alpha_i) + e(\theta), \quad i = 0,1,\ldots,n.$$

Through appropriate linear combination

$$c(\theta) = \Sigma a_i v_i(\theta) = \Sigma a_i s(\theta + \alpha_i)$$

where

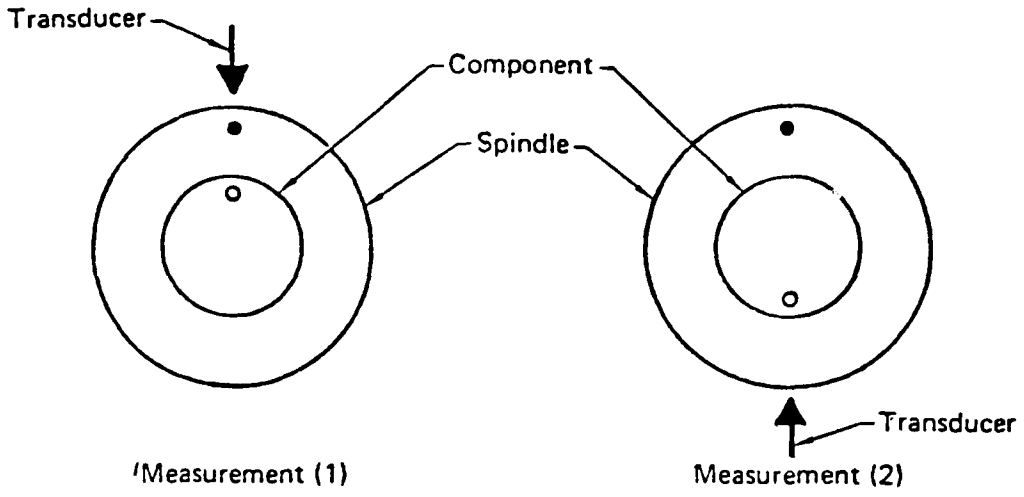

Figure 2.11 Reversal Method for In-Process Measurement

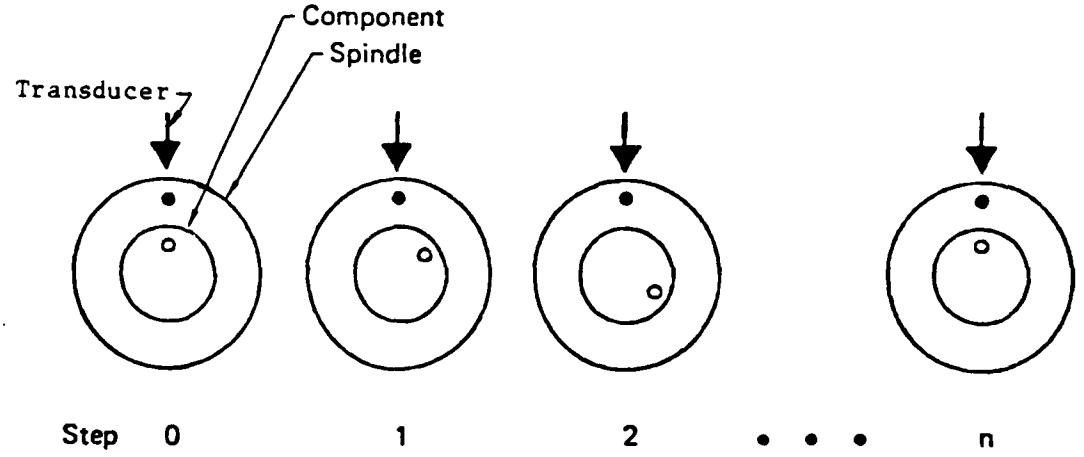

Figure 2.12 Multi-Step Method for In-Process Measurement

$$\Sigma a_i = 0$$

$s(\theta)$ can be evaluated from the Fourier expansion of $c(\theta)$. Although the reversal method has more mechanical problems, the multi-step method suffers harmonic distortion. Both of these methods assume that the spindle error motion is repetitive, which is not generally true in practice. Thus, Whitehouse [111] proposed the multiprobe method for non-repetitive spindle errors. This is particularly good for our GAC system. It will be discussed in Chapter 4.

2.2 Machine Tool Dynamics

As discussed in Chapter 1, there are many error sources which contribute to the inaccuracies of a machined part. Machine tool dynamics plays a very important role in transforming the error sources into the geometrical inaccuracies. Also, in developing a GAC system for reducing the inaccuracies, the dynamic stability of the machining system should not be sacrificed, however. Thus, it is imperative to understand machine tool dynamics before the development of the GAC system.

In general, machine tool dynamics deals with the interaction between the cutting process and the machine tool structure as shown in Fig. 2.13. The interest in the investigation of machine tool dynamics can be attributed to the most obscure and delicate problem in metal cutting - chatter [94]. Chatter, usually, is an unwanted vibration phenomenon during the machining operation. It spoils the finish and the dimensional accuracy of the workpiece, shortens the lives of the tool and the machine, and generates uncomfortable noise and vibration.

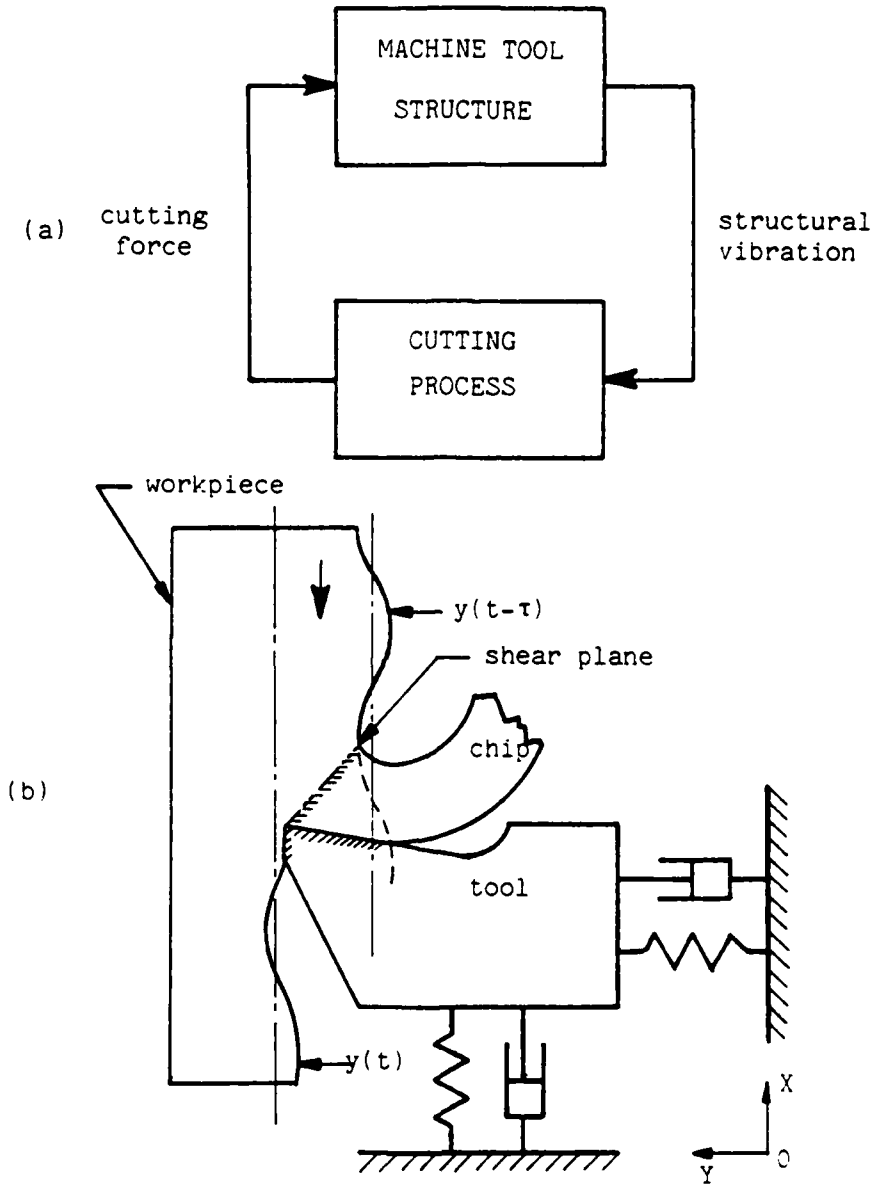

Figure 2.13 Machine Tool Dynamics

There are two basic types of chatter: forced chatter and self-excited chatter. Forced chatter typically results from periodic disturbances, such as unbalanced rotating members, intermittent cutting, gear backlash, and motions transmitted through the floor [16]. This type of chatter, though important in practice, relates to fairly simple structural dynamics and offers no insight into the dynamics of the cutting process. Self-excited chatter, on the other hand, occurs only when there are any machining operations. The interaction of cutting dynamics and structural dynamics, under certain conditions, may result in dynamic instability of the machining process. Normally, the resulting vibration is much more violent than that resulting from the former type. Thus, without any confusion, the term "chatter" specifically refers to the self-excited type in the following text.

2.2.1 Chatter and Cutting Dynamics

The theory of chatter in metal cutting was first explored by Arnold [4]. He proposed the falling characteristic of force-speed relationship for explaining the chatter phenomenon. Although this concept is still quite controversial [40,98], his work shed some light on the research in cutting dynamics. Basically, the cutting process can be visualized from the three boundaries in Fig. 2.13(b) [30]. On the boundary of the shear plane, the length and the angle of the plane determine major cutting forces exerted on the tool faces [64]. On the boundary of the tool-chip interface, the tool tip, tool holder, and workpiece may deflect owing to the cutting forces on the tool rake face. The geometry and the tip position of the tool are

thus varied. Besides, the sliding motion of the chip over the tool face is sometimes complicated by the built-up-edge and the wear on the rake face, which change the tool geometry further.

Similar observations occur on the boundary of the tool-workpiece interface. The flank wear resulting from the sliding motion changes the effective clearance angle of the tool and affects the reacting forces on the boundary. The tool and the workpiece, again, are deflected by the reacting forces. Conceivably, the whole machining process is quite nonlinear in nature; the associated factors are interrelated. These explain the frequent inconsistencies in the experimental findings among the researchers.

The mechanisms of chatter, generally, can be divided into the velocity-dependent type, regenerative type, and mode-coupling type [104]. Although they act simultaneously in practice, regenerative chatter is recognized to dominate most of the unstable vibrations in metal cutting [43,52,97]. Furthermore, Tobias [98] elaborated the theory of regenerative chatter and derived a stability chart which matches very well with the test results as shown in Fig. 2.14. The lobing characteristic of the stability chart, which is common to most of the machining processes, can hardly be explained by other chatter theories. These facts justify the regenerative process or effect as being the key phenomenon of the machining process.

Regenerative effect is the chip-thickness variation effect caused by the surface undulation, $y(t-\tau)$, which is formed in a previous cut [98]. Hence, as seen in Fig. 2.13(b), the uncut chip

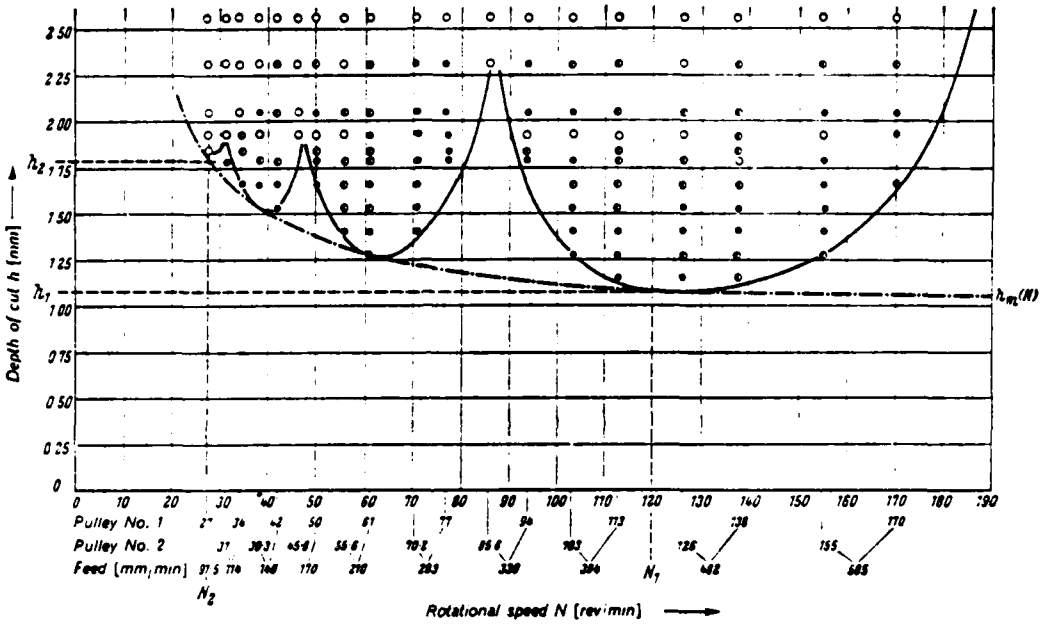

Figure 2.14 Stability of a Milling Process [98]
- O large amplitudes
- ◐ moderate amplitudes
- ● small amplitudes

thickness for a cylindrical machining process is given by

$$\delta(t) = y(t) - \mu y(t-\tau)$$

where τ is the time required for each revolution of the spindle and μ, overlap factor, is introduced to account for the degree of overlap in successive cuts. μ is equal to one for plunge cutting, but zero for thread cutting. In general,

$$0 \leq \mu \leq 1$$

The analytical prediction of μ is very difficult; nevertheless, some attempts have been made by Srinivasan and Nachtigal [91].

Machine tool dynamics can be conveniently represented by the block diagram of Fig. 2.15, where regenerative effect is separated from cutting dynamics for its particular significance. We deliberately generalize the complexity of cutting dynamics by expressing it as $k_c G_c'$. k_c represents the static cutting stiffness, which can be measured in steady state cutting. The dynamic cutting stiffness G_c' can be as complex as the theoretical derivations of Albrecht [2] and Wu [114]. However, linear dynamics as expressed by

$$G_c'(s) = 1 + Ks$$

is adequate to account for the physics of small vibration and to accommodate the important effect of penetration rate [98,89].

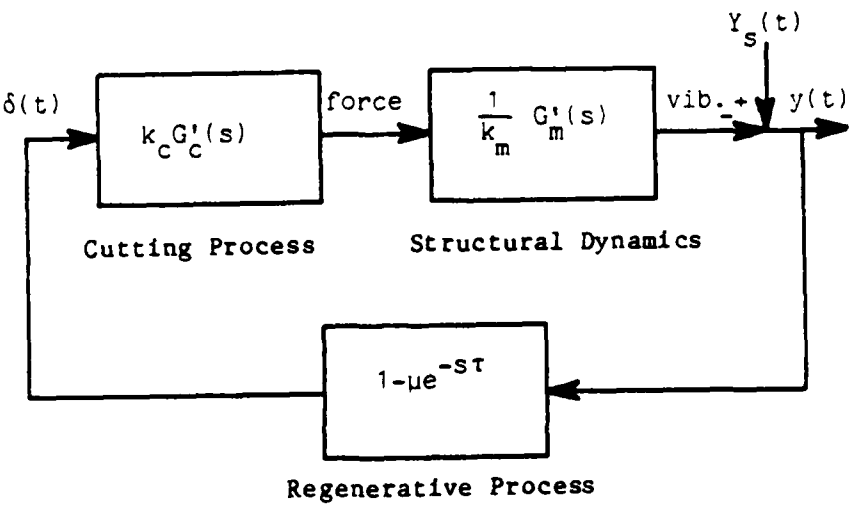

Figure 2.15 Machine Tool Dynamics in Control Block Diagram

As for structural dynamics, k_m is the static structural stiffness of the tool-workpiece-machine system. The dynamic structural stiffness, G_m', basically has the transfer function

$$G_m'(s) = \sum_i \frac{g_i \omega_{ni}^2}{s^2 + 2\zeta_i \omega_{ni} s + \omega_{ni}^2}$$

which is a multi-degree of freedom system with damping ratios ζ_i's and natural frequencies ω_{ni}'s. If there is any mode-coupling effect, G_m' can be expanded into a transfer matrix to correlate the vectors of cutting forces and structural deflections.

A further simplification of the representation can be made by letting

$$G_m = G_c' G_m'$$

The stability borderline in the stability chart can be constructed by solving the characteristic equation of the system in Fig. 2.15

$$1 + \frac{k_c}{k_m}(1 - \mu e^{-s\tau}) G_m(s) = 0, \quad s = j\omega, \; j = \sqrt{-1}$$

Thus

$$g_R(\omega) = \frac{k_m}{k_c} \frac{1 - \mu \cos \omega\tau}{1 + \mu^2 - 2\mu \cos \omega\tau} \tag{2.5}$$

$$g_I(\omega) = \frac{k_m}{k_c} \frac{\mu \sin \omega\tau}{1 + \mu^2 - 2\mu \cos \omega\tau} \tag{2.6}$$

where

$$G_m(j\omega) = g_R(\omega) + jg_I(\omega)$$

If $G_m(j\omega)$ and μ are known in advance, the chatter frequency ω_c can be found, for each given $\omega_c\tau$, by solving

$$\frac{g_I(\omega_c)}{g_R(\omega_c)} = -\frac{\mu \sin \omega_c\tau}{1 - \mu \cos \omega_c\tau}$$

Then, k_c/k_m can be obtained from either (2.5) or (2.6).

Fig. 2.16 is the stability chart for the special case when

$$\mu = 1$$

$$G_m(s) = \frac{\omega_n^2}{s^2 + 2\zeta\omega_n s + \omega_n^2} \tag{2.7}$$

The chart shows that the stability of machining is determined by the stiffness ratio, k_c/k_m, and the ratio of the cutting speed, Ω or $2\pi/\tau$, to the chatter frequency, ω_c. In this case the asymptotic borderline for absolute stability is [65]

$$(k_c/k_m)_{min} = -\frac{1}{2[g_R(\omega)]_{min}} = 2\zeta + 2\zeta^2$$

The term $(k_c/k_m)_{min}$ represents the minimum ratio of static cutting stiffness to static structural stiffness. If the actual stiffness ratio is smaller than this limit, the system will be unconditionally stable at any cutting speed. Thus, the term $(k_c/k_m)_{min}$ can be used

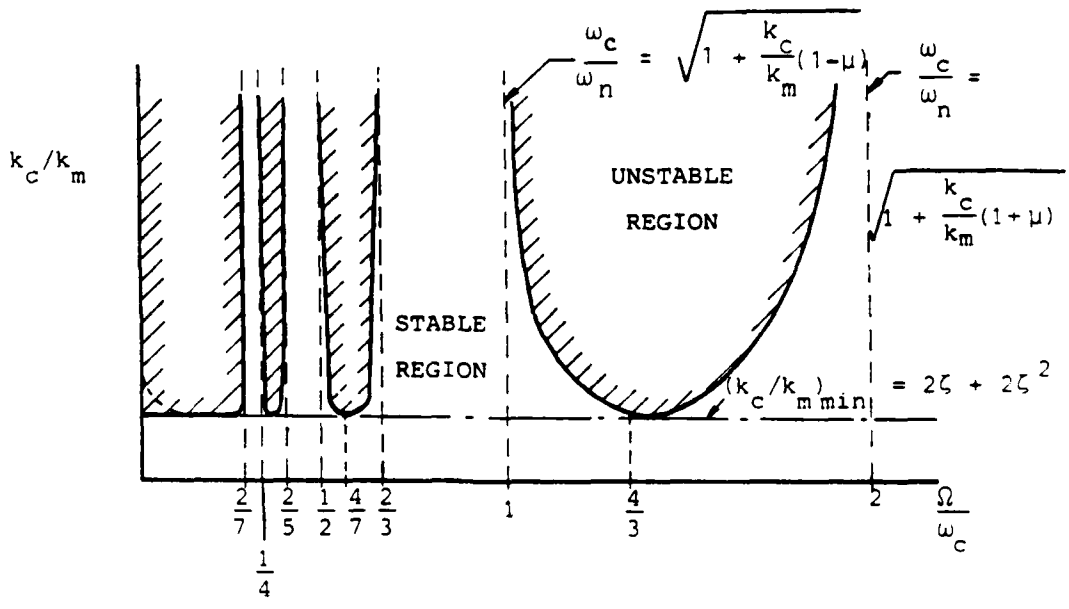

Figure 2.16 A Theoretical Stability Chart of Fig. 2.15

μ=1, ω_c - chatter frequency, ω_n - natural frequency, Ω- spindle angular speed

as a measure of the stability of machining. For the above simple system, with typical damping ratio of $\zeta = 0.05$, the maximum degree of stability is $k_c/k_m = 0.105$.

2.2.2 Methods for Chatter Reduction

There are many ways of increasing the stability of machining or chatter control [16,98]. Increasing the damping in the vibration direction is the most obvious one. Increasing the structural stiffness by preloading the spindle can also enhance the stability. In the shop floor, changing the cutting conditions is is frequently used for avoiding chatter. Small depth of cut or width of cut, which reduces cutting stiffness, is beneficial in stabilizing the machining process. It can be seen from Figs. 2.14 and 2.16 that the dynamic stability, sometime., can be achieved by using high cutting speed which exceeds a certain critical value. Weck et al. [103] even used the lobing characteristic of the stability chart to avoid chatter vibration by shifting the spindle speed to the stable region.

Most of the above methods usually restrict the productivity or need redesign of the machine. To overcome these deficiencies, active chatter control was introduced in the late 1960's. The system of active chatter control normally has a feedback controller which is designed according to the machine tool dynamics as shown in Fig. 2.15. The feedback system of Comstock et al. [29] measures the relative displacement between the tool and the spindle, and controls the infeed motion of the tool during plunge cutting. Nachtigal and his coworkers [74,75,60] use force feedback to control the same machining process.

Later, adaptive active chatter control, using both force and displacement feedbacks, was proposed to handle the problems of the variation of machine tool dynamics during operation [76,67]. Basically, these methods use a deterministic model of machine tool dynamics for stabilizing the machining operation. They may also attenuate disturbances through the increase of the controller gain [66]. However, for geometric adaptive control, where accuracy is more important than stability, the gain increase may not be adequate for the unknown nature of random disturbances. Therefore, it is essential to develop a stochastic model, based on the similar reasoning of machine tool dynamics, to control the random disturbances more effectively. Also, the control algorithms must be more adaptive, versatile, and easy to implement for automated machining systems.

CHAPTER 3

SELF-TUNING CONTROL THEORY

Although we are able to recognize and model the fundamental properties of machine tool dynamics as shown in Chapter 2, the characteristic parameters of the system can never be assessed exactly through off-line testings and analyses. The value of the parameters may change with the type of working material, part geometry, tool geometry, and cutting conditions. Also, the changes may occur during the operation because of cutting force, wear, heat, and other disturbances. Thus, in GAC, we need an adaptive control technique which can assess the system characteristics on line and maximize the performance of the machining process.

As shown in Fig. 1.1, the adaptive controller basically consists of two important functions:

*on-line identification of characteristic parameters

*real time control for optimizing the performance index.

An ideal or optimal adaptive controller, also called dual controller, is very difficult to achieve and implement due to the nonlinear nature of the interaction between the identification function and the control function [35,9] The interaction is nonlinear in the sense that the controller has to consider the future uncertainties of the parameters in giving the control inputs. And the uncertainties or

probability distributions of the parameters, called hyperstate, are functions of the control inputs [112,5].

3.1 Self-tuning Control (STC)

Self-tuning control is a suboptimal adaptive control technique which uses the certainty equivalence principle. The optimal controller is designed by considering the estimated parameter values as the true parameter values, that is, by ignoring any uncertainties of the estimated parameters. This simplification makes the adaptive control system linear and reduces the work of both analysis and computation considerably.

The earliest STC is Kalman's [51] self-optimizing control, which tried to adapt the controller automatically to the changes of the process characteristics. Peterka [79] extended this idea to the stochastic system with constant parameters. It is Astrom and Wittenmark [10] who first analyzed the properties of a self-tuning regulator, and showed that optimal control can still be obtained despite the approximation introduced by the certainty equivalence principle. Since then, the interest in STC increased rapidly. Further analysis of convergence and stability has provided much deeper insight into the STC theory. Various algorithms for both identification and control have been proposed to make STC more efficient and versatile. And many successful applications of STC have been reported justifying its substitution for PID controllers. Furthermore, the sampled data based algorithms of STC are particularly suitable for today's low cost microprocessor control.

Most of these developments can be reviewed by studying the following representative work: Astrom [6,7]; Astrom and Wittenmark [12]; Clarke and Gawthrop [27,28]; Goodwin and Sin [39]; Harris and Billings [41]; Isermann [45,46]; Unbehauen [100]; Wellstead [105].

3.2 Self-tuning Techniques

Assume that the system to be controlled can be described by an ARMAX model [39]

$$A(z^{-1})y_t = B(z^{-1})u_{t-k} + C(z^{-1})e_t \tag{3.1}$$

where k, an integer, is the time delay of the control system and

$$A(z^{-1}) = 1 + a_1 z^{-1} + \ldots + a_{n_a} z^{-n_a}$$

$$B(z^{-1}) = b_0 + b_1 z^{-1} + \ldots + b_{n_b} z^{-n_b}$$

$$C(z^{-1}) = 1 + c_1 z^{-1} + \ldots + c_{n_c} z^{-n_c}$$

are associated with the dynamics of the system. y_t, u_t and e_t denote the system output, the control input, and the white noise disturbance at the sampling time instant t, respectively.

The general form of a self-tuning controller can be expressed as

$$H(z^{-1})y^*_{t+k} = F(z^{-1})y_t + G(z^{-1})u_t \tag{3.2}$$

where y_t^* is the desired output of the system. The polynomials F, G and H are determined by the polynomials A, B and C in (3.1) and the specified control criteria. Depending on the methods for determining the parameters of the controller, self-tuning controllers can be divided into two categories, explicit and implicit algorithms. The explicit or indirect algorithm needs to estimate the polynomials A, B and C before assessing the parameters of the controller. In the implicit or direct algorithm the model (3.1) can be reparameterized into a certain form so that the parameters of the controller can be estimated directly.

3.2.1 Parameter Estimation

Both the explicit and implicit algorithms need a recursive parameter estimation scheme. The scheme can be one of the following recursive estimation methods [46,33]:

recursive least squares (RLS)

recursive extended least squares (RELS)

recursive maximum likelihood (RML)

recursive instrumental variables (RIV)

stochastic approximation (STA)

The RML or recursive prediction error method (RPEM) is the most general and complex algorithm [59]. It has a unified form as shown below:

$$\hat{\theta}(t) = \hat{\theta}(t-1) + L(t)\varepsilon(t) \tag{3.3a}$$

$$L(t) = P(t)\psi(t)$$

$$= \frac{P(t-1)\psi(t)}{1 + \psi^T(t)P(t-1)\psi(t)} \tag{3.3b}$$

$$P(t) = [I - L(t)\psi^T(t)]P(t-1) \,/\, \alpha(t) \tag{3.3c}$$

$$\varepsilon(t) = y(t) - \hat{y}(t)$$

$$= y(t) - \hat{\theta}^T(t-1)\phi(t) \tag{3.3d}$$

$$\hat{\theta}^T(t) = [\hat{a}_1(t),\ldots,\hat{a}_{n_a}(t),\hat{b}_1(t),\ldots,\hat{b}_{n_b}(t),$$

$$\hat{c}_1(t),\ldots,\hat{c}_{n_c}(t)] \tag{3.4a}$$

$$\phi^T(t) = [-y(t-1),\ldots,-y(t-n_a),u(t-k),\ldots,u(t-k-n_b+1),$$

$$\bar{\varepsilon}(t-1),\ldots,\bar{\varepsilon}(t-n_c)] \tag{3.4b}$$

$$\bar{\varepsilon}(t) = y(t) - \hat{\theta}^T(t)\psi(t) \tag{3.4c}$$

$$\psi^T(t) = [-\hat{y}(t-1),\ldots,-\hat{y}(t-n_a),\tilde{u}(t-k), \ldots,\tilde{u}(t-k-n_b+1),$$

$$\varepsilon(t-1),\ldots,\varepsilon(t-n_c)] \tag{3.4d}$$

$$\hat{C}(z^{-1},\hat{\theta}(t-1))\begin{bmatrix}\hat{y}(t)\\ \tilde{u}(t)\\ \varepsilon(t)\end{bmatrix} = (1 + \hat{c}_1(t-1)z^{-1} + \ldots$$

$$+ \hat{c}_{n_c}(t-1)z^{-n_c}) \begin{bmatrix} \tilde{y}(t) \\ \tilde{u}(t) \\ \tilde{\varepsilon}(t) \end{bmatrix}$$

$$= \begin{bmatrix} y(t) \\ u(t) \\ \bar{\varepsilon}(t) \end{bmatrix} \tag{3.4e}$$

where matrix I is a unit matrix and $\alpha(t)$ is the forgetting factor for discounting the old data. The a posteriori prediction error $\bar{\varepsilon}(t)$ in (3.4b and c) can improve the convergence rate of the estimation algorithm. Most of the time, however, it is approximated by $\varepsilon(t)$ for simplicity. Further simplification can still be made. If $\psi(t)$ is approximated by $\phi(t)$, the algorithm reduces to RELS. If n_c is equal to zero, i.e., $C(z^{-1}) = 1$, the algorithm reduces to RLS. RIV and STA can be obtained by modifying or simplifying RLS; however, they are seldom used in STC.

3.2.2 Control Criteria

In general, there are two types of control criteria, classical and optimal [109]. From (3.1) and (3.2), the closed loop system is of the form

$$(AG+BF)y_{t+k} = BHy^{*}_{t+k} + CGe_{t+k} \tag{3.5}$$

With the classical type , the parameters of the controller, $\hat{F}$ and $\hat{G}$, are determined such that

$$\hat{A}\hat{G} + \hat{B}\hat{F} = \hat{C}T \tag{3.6}$$

where $\hat{A}$, $\hat{B}$, and $\hat{C}$ are the estimated polynomials of A, B, and C. T is the prespecified characteristic polynomial of the closed loop system. For a regulator system, $y^* = 0$, T is chosen to have the properties of good noise rejection, a pole placement control [106,107]. For a servo system, $e_t = 0$, T and H are designed to assure good tracking capability. It belongs to the pole-zero placement control [11]. The extended STC of Wellstead and Sanoff's [108] chooses T and H for both output tracking and noise rejection.

With the optimal type, the controller of (3.2) is taken to minimize the cost function

$$I = E[\phi^2(t+k)|t]$$

$$\phi(t+k) = Py_{t+k} + Qu_t - Ry^*_{t+k} \tag{3.7}$$

where P, Q and R are polynomials in operator z^{-1}. Consequently, $\hat{F}$, $\hat{G}$ and $\hat{H}$ can be determined from

$$P\hat{C} = \hat{A}\hat{E} + z^{-k}\hat{F}$$

$$\hat{G} = \hat{B}\hat{E} + Q\hat{C}$$

$$\hat{H} = \hat{C}R \tag{3.8}$$

The alternative form of (3.5) is thus

$$y_t = \frac{BR}{PB + QA} y^*_t + \frac{EB + QC}{PB + QA} e_t$$

This is called generalized minimum variance control [23,25,26,38]. When $P = 1$, $y_t^* = 0$, and $Q = 0$, the controller reduces to the famous self-tuning regulator, a minimum variance controller [10]. Normally, the cost function is specified with

$$P = R = 1, \quad Q = \lambda > 0$$

for weighted minimum variance control [39].

The cost function of the optimal type can be extended to state space variables for more sophisticated control [56]; however, it is beyond our scope of interest. The generalized STC proposed by Allidina et al. [3] is a unification for the classical type and the optimal type.

3.3 Implementation Aspects

In the practical implementation of STC there are several factors which should be considered. They can be classified into identification, control, and general issues.

3.3.1 Identification Issues

In identification or parameter estimation, we consider the following factors:

i. Orders of system, n_a, n_b, and n_c: They should be known a priori. Normally, by knowing the upper bound, we can let $n_a = n_b = n_c = n$. For implicit self-tuning algorithms, the information on time delay k is also needed. These integers determine the total number of parameters to be estimated.

ii. Bias of estimation: Explicit algorithms require identification schemes with less bias error in estimated parameters, such as RML and RELS. These schemes, however, are complex computationally and are susceptible to numerical instabilities. Implicit algorithms, on the other hand, may use the simple scheme as RLS and still have satisfactory control performance.

iii. Computation accuracy and speed: In microprocessor based control systems the accuracy of data words is much more limited than that in general purpose computers. The accumulated computational errors may cause numerical difficulties. To overcome this problem, the square roots method [92] and the UD method [14,96] of RLS can be used to convert the computation from single precision to double precision without slowing down the computational speed. If the computational speed is critical, a fast algorithm is recommended [71,57].

iv. Forgetting factors: A forgetting factor is very important in STC. It not only determines the tracking speed of identification for systems with time varying parameters, but also may affect the convergence of the STC output. Normally, it is in the range of .95 to 1.0. A low forgetting factor is good for initial coarse tunings, fast varying parameters, and abrupt changes in the desired output. However, it may destabilize the control system if the value is too low, and may cause estimator wind-up in servo control [5,12]. A time varying forgetting factor [36] can be used to avoid those problems.

v. Initial data: This is not a crucial issue in STC. The general rule is to make an initial guess of the parameters as close to the true values as possible. If the confidence of the guess is low, the determinant of the covariance matrix should be large.

vi. Identifiability: Astrom and Wittenmark [10] showed that in an implicit self-tuning regulator it is possible to have the problem of identifiability in estimation. To avoid any numerical difficulties, the simplest way is to give a certain parameter a constant value.

3.3.2 Control Issues

The selection of control criterion depends on the following factors:

i. Performance specifications: This includes steady state error, noise rejection, convergence, stability, and robustness. These factors usually conflict with each other. Therefore, the selected criterion must be a compromise of these factors. At this moment we are unable to evaluate or justify any control criteria for the lack of theoretical analysis. Some general guidelines can still be found [12].

ii. Nonminimum phase problem: The nonminimum phase problem refers particularly to some of the zeros of B in (3.1) falling outside the unit circle Minimum variance control is very likely to be unstable for this kind of systems. Pole placement or weighted minimum variance control can overcome this problem [24].

iii. Constraints on control input: Another deficiency of minimum variance control is the large amplitude or energy of control inputs frequently required during control. The control hardware or actuator can be easily overloaded or saturated. Like the nonminimum phase problem, pole placement and weighted minimum variance control are possible solutions. Or, the constraints can be incorporated into the cost function of optimal control [62,61].

iv. Deterministic disturbances: In this text, deterministic disturbances refer to the slowly varying disturbances and the periodic disturbances with unknown frequencies and amplitudes. This type of disturbances is important in practical control systems; however, they are rarely discussed previously in STC. The analysis and simulation of Goodwin and Sin [39] reveal that the deterministic disturbances can be well compensated for by STC.

3.3.3 General Issues

i. Simplicity in implementation: STC should always be designed as simple as possible for practical applications. The self-tuning algorithms with weighted minimum variance criterion and RLS estimation usually give more satisfactory results than other sophisticated algorithms. Also, implicit algorithms are simpler and more robust than explicit ones in general [12].

ii. Sampling rate: Sampling rate, in general, should be high enough to cover the desired bandwidth of the closed loop system. Its

upper bound is limited by some considerations. It should not exceed the response speed of the actuator. It should be low enough so that the computer can accomplish all the digital signal processing, and the variation of system delay is insignificant compared to the sampling time interval. Further considerations can be seen in [12].

CHAPTER 4

THEORETICAL DEVELOPMENT

As mentioned in Chapter 2, the geometrical inaccuracies of the machined part result from the relative error motion between the tool tip and the part surface during machining operations. The error motion in radial direction is particularly important in determining the geometrical errors. There are numerous sources which contribute to such kind of error motion. Three major types of error sources considered in this text are: stochastic, deterministic, and regenerative types.

The stochastic type is mainly induced by the play in the imperfect spindle bearings. Fig. 2.10 is a typical polar plot of spindle error motion measured from the idling spindle. The randomness of the error motion suggests statistical models, such as autoregressive model [83] and moving average model, for describing this error motion mathematically. In real cutting, this error motion is complicated further by the chip breakage, nonstationary built-up-edge, hard grains in work material, floor noises, and change of the bearing play due to cutting forces and thermal drifts.

The deterministic type can be further divided into linear errors and periodic errors. Linear errors refer to those caused by steady or slowly varying disturbances, such as the structural deflection

induced by the mean cutting forces, tool wear, and thermal expansion. Periodic errors mostly come from the unbalanced rotating parts, such as the spindle, grinding wheel, and gear train. The resulting error motion is characterized by the periodic movement with frequencies having integer multiples of the angular frequency of the spindle. The fundamental or lowest frequency component of error motion results in the eccentricity of the machined part, while the higher harmonics produce lobe-shape errors on the part surface. Periodic errors may also result from directional stiffness variation caused by the chuckhead [81].

The regenerative type is the regenerative effect discussed in Chapter 2. It relates to the interaction between the cutting force and the machine tool structure. The frequency of this type of error motion is close to the natural frequency of the tool-workpiece structure. It is an unstable phenomenon during machining operations. Whether this unacceptable error motion will occur or not is determined by the stiffness and the damping of the machining system.

Most of the above error sources are dynamic. They are difficult to identify because the error sources are interrelated. Moreover, these error sources differ with part designs and machining conditions. Therefore, they can be best compensated for by a GAC system. The GAC system proposed in the next section assumes that direct measurement of the part geometry is used. Thus, the effect of the above major error sources, except the thermal effect, on geometrical accuracy can be detected and corrected by the controller. The thermal effect is the dimensional expansion of the workpiece due

to the cutting heat. The GAC system tends to generate the geometrical accuracies at the elevated workpiece temperature during machining. Thus, a certain temperature measurement and calibration is needed for the true dimensional accuracy. In this text, however, this effect is assumed to be negligible for simplicity.

4.1 Model of the GAC System

The physical model of a cylindrical machining process, plunge cutting in particular, is shown in Fig. 4.1. The tool cuts into the rotating workpiece, which is clamped to the spindle. The forces generated during the cutting process excite the tool-workpiece structure, which is basically a spring-mass-damper system. Meanwhile, the induced structural or regenerative type error motion together with the other two types of error motions determine the actual tool path on the workpiece. The instantaneous part surface and the depth-of-cut are thus formed.

Based on the above investigation, a control diagram of the GAC system for plunge cutting is constructed as shown in Fig. 4.2. The profile of the part surface at the tool tip is denoted by Y_t, which is the reduction of radius measured from a base circle as shown in Fig. 4.1. Due to the regenerative effect in plunge cutting, the instantaneous depth-of-cut is $Y_t - Y_{t-p}$, where p is the time interval for the spindle to rotate in one revolution. The cutting process CP is related to the depth-of-cut and the cutting force. Through the structural dynamics, MT, a spring-mass-damper system, the error motion X_t is induced. Thus, surface profile Y_t is the summation of

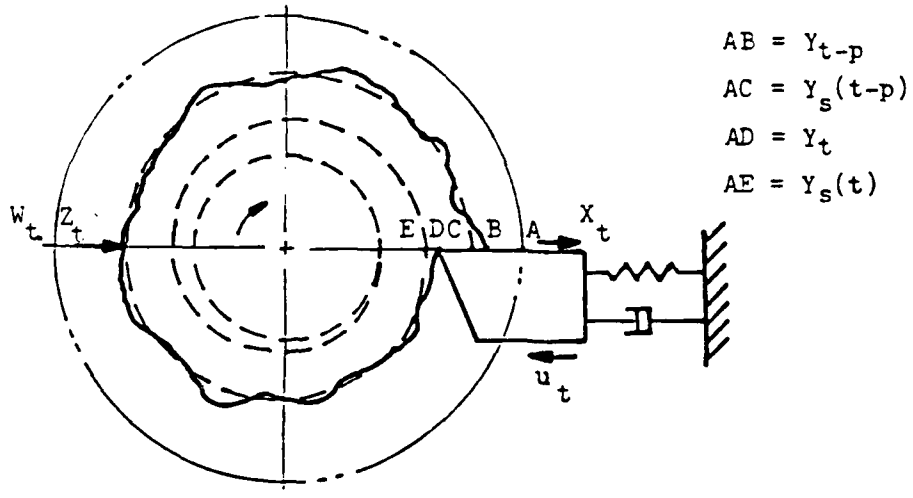

Figure 4.1 Structural Dynamics and Regenerative Effect of Plunge Cutting

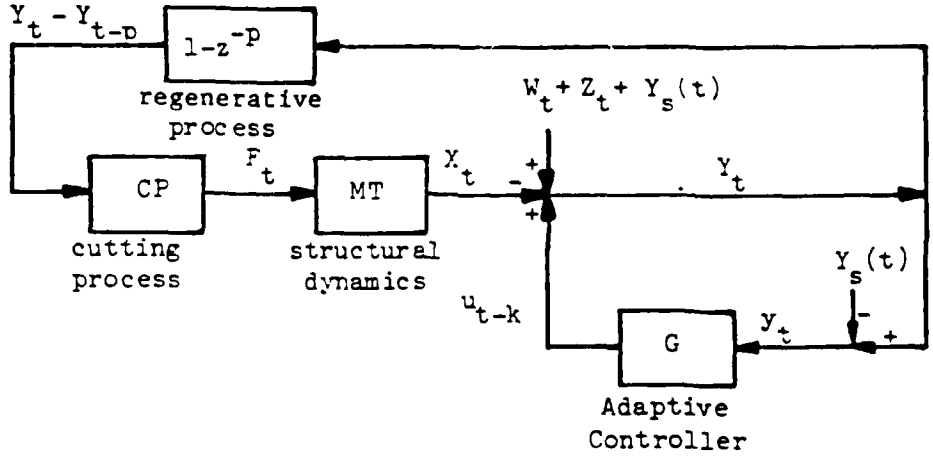

Figure 4.2 Control Diagram of the GAC System

structural error motion $-X_t$, deterministic error motion Z_t, stochastic error motion W_t, specified infeed of the tool $Y_s(t)$, and the control action u_{t-k} from the adaptive controller. The controller G constantly measures the geometrical error y_t, defined by $Y_t - Y_s(t)$, identifies the system model, and gives appropriate control action to reduce y_t.

From Appendix 1, a linear model of the GAC system is derived and expressed by a stochastic difference equation as follows:

$$A(z^{-1})(y_t - y_{t-p} + \delta_t)$$

$$= B(z^{-1})(u_{t-k} - y_{t-p} + \delta_t) + C(z^{-1})\xi_t \qquad (4.1)$$

with

$$A(z^{-1}) = 1 + a_1 z^{-1} + \ldots + a_n z^{-n}$$

$$B(z^{-1}) = b_0 + b_1 z^{-1} + \ldots + b_n z^{-n} \qquad (4.2)$$

$$C(z^{-1}) = 1 + c_1 z^{-1} + \ldots + c_n z^{-n}$$

where z^{-1} is the backward shift operator, that is, $z^{-1} y_t = y_{t-1}$. The inclusion of y_{t-p} in (4.1) explains the regenerative effect in plunge cutting process. δ_t, equal to $Y_s(t) - Y_s(t-p)$, is the depth-of-cut corresponding to the specified infeed. The coefficients of $A(z^{-1})$ and $B(z^{-1})$ are parameters associated with the characteristic properties of CP and MT. They are not known in general. $C(z^{-1})\xi_t$

characterizes the stochastic error source in machining, where ξ_t represents a white noise process with zero mean and variance σ_ξ^2. The deterministic error source is embedded in (4.1) by the common zeros of A, B, and C on the unit circle. In the following control algorithms the order of the model, n, and time delay, k, are assumed to be known. The delay, k, which accounts for the computation or measurement delay, is far smaller than the regenerative delay p in practice. The minimum value of k in digital control system is equal to one.

4.2 STC Algorithm

By solving the Diophantine equation

$$C(z^{-1}) = A(z^{-1})E(z^{-1}) + z^{-k}F(z^{-1}) \tag{4.3}$$

where

$$E(z^{-1}) = 1 + e_1 z^{-1} + \ldots + e_{k-1} z^{-k+1}$$

$$F(z^{-1}) = f_0 + f_1 z^{-1} + \ldots + f_{n-1} z^{-n+1}$$

Equation (4.1) can be written as

$$C(z^{-1})y_t = F(z^{-1})(y_{t-k} - y_{t-p-k} + \delta_{t-k}) +$$

$$G(z^{-1})(u_{t-k} - y_{t-p} + \delta_t) +$$

$$C(z^{-1})(y_{t-p} - \delta_t) + C(z^{-1})E(z^{-1})\xi_t \tag{4.4}$$

where

$$G(z^{-1}) = B(z^{-1})E(z^{-1})$$

Thus,

$$y_{t+k} = \frac{F}{C}(y_t - y_{t-p} + \delta_t) + \frac{G}{C}(u_t - y_{t-p+k} + \delta_{t+k}) +$$

$$(y_{t-p+k} - \delta_{t+k}) + E\xi_{t+k}$$

$$= y_{t+k|t} + E\xi_{t+k} \tag{4.5}$$

where the operator z^{-1} is omitted for simplifying the representation. $y_{t+k|t}$ is the conditional expectation of y_{t+k} based on the observations $y_t, y_{t-1}, \ldots, u_t, u_{t-1}, \ldots$, and the parameters of A, B, and C. Thus, for the minimum variance control criterion

$$\text{Min } E[y^2_{t+k}|t], \quad E[.]: \text{ an expectation function} \tag{4.6}$$

it gives the following control law

$$y_{t+k|t} = 0 \tag{4.7}$$

or

$$Cy_{t+k|t} = F(y_t - y_{t-p} + \delta_t) + G(u_t - y_{t-p+k} + \delta_{t+k}) +$$

$$C(y_{t-p+k} - \delta_{t+k}) = 0 \tag{4.8}$$

with variance

$$\text{Var}\,[y_t] = [1 + e_1^2 + \ldots + e_{k-1}^2]\sigma_\xi^2 \tag{4.9}$$

In self-tuning control, since all the parameters are unknown, (4.8) should be written as

$$\begin{aligned} &\hat{y}_{t+k|t} + \hat{c}_1\hat{y}_{t+k-1|t-1} + \ldots + \hat{c}_n\hat{y}_{t+k-n|t-n} \\ &= \hat{F}(y_t - y_{t-p} + \delta_t) + \hat{G}(u_t - y_{t-p+k} + \delta_{t+k}) + \\ &\quad \hat{C}(y_{t-p+k} - \delta_{t+k}) \\ &= 0 \end{aligned} \tag{4.10}$$

where all the estimated quantities are represented by placing the symbol, $\hat{}$, on the top of the notations. Therefore, based on the certainty equivalence principle, the control law corresponding to (4.7) is to find u_t such that

$$\begin{aligned} \hat{y}_{t+k|t} &= \hat{F}(y_t - y_{t-p} + \delta_t) + \hat{G}(u_t - y_{t-p+k} + \delta_{t+k}) \\ &\quad + \hat{C}(y_{t-p+k} - \delta_{t+k}) \\ &= 0 \end{aligned} \tag{4.11}$$

(4.11) is derived from (4.10) by dropping the terms, $\hat{y}_{t+k-i|t-i}$, $i=1, 2, \ldots, n$. Consequently, the model for estimating the parameters, $\hat{F}$, $\hat{G}$, and $\hat{C}$, is

$$y_t = \hat{F}(y_t - y_{t-p+k} - \delta_{t+k}) + \hat{G}(u_{t-k} - y_{t-p} + \delta_t)$$

$$\hat{C}(y_{t-p} - \delta_t) + \varepsilon_t \qquad (4.12)$$

where ε_t corresponds to $E\xi_t$. If the system is optimally controlled, the control output y_t should satisfy (4.11).

The STC algorithm, represented by (4.11) and (4.12), belongs to the implicit type. All the parameters in (4.12) can be updated by the recursive least squares (RLS) scheme as shown in Appendix 2. The recursive scheme can be further subjected to UD factorization for improving the accuracy of computation [27,14]. A forgetting factor is used for tracking the specified input and the time-varying parameters. Also, it is helpful to enhance the convergence rate of the output at the outset of control.

4.3 Stability, Convergence, and Robustness

In optimal control, it can be shown that the control law (4.7) gives a closed loop system satisfying

$$Cy_t = CE\xi_t$$

$$CBu_t = C(B - A)(y_{t-p+k} - \delta_{t+k}) - CF\xi_t \qquad (4.13)$$

The characteristics of the closed loop system, thus, depend on the polynomials, B and C. That is, for a stable minimum variance control, the zeros of $B(z^{-1})$ and $C(z^{-1})$ must be within the unit circle. The zeros of A, however, plays no important role in the

minimum variance control system. Therefore, even though the open loop system is unstable, this closed loop system may remain stable and optimally controlled. Conceivably, the self-tuning control system will inherit the properties of the optimal control system. This can be seen from the following stability and convergence analysis conducted by Goodwin and Sin [39,88].

The existence of C in (4.12) is due to the specified infeed and the regenerative effect. Hence, it is a servo control problem. By introducing the following substitutions

$$y^*(t) = Y_s(t)$$

$$y(t) = y_t + y^*(t)$$

$$u(t-k) = u_{t-k} + y^*(t)$$

$$A' = A + (B - A)z^{-p}$$

$$\omega(t) = \xi(t)$$

the model, (4.1), can be converted into

$$A'y(t) = Bu(t-k) + C\omega(t)$$

and the control law, (4.10), into

$$\phi(t)^T\hat{\theta}(t) = y^*(t+k)$$

where $\phi(t)$ and $\theta(t)$ are defined in [39]. The term $\omega(t)$ is assumed to be a white noise process, which satisfies the following conditions:

(i) $E[\omega(t)|t-1] = 0$

(ii) $E[\omega^2(t)|t-1] = \sigma^2$

(iii) $\lim_{N\to\infty} \text{Sup} \frac{1}{N} \sum_{t=1}^{N} \omega(t)^2 < \infty$

Also, the following assumptions are made about the system:

1. k is known.

2. The upper bound for model order is known.

3. $B(z^{-1})$ and $C(z^{-1})$ have all zeros inside the unit circle.

4. $\frac{1}{C(z)} - \frac{1}{2}$ is strictly passive.

By using a modified RLS [88], the self-tuning controller can be shown to ensure with probability one that

$$\lim_{N\to\infty} \text{Sup} \frac{1}{N} \sum_{t=1}^{N} y(t)^2 < \infty \tag{4.14}$$

$$\lim_{N\to\infty} \text{Sup} \frac{1}{N} \sum_{t=1}^{N} u(t)^2 < \infty \tag{4.15}$$

$$\lim_{N\to\infty} \text{Sup} \frac{1}{N} \sum_{t=1}^{N} E[(y(t) - y^*(t))^2|t-1] = \sigma^2 \sum_{i=0}^{k-1} e_i^2 \tag{4.16}$$

Properties (4.14) and (4.15) yield the stability of the closed loop system. The energy of both the system output and the control input are bounded. Condition (4.16) stands for the output convergence. That is, the desired output $y^*(t)$ is asymptotically and optimally tracked. The passivity or positive real assumption on $\frac{1}{C} - \frac{1}{2}$, a stronger assumption than C having asymptotically stable zero [58], is important to the output convergence.

From Appendix 1, A', B, and C may have common zeros on the unit circle because of the deterministic disturbance. When the sampling rate is sufficiently high B may have unstable zeros due to the excess number of poles [8]. As for the former case, the common zeros characterize the uncontrollable part of the system. In optimal control, Goodwin and Sin [39] showed that if C is split into

$$C = C_s + C_r$$

where C_s has only asymptotically stable zeros and C_r is the remainder which can be as small as desired by the choice of C_s, the use of C_s instead of C in the Diophantine equation (4.3) will result in a suboptimal but stable control. By the same token, in self-tuning control, if the zeros of $\hat{C}$ is kept within the unit circle by projection method [39], the closed loop system will be nearly optimal and stable.

For the later case, u_t in (4.13) will be unbounded when B has unstable zeros. If lowering the sampling rate is not permissible, the weighted minimum variance control as shown in Appendix 2 can be used to get a suboptimal but stable control.

The above analysis is based on the assumption that the model order n is sufficiently large to cover all the natural frequencies of the system. In practice, a lower order model, however, is desirable to simplify the algorithm and minimize the computation time. This prompts the robustness issue of self-tuning control. Again, the weighted minimum variance control can be used for ensuring the robustness of the low order controller [12]. Furthermore, by properly varying the weighting factor on-line, the control input can be assured to fall within the constraints.

4.4 Multiprobe Measurement in GAC

To separate the spindle error motion from the measurement of the surface profile, Whitehouse [111] devised the multiprobe method, which uses three probes of different sensitivities without requiring any masters. The probes are spaced around the workpiece as shown in Fig. 4.3. The centerlines of these probes intersect at a fixed point O. Due to the spindle error motion, the axis of rotation O′ moves around the fixed center randomly. The amplitude of this movement, e, is assumed to be far less than the nominal radius of the part, normally below 10^{-3}R [110].

The geometric error $y_i(t)$ and the sensor measurement $v_i(t)$ at each probe location are defined by

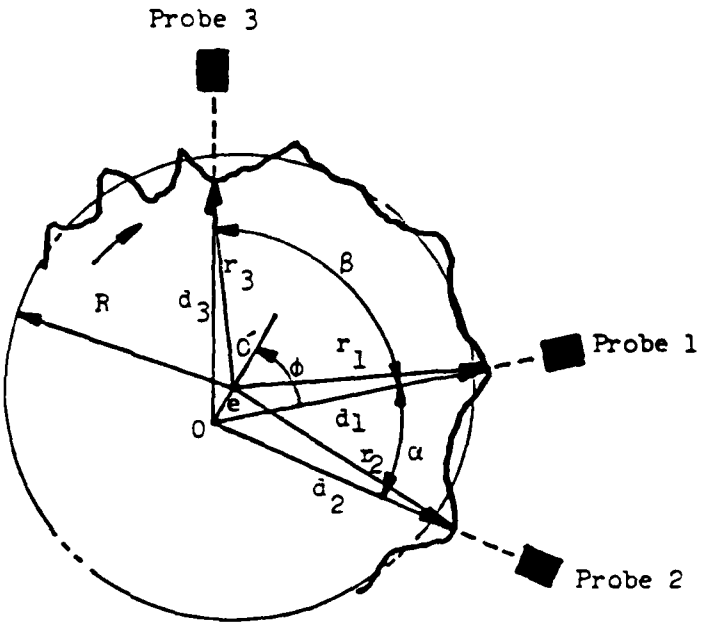

Figure 4.3 Multiprobe Measurement

$$y_i(t) = R - r_i(t)$$

$$v_i(t) = R - d_i(t), \quad i = 1, 2, 3. \tag{4.17}$$

where $r_i(t)$ and $d_i(t)$ are illustrated in Fig. 4.3. Hence,

$$v_i(t) = y_i(t) + (r_i(t) - d_i(t)), \quad i = 1, 2, 3. \tag{4.18}$$

It can be seen from Fig. 4.3 and (4.18) that the spindle error motion involves two unknown quantities: amplitude, e, and angle, ϕ. At least three probes are thus needed to remove the spindle error motion from the probe measurements; however, the geometrical error, $y_i(t)$, can never be obtained for the number of unknown quantities always exceeds that of known quantities in (4.18). Therefore, only three probes are sufficient for solving the separation problem. Additional probes can be regarded as redundant.

With the three probes as shown in Fig. 4.3, it can be proved that

$$d_t = cv_1(t) + av_2(t) + bv_3(t)$$

$$= cy_1(t) + ay_2(t) + by_3(t) \tag{4.19}$$

with

$$a = \sin\beta \,/\, \sin(\alpha + \beta)$$
$$b = \sin\alpha \,/\, \sin(\alpha + \beta) \tag{4.20}$$
$$c = -1$$

and

$$\alpha + \beta \neq \pi, 2\pi$$

$$\alpha , \beta > 0$$

where d_t is the combined measurement of probes 1, 2, and 3 with the scaling factors -1, a, and b, respectively. Thus, (4.19) shows that the spindle error motion has been separated from the measurement of the surface geometry. During the plunge cutting process, R in (4.17) should be replaced by R_i. Nevertheless, (4.19) and (4.20) hold in this situation. Instead of applying Fourier analysis to reconstruct the surface geometry as Whitehouse did, the combined signal d_t is used in the GAC system by the following manipulation.

According to the angular spacing of these probes and the direction of rotation, the geometrical errors $y_1(t)$, $y_2(t)$, and $y_3(t)$ can be expressed by sampled variables, y_{t-f}, y_{t-g}, and y_t respectively. Thus, (4.19) can be written as

$$d_t = by_t - y_{t-f} + ay_{t-g}, \quad t = 1, 2, 3, \ldots$$

$$f = p\beta/2\pi$$

$$g = p(\alpha + \beta)/2\pi$$

where p is the number of sampled points per revolution. Define

$$P_d(z^{-1}) = b - z^{-f} + az^{-g} \tag{4.21}$$

then

$$d_t = P_d(z^{-1})y_t \tag{4.22}$$

Before proceeding to the design of a GAC system, the characteristics of the polynomial, $P_d(z^{-1})$, should be analyzed.

4.4.1 Properties of Multiprobe Measurement

The characteristic roots of $P_d(z^{-1})$ can be found by solving

$$P_d(z^{-1}) = 0$$

or

$$z^g \sin \alpha - z^{g-f} \sin(\alpha + \beta) + \sin \beta = 0 \tag{4.23}$$

Let

$$z = re^{j2\pi m/p}, \quad j = \sqrt{-1}$$

where m is a real number and

$$0 \leq m < p$$

then (4.23) can written as

$$r^g[\cos m(\alpha + \beta) + j \sin m(\alpha + \beta)]$$

$$- r^{g-f}(\cos m\alpha + j \sin m\alpha)\sin(\alpha + \beta) + \sin \beta = 0$$

Thus,

$$r^g \cos m(\alpha + \beta) \sin \alpha - r^{g-f} \cos m\alpha \sin(\alpha + \beta) + \sin \beta = 0 \qquad (4.24)$$

$$r^g \sin m(\alpha + \beta) \sin \alpha - r^{g-f} \sin m\alpha \sin(\alpha + \beta) = 0 \qquad (4.25)$$

If $\sin m(\alpha + \beta) \neq 0$, from (4.25)

$$r^f = \frac{\sin m\alpha}{\sin \alpha} \frac{\sin (\alpha + \beta)}{\sin m(\alpha + \beta)} \qquad (4.26)$$

and, from (4.25) * cos $m\alpha$ - (4.24) * sin $m\alpha$,

$$r^g = \frac{\sin m\alpha}{\sin \alpha} \frac{\sin \beta}{\sin m\beta} \qquad (4.27)$$

If $\sin m(\alpha+\beta) = 0$, (4.25) gives

$$\sin m\alpha = 0$$

and

$$\sin m(\alpha+\beta) = \sin m\alpha \cos m\beta + \sin m\beta \cos m\alpha$$

$$= \sin m\beta \cos m\alpha$$

$$= 0$$

Hence,

$$\sin m\beta = 0$$

And, in this case, (4.24) gives

$$(\pm)r^{g}\sin\alpha - (\pm)r^{g-f}\sin(\alpha+\beta) + \sin\beta = 0 \qquad (4.28)$$

Therefore, if there exists a characteristic pair (r^*, m^*), it must either satisfy (4.26) and (4.27), or (4.28). The magnitude of r^* can be any positive finite value. One special characteristic pair is

$$r^* = 1,\ m^* = 1$$

for all admissible α and β. The solution means that if y_t is a sinusoidal function with frequency $\frac{1}{p}$

$$y_t = \sin 2\pi t/p$$

then

$$P_d(z^{-1})y_t = 0$$

In measurement, this means that the multiprobe method can not detect the eccentricity error of the part, that is, the sinusoidal form error with once-per-revolution frequency. This is the major constraint of multiprobe method [111]. If this error is caused by the unbalanced motion of a certain machine member, a balancing operation should be performed before machining. The higher harmonics, corresponding to $r^* = 1$ and $m^* = 2,3,4,\ldots$, may also be undetectable to the measurement setup if α and β are not properly chosen. To avoid this, the following analysis is needed.

Let

$$\alpha = 2\pi m_\alpha / p$$

$$\beta = 2\pi m_\beta / p$$

$$m_\alpha, m_\beta < p$$

From (4.26) and (4.27), the suppression of higher harmonics occurs when $m = m^*$ and

$$m^* m_\alpha / p = k_\alpha (1 \pm m_\alpha / p) = 1, 2, 3, \ldots$$

$$m^* m_\beta / p = k_\beta (1 \pm m_\beta / p) = 1, 2, 3, \ldots$$

or

$$m^* = m_0 \pm 1, \quad m_0 = \frac{k_\alpha p}{m_\alpha} = \frac{k_\beta p}{m_\beta} \tag{4.29}$$

From (4.29)

$$m_\alpha k_\beta = m_\beta k_\alpha = k[\mathrm{lcm}(m_\alpha, m_\beta)]$$

where "lcm" is lowest common multiplier. And

$$m_0 = \frac{kp[\mathrm{lcm}(m_\alpha, m_\beta)]}{m_\alpha m_\beta} = \frac{kp}{\gcd(m_\alpha, m_\beta)}$$

where "gcd" is greatest common divisor and k can be any integers which make m_0 an integer. Hence,

$$m^* = \frac{kp}{\gcd(m_\alpha, m_\beta)} \pm 1$$

or more precisely,

$$m^* = \mathrm{mod}\left[\frac{kp}{\gcd(m_\alpha, m_\beta)} \pm 1,\ p\right] \tag{4.30}$$

From (4.30), if m_α is relatively prime to m_β, or $\gcd(m_\alpha, m_\beta)$ is relatively prime to p, then

$$m^* = 1,\ p-1\ (\text{or } -1)$$

that is, no higher harmonics are suppressed. Sometimes, it is neither easy nor necessary to achieve this property. A probe configuration with sufficiently large m^* is acceptable. This is because of the fact that higher harmonics usually have very low amplitudes.

The other desired property of the multiprobe method, which will be important to the following controller design, is to select angles α and β such that the number of characteristic pairs having $r^* > 1$ is minimal or none.

It seems that we are not able to derive any explicit function in terms of α and β for r from (4.26), (4.27), and (4.28). However, the following rules can help us approach the desired property.

Rule 1: It can be shown that if α equals to β, the characteristic pair will be

$$[r^* = 1,\ (\frac{kp}{m_\alpha} \pm 1)], \quad k = 0, 1, 2, \ldots, m_\alpha - 1$$

Therefore, if m_α is relatively prime to p, there are no zeros of (4.23) outside the unit circle, and there is no suppression of higher harmonics of y_t.

Rule 2: From (4.23), if $|\sin\beta/\sin\alpha| < 1$, the chance to get all the zeros to lie within unit circle is high, but it is still not guaranteed.

After this preliminary selection process, all zeros of (4.23) can be checked by numerical solution. Reselections of α and β may be needed.

4.4.2 STC With Multiprobe Measurement

Multiplying (4.1) by p_d, the model of the GAC system becomes

$$A(d_t - d_{t-p} + \delta_t') = B(u'_{t-k} - d_{t-p} + \delta_t') + C(z^{-1})\xi_t' \quad (4.31)$$

where d_t is the measurement from the multiprobe method and

$$u'_{t-k} = P_d(z^{-1})u_{t-k} \quad (4.32)$$

$$\delta_t' = P_d(z^{-1})\delta_t$$

$$\xi_t' = P_d(z^{-1})\xi_t$$

For the minimum variance control criterion,

$$\text{Min } E[d^2_{t+k}|t]$$

the self-tuning control algorithm is similar to (4.11) and (4.12).

The model for parameter estimation is

$$d_t = \hat{F}(d_{t-k} - d_{t-p-k} + \delta'_{t-k}) +$$

$$\hat{G}(u_t' - d_{t-p+k} + \delta'_{t+k}) + \hat{C}(d_{t-p} - \delta_t') + \varepsilon_t' \qquad (4.33)$$

and the control law is

$$\hat{F}(d_t - d_{t-p} + \delta_t') + \hat{G}(u_t' - d_{t-p+k} + \delta'_{t+k})$$

$$+ \hat{C}(d_{t-p+k} - \delta'_{t+k}) = 0 \qquad (4.34)$$

Since P_d has at least one zero on the unit circle, and possibly has unstable zeros, the control input u_t can not be calculated directly by using (4.32). Any errors in u_t' and $u_0, u_{-1}, \ldots,$ will not be damped out by P_d^{-1}. The solution for this problem is to compute

$$\bar{u}_t = (u_t' + u_{t-f} - au_{t-g}) / b$$

and

$$u_t = \rho \bar{u}_t \qquad (4.35)$$

where ρ, called detuning factor, is a scalar and

$$0 < \rho < 1$$

The introduction of $\bar{u}_t$ and ρ is similar to that used in [26]

$$u_t = \frac{\bar{u}_t}{1 + Q/g_0}$$

where Q/g_0 is the weighting factor of u_t to stabilize the nonminimum phase system in the generalized variance control. The selection criterion of ρ is that the more unstable the zeros of P_d are, the smaller ρ is. Normally, a smaller detuning factor results in less optimal output.

The previously mentioned properties of stability, convergence, and robustness can be readily applied here. Conceivably, however, the performance would be slightly affected, since the objective function is d_t instead of y_t, and the detuning factor is less than one.

CHAPTER 5

SIMULATION OF THE GAC SYSTEM

Simulation is an important tool for evaluating the effectiveness of the self-tuning control algorithm. The stability and convergence properties described in the last chapter are based on certain idealized assumptions. They provide, at best, qualitative guidelines for assuring or improving the algorithms. Still, there are some questions in real applications that are very difficult to answer through theoretical analysis. Most of them are related to the robustness of the algorithms, such as: nonlinearities in the physical process and controller, insufficient number of order in the system model, finite precision in numerical computation, and so forth. Simulation can, however, easily and quantitatively show the best performance that the control algorithm can achieve under these practical considerations. And simulation can determine the appropriate numerical range for the ad hoc factors, such as: the forgetting factor in parameter estimation, the weighting factor in weighted minimum variance control, and detuning factor in GAC system with multiprobe measurement. Also, another important advantage of simulation is that it can provide experience in significantly lowering the possibility of failures or damage in setting up a real system.

There are two approaches for simulating a physical process: digital and analog. The analog approach is to simulate the process by using electric or electronic wirings. The analog one is convincing, while the digital approach, by using a digital computer, is superior as it is versatile enough to simulate various complex situations in the real system such as, time delays. Therefore, this chapter is devoted to the simulation on a general purpose digital computer, a CDC 6000 system. The simulation with analog wirings and microprocessor controller will be discussed in the next chapter.

A proper simulation model is not merely the one which contains as much complexity as the process may have, but it must also be one whose dynamic behavior is in coincidence with the practical observations. For machining processes it is well known that chatter or instability will occur whenever the machining system has insufficient stiffness and damping. This important phenomenon will be shown in the following simulation.

5.1 Simulation Model and Conditions

A finishing process of plunge grinding or cutting, as shown in Fig. 4.1 and Fig. 5.1, is simulated. The specified infeed, $Y_s(t)$, increases at a constant rate and then stays at a desired part dimension for two or more revolutions. In this text we assume that this feed motion is provided by a conventional hydraulic or electric drive. The control action, which is usually small and of high frequency, can be generated by a separate precision actuator embedded in the tool holder or in the spindle housing. The piezeoelectric

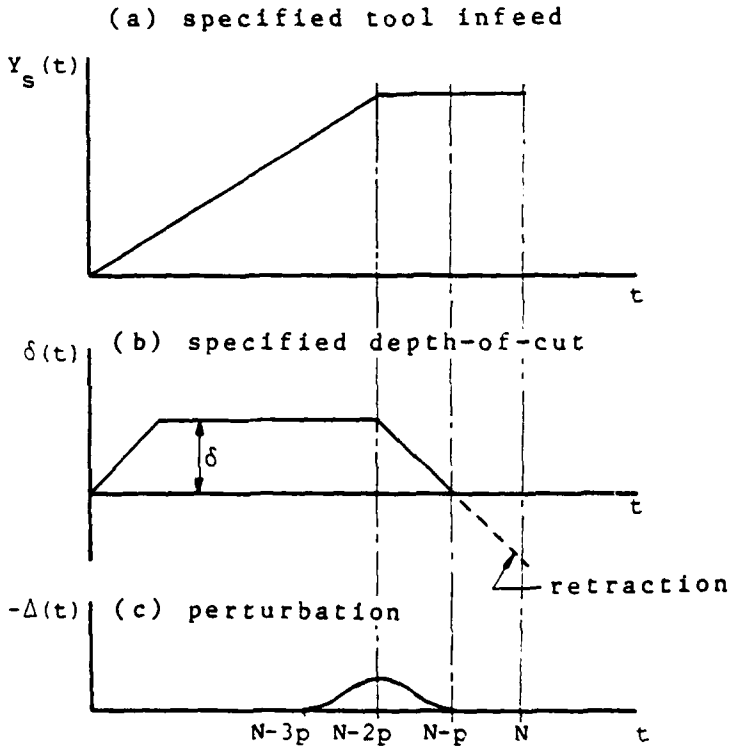

Figure 5.1 Plunge Cutting Process

translator [54,21,19] is an excellent device for implementing the precision actuator. The separation of the control motion and the feed motion is advantageous in releasing the complicate coordination between the basic NC functions and the feedback control. Also, the specially designed tool holder, with the kit consisting of a sensor and a microcontroller, can be easily reinstalled in any other similar machine tools. This will simplify the manufacturing of the machine tool and the maintenance of the precision actuator.

To simulate the machining dynamics on the digital computer, the discrete transfer function of the machine tool structure given in Appendix 1 is used. A nonlinear process, $Y_t = \max\{Y_t', Y_{t-p}\}$ as shown in Fig. 5.2, is added to account for the loss of contact which may occur in finish cutting. Nevertheless, the derived self-tuning control algorithm, based on the linear model, will be used for testing its robustness. Unless stated otherwise, the simulation uses the following data:

damping ratio of MT (S) = .05

natural frequency of MT (ω_n) = 9.55 Hz = 60 rad/sec

speed of work spindle (Ω) = 100 rpm

sampling period (T) = 10 msec

regenerative time delay (p) = 1/ (ΩT) = 60

total number of samplings (N) = 900 (i.e. 15 revolutions)

system time delay (k) = 1

feedrate = .24 unit/rev = .004 unit/sample

The dimensionless data of feedrate is chosen only for numerical convenience. Thus, appropriate sensitivities of the transducers and

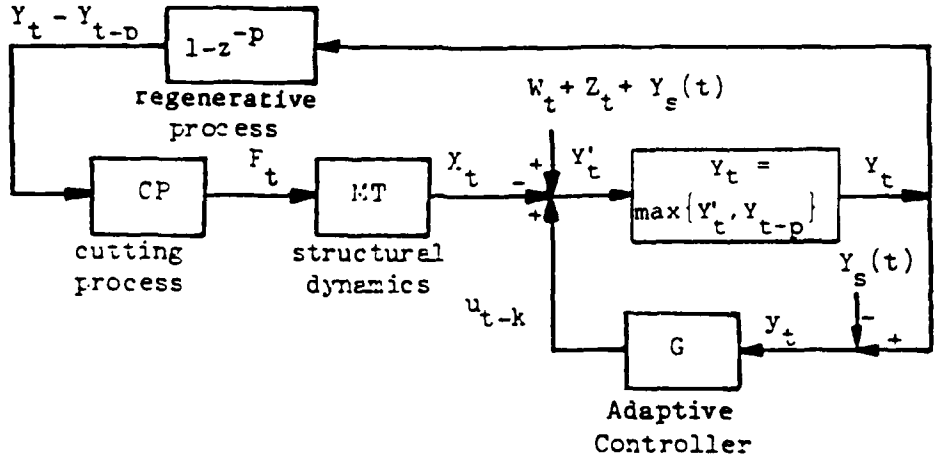

Figure 5.2 Simulation Model

the power amplifiers are assumed for the simulated geometrical errors and control inputs. The selection of natural frequency, ω_n, and sampling period, T, is done according to the rule of thumb, $\omega_n T$ in the range of 0.25-1, or 6-25 samples in each period of the resonant response of the closed loop system [113]. It can be easily shown that for different ω_n's the simulation results will be identical, if $\omega_n T$ remains the same. Therefore, the simulation results in this chapter can be applied to systems having higher natural frequencies. The system delay, k, can be greater than one if the positions of measurement and control are not at the same spot. The delay due to computation is assumed to be negligible.

Another important parameter not mentioned above is the stiffness ratio, (k_c/k_m), discussed in Chapter 2. The larger the ratio is, the more unstable the uncontrolled machining system is. Therefore, this ratio will be varied to test the control performance at different stability levels of the machining system.

The simulation is divided into two major parts. The first part is to test the performance of the control strategy by assuming that the geometrical error y_t can be measured directly. The second part is to include the reality of measurement problem and to test the feasibility of the GAC system with multiprobe measurement. Table 5.1 summarizes the simulation conditions for both parts.

In the simulation results, the geometrical error y_t is represented by three conventional terms: dimensional error, which is the mean value of y_t, out-of-roundness, which is the maximum peak to

Table 5.1 Simulation Conditions

simulation	n	k	STF	σ	AMPL	m(Ω)	γ	f1	f2	S	f	g	ρ	@
I-1	2	1	.1	0	.004	2	0	.995	.5	50	NA	NA	NA	#
I-2	"	"	"	"	"	"	"	"	0.	"	"	"	"	"
I-3	"	"	"	"	"	3*	.8	1.0	.5	"	"	"	"	"
I-4	"	"	"	"	.004 .002	8.5 1	0 0	.995	"	"	"	"	"	"
I-5	4	"	"	"	"	"	"	.99	"	"	"	"	"	"
I-6	2	3	"	"	.004	2	"	"	"	"	"	"	"	%
I-7	2	1	"	.002	"	"	"	.995	"	"	"	"	"	#
I-8	"	"	"	.004	.008	"	"	"	"	"	"	"	"	"
I-9	"	"	"	.008	.016	"	"	"	"	"	"	"	"	"
I-10	"	2	"	.002	.004	"	"	"	"	10	"	"	"	%
I-11	"	3	"	"	"	"	"	"	"	50	"	"	"	%
I-12	"	1	.2	"	"	"	"	"	"	"	"	"	"	#
I-13	"	"	6.	"	"	"	"	"	"	"	"	"	"	"
I-14**	"	"	2.	"	"	"	"	"	"	10	"	"	"	"
II-1	"	"	.1	0	"	"	"	"	"	50	5	20	1.0	-
II-2	"	"	"	"	"	"	"	"	"	"	"	"	.95	"
II-3	"	"	"	"	"	1	"	"	"	"	"	"	"	"
II-4	"	"	"	"	"	11	"	1.0	"	"	"	"	.85	"
II-5	"	"	"	"	"	"	"	"	"	"	"	27	"	"
II-6	"	"	"	.002	"	2	"	"	"	"	"	20	.88	"
II-7	"	"	.2	"	"	"	"	"	"	"	"	"	"	"
II-8	"	"	2.	"	"	"	"	"	"	10	"	"	"	"

STF: stiffness ratio, AMPL: amplitude of periodic disturbance
S: init. value of cov. matrix for param. estimation
@: $\delta(t)$, #:with retract, %: with pert. input, -: dwell
*: disturb. from clamping, **: use general STC algorithm

peak error of y_t, and roughness, which is the root mean square of y_t. Since roughness refers to the high frequency error, its value will not be counted and shown in deterministic systems. Notice that the definitions of these terms are a little different from those used in practice. However, they are convenient for evaluating the performance of the simulated GAC system. These data are shown with polar plots for comparison. Time responses are plotted to check the performance of both controlled and uncontrolled systems. Negative value of the responses means that the tool is away from the workpiece with respect to the specified tool path. The plots of the estimated parameters are used for examining the behavior of the STC algorithms.

5.2 Simulation With Ideal Measurement

In the first part of the simulation, we begin to test a stable machining system without stochastic disturbance in order to see how well the deterministic disturbance can be compensated for by the self-tuning controller. Then, some stochastic disturbance is added to the system for examining the noise rejection capability of the controller. The increase in stability of the self-tuning controller can be visualized by increasing the stiffness ratio. The importance of incorporating the physical insight into the mathematical model in Chapter 4 can be seen by comparing the control performance with that of the controller which uses the general self-tuning algorithm as described in Chapter 3.

5.2.1 Deterministic Systems

Fig. 5.3 depicts a simulation run with the periodic disturbance having frequency 2Ω and amplitude 0.004. Stochastic disturbance is not added in simulation. It is a stable machining system with stiffness ratio, $k_c/k_m=1$. The polar plots show that dimensional error and out-of-roundness are almost eliminated in the GAC system. Moreover, Fig. 5.3 shows that the GAC system makes perfect tracking of the desired tool path through the control input which is nearly equal but opposite to the uncontrolled response. Because of this, the time-consuming dwell cutting or spark-out process is not needed for acquiring satisfactory accuracy. Hence, we can have the tool retract from the workpiece smoothly, at the last revolution of cut, by letting δ_t in equations (4.11) and (4.12) linearly decrease as shown in Fig. 5.1b. The simulated control input also demonstrates this kind of arrangement.

The estimated parameters in Fig. 5.3 quickly converge to steady state values, although the adopted model order, n, is two instead of four, the full order of the simulated system. By substituting those steady state estimates into (4.12), the behavior of the controller can be explained. Since the controlled y_t is very near to zero in the middle of cutting, the estimated model can be written as

$$(1.37062 - .53975z^{-1})\delta_{t-1} + (.86733 - 1.69675z^{-1} + .86733z^{-2})(u_{t-1} + \delta_t) - (1 - .5364z^{-1} + .40897z^{-2})\delta_t = 0$$

In addition, at that time, δ_t is a constant

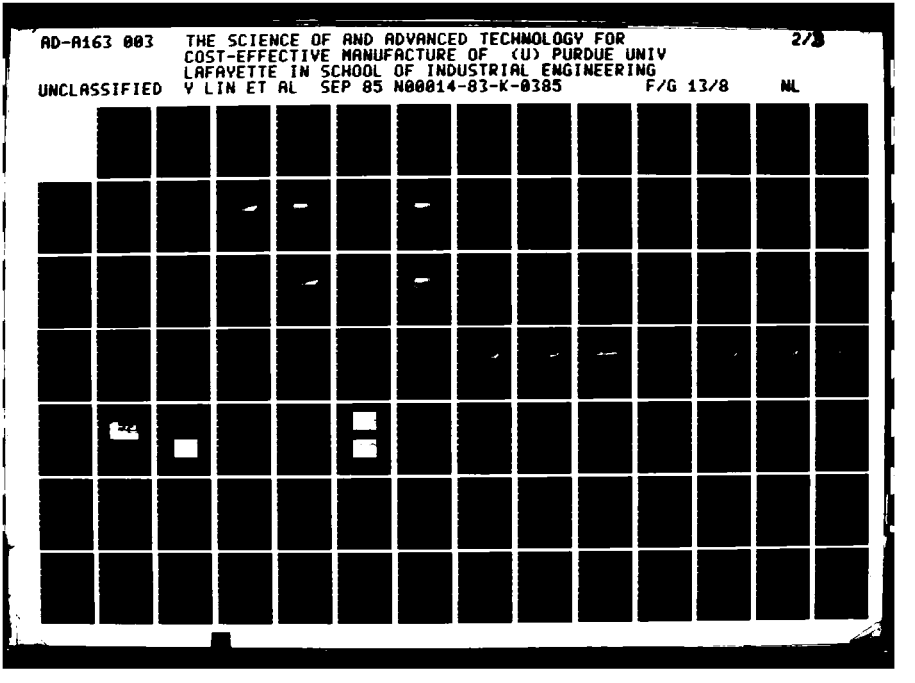
AD-A163 003 THE SCIENCE OF AND ADVANCED TECHNOLOGY FOR 2/3
COST-EFFECTIVE MANUFACTURE OF (U) PURDUE UNIV
LAFAYETTE IN SCHOOL OF INDUSTRIAL ENGINEERING
UNCLASSIFIED Y LIN ET AL SEP 85 N00014-83-K-0385 F/G 13/8 NL

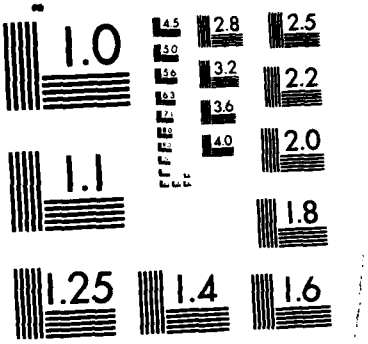

MICROCOPY RESOLUTION TEST CHART
NATIONAL BUREAU OF STANDARDS-1963-A

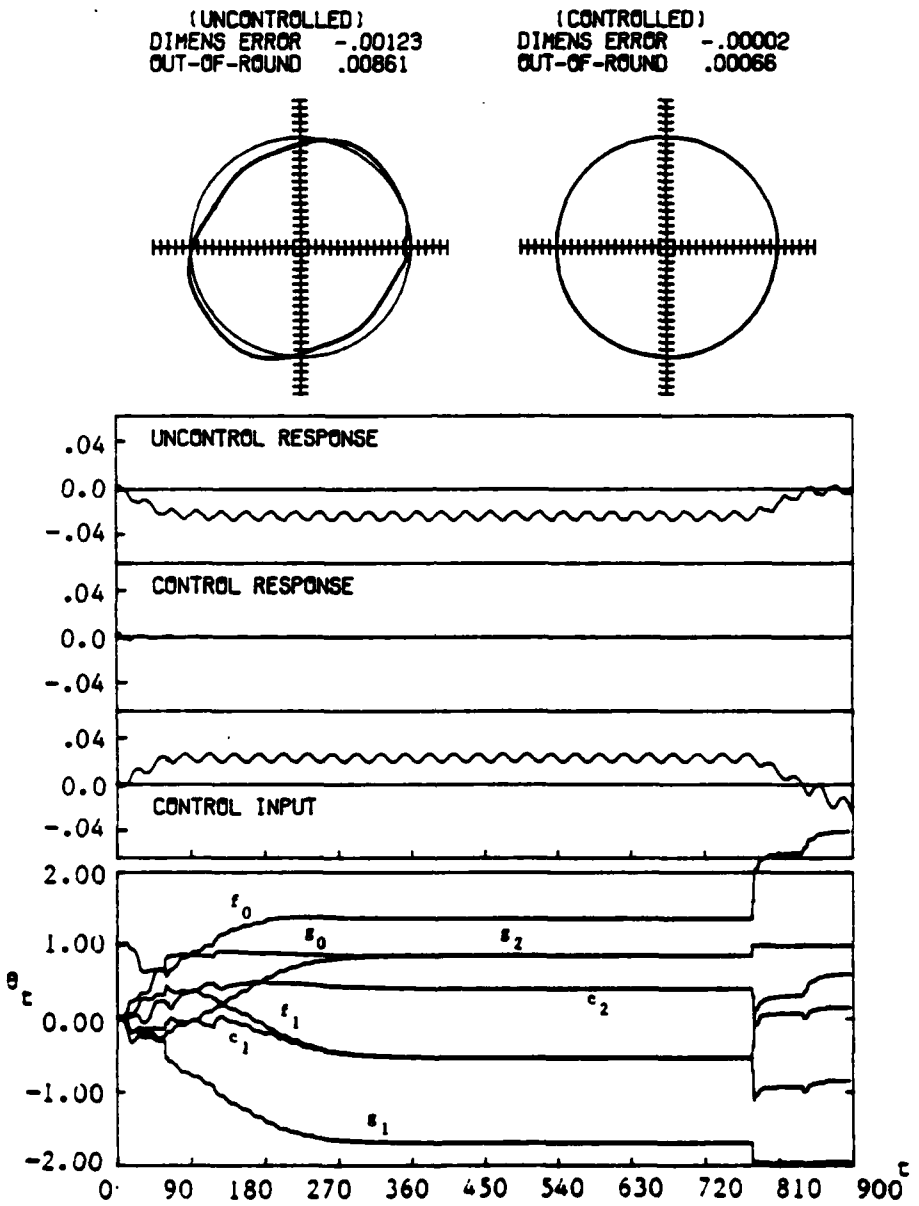

Figure 5.3 GAC System With Periodic Disturbance Only (Simulation I-1)

$$\delta_t = \delta = .24$$

Thus

$$(1 - 1.9562912z^{-1} + z^{-2})u_{t-1} = .00437\delta \qquad (5.1)$$

The polynomial on the left hand side of the above equation can be expressed as

$$1 - 2(\cos 2\pi\omega T)z^{-1} + z^{-2}$$

which represents a sinusoidal wave of frequency ω. Solving for ω gives

$$\omega = 200 \text{ rpm} = 2\Omega$$

which is the frequency of the periodic disturbance in the simulation. This explains the usage of a sinusoidal control input in Fig. 5.3 for countering the periodic disturbance. In addition, let

$$u_t = u_p + u_s \qquad (5.2)$$

where u_p is the sinusoidal component and u_s is the static component. Substituting (5.2) into (5.1) gives

$$u_s = (.1)\delta = (k_c / k_m)\delta$$

The above solution explains why the self-tuning controller can automatically compensate for the static deflection during the cutting operation.

Because of the discrepancy of the model order and the nonpersistent excitation of the output, the converged parameters are merely a set of estimates which satisfy the minimum variance criterion as shown above. When the specified depth-of-cut begins to change at the end of the cut, it can be seen in Fig. 5.3 that these estimates also change to a new set of values, accordingly, to maintain the optimality.

A time varying forgetting factor is used in the above simulation to improve the convergence rate of the estimates and the output; it is of the form shown below:

$$\lambda = f_1 - f_2 / t$$

where t is the sampling time instant at t = 1, 2, 3, ... , and

$$f_1 = .995, \quad f_2 = .5$$

This forgetting factor is low at the start-up of tuning so that the inaccuracy of the initial guesses can be forgotten as fast as possible. The forgetting factor then increases to f_1 asymptotically. f_1 is slightly smaller than one to permit the self-tuning controller to adjust itself for the environmental changes or modeling errors. Fig. 5.4 shows a similar simulation run with constant forgetting factor

$$\lambda = .995$$

It shows that the controlled response and the estimated parameters

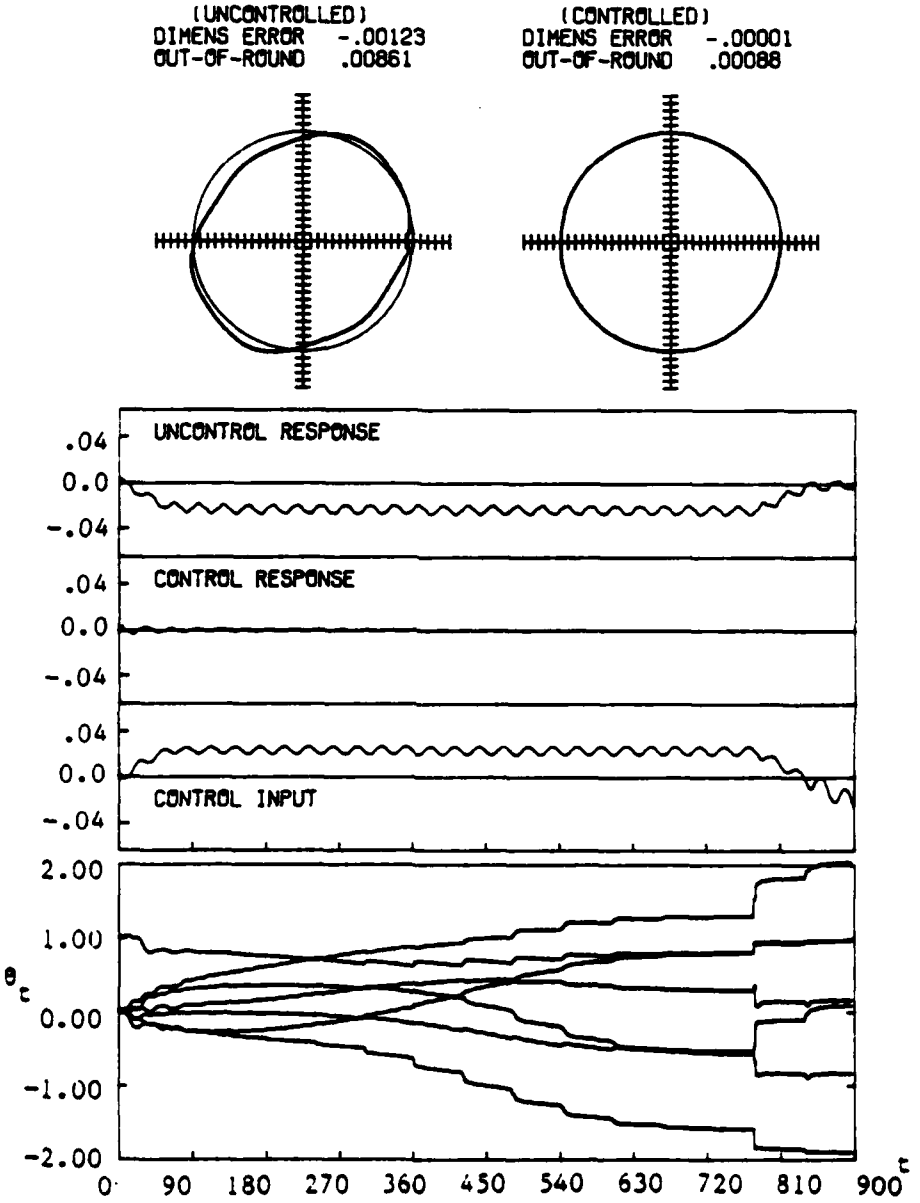

Figure 5.4 The Effect of Forgetting Factor on the Convergence of GAC System (Simulation I-2)

converge far slower than they do in the simulation run shown in Fig. 5.3. A rule of thumb, gained from simulation experience, for selecting f_1 and f_2 is

$$.99 < f_1 < 1.0$$

$$.1 < f_2 < 1.0$$

Faster convergence rate means that the GAC system can take larger depth-of-cut, shorten the production time, and still have good accuracy.

As it was mentioned, the periodic disturbance may result from the stiffness variation of the clamped workpiece. A work-chuck assembly with three clamping jaws is simulated by using a time varying stiffness ratio

$$(k_c / k_m)(1 + \varepsilon \sin(3\Omega t + \gamma))$$

$$\varepsilon = .2, \quad \gamma = .8$$

Fig. 5.5 shows that the self-tuning controller can compensate for this kind of error source as nicely as it does for the former periodic disturbance. When the phase angle γ is varied to any other value, the simulation results remain very similar. This is an advantage of using STC because, in practice, different diameters of the workpiece have different phase shifts of the jaws [81].

The polar plot of the uncontrolled geometrical error has six lobes instead of three in Fig. 5.5. This is due to the loss of

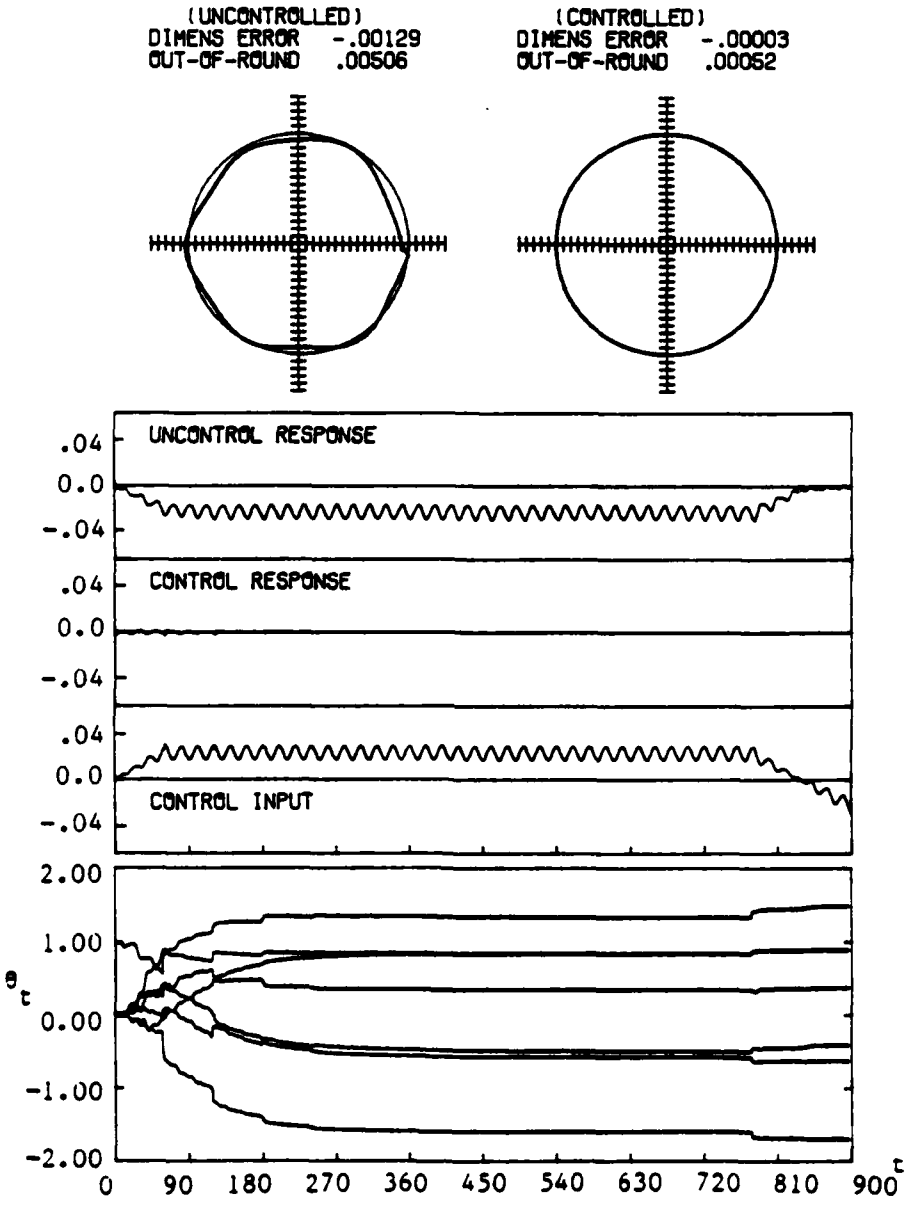

Figure 5.5 GAC System With Periodic Disturbance From Stiffness Variation of Chucked Workpiece (Simulation I-3)

contact which occurs in the last two revolutions. Same nonlinear effect can also be seen in Fig. 5.3, which has four lobes rather than two.

To see if the self-tuning controller can compensate for two or more periodic disturbances, two sinusoidal functions

$$.004 \sin(\Omega t + \gamma) + .002 \sin(8.5\Omega t)$$

are simulated as shown in Fig. 5.6. It shows that the geometrical error is reduced somewhat but not satisfactorily enough, if the same self-tuning model and model order are used. The time varying estimates, together with the coarse control accuracy, indicate that the assumed model order is insufficient. As we have shown that the cancellation of the periodic disturbance is due to the estimated control model having the same dynamics as that of the disturbance function, therefore, the model order must increase to four when there are two sinusoidal disturbances. Under the same simulation conditions except that

$$n = 4$$

and

$$\lambda = .99 - .5 / t$$

Fig. 5.7 shows that the geometrical error significantly reduces and the parameter estimation converges fast again. Besides these, the simulation shows that the frequency of the periodic disturbance need not be integer multiples of the angular speed of the spindle.

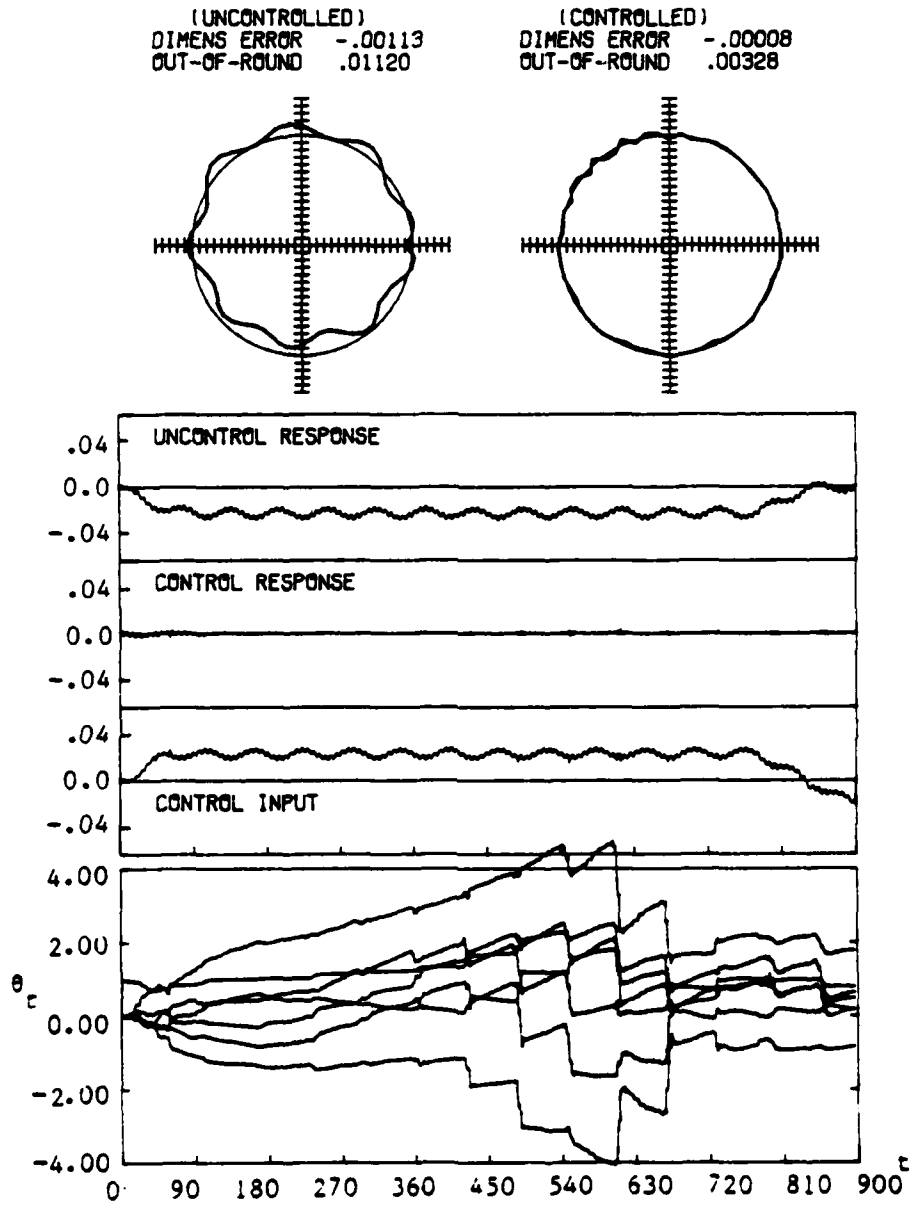

Figure 5.6 GAC System With Insufficient Model Order for Two Periodic Disturbances (Simulation I-4)

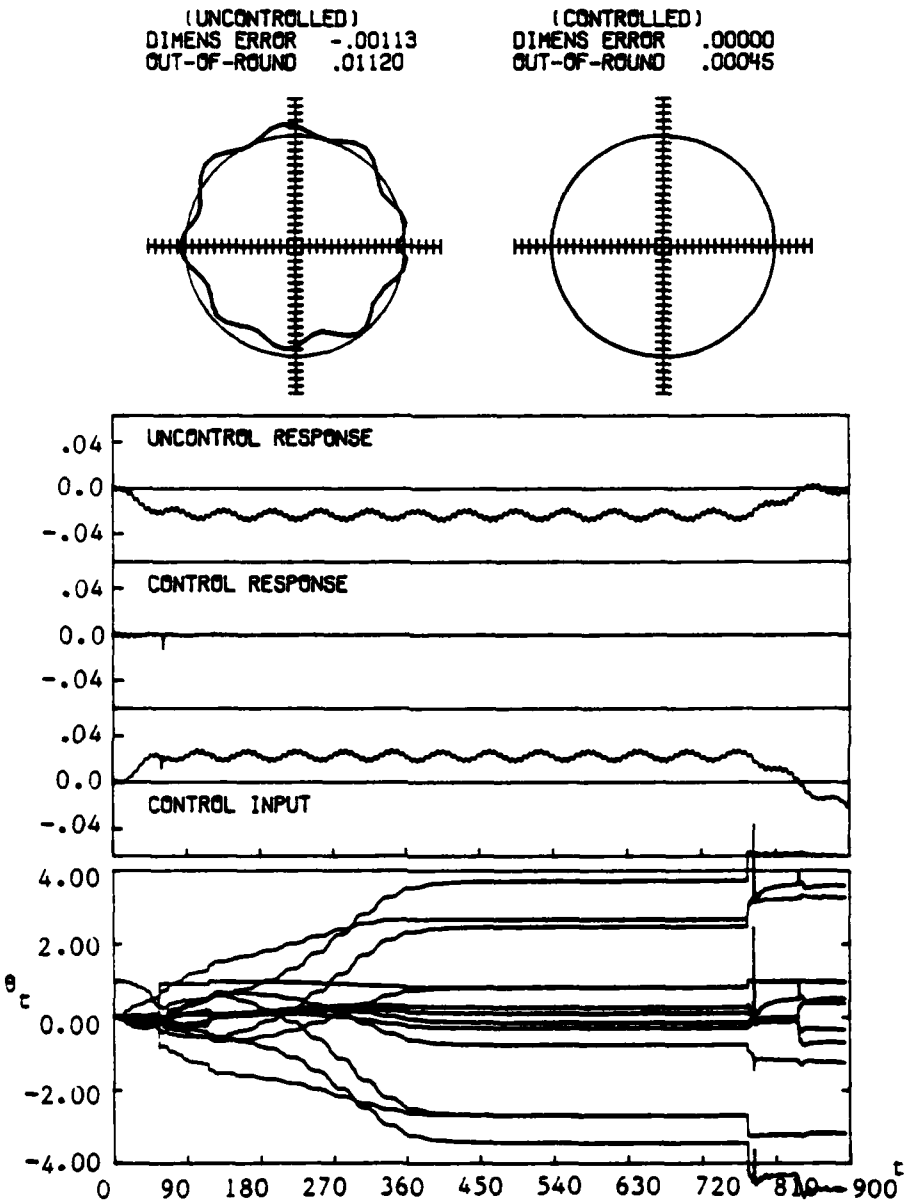

Figure 5.7 GAC System With Sufficient Model Order for Two Periodic Disturbances (Simulation I-5)

It is sometimes convenient and desirable to offset the sensing area from the tool tip during the machining operation. The system time delay will be greater than one in this circumstance. When k = 3, simulation shows that the self-tuner we used is not fast enough to minimize the transient response due to the abrupt change of slope of the depth-of-cut in the last but one revolution, and is unstable in the last revolution where loss-of-contact occurs most often. A rational solution is to alleviate the change of slope by introducing a perturbation input as shown in Fig. 5.1c, where

$$\Delta(t) = -\frac{\delta}{2p}\left[1. + \cos \pi\frac{t-(N-2p)}{p}\right], \quad \text{if } N-3p \leq t \leq N-p$$

$$= 0, \text{ otherwise} \tag{5.3}$$

The perturbation provides excitation for activating the tuning of the controller parameters to cope up with the input changes. Fig. 5.8 shows that before applying perturbation $\Delta(t)$ the controlled response is still perfectly regulated despite the large time delay. The perturbation, then, starts at the time instant N-3p. The transient response is significantly reduced and satisfactory out-of-roundness, 0.00125, is thus obtained. Since the perturbation tends to slow down the infeed, the tool should stay at the final position rather than retract at the last revolution.

The simulation of the above deterministic systems clearly illustrates how the self-tuner behaves to achieve the optimal performance. Next we shall find how the same controller reacts in the presence of stochastic disturbances.

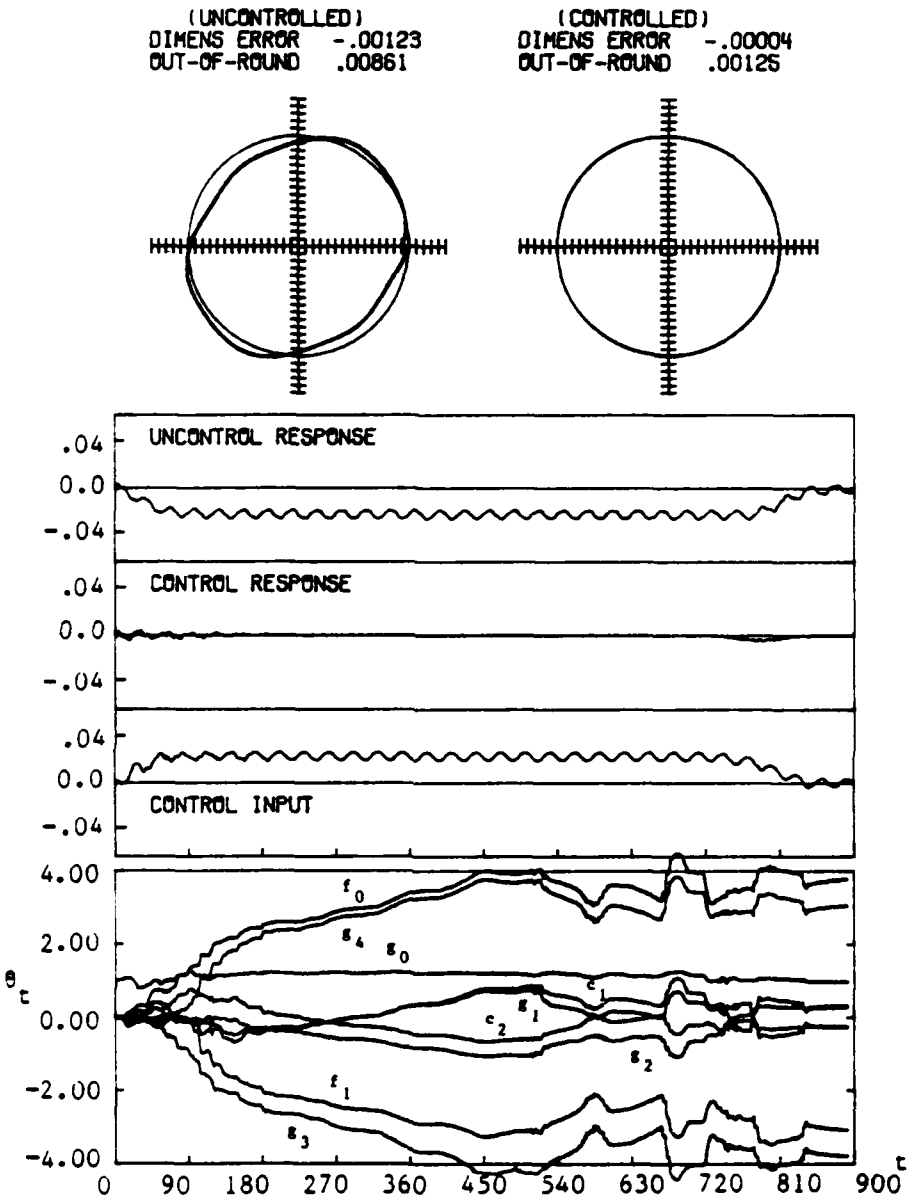

Figure 5.8 Perturbation Input for GAC System With Large Time Delay (Simulation I-6)

5.2.2 Stochastic Systems

By adding the following stochastic disturbance

$$W_t = e_t + 2.0e_{t-1} + 1.31e_{t-2} + .28e_{t-3}$$

e_t: Gaussian white noise with zero mean and rms .002

to the same machining system, Fig. 5.9 shows that, compared to the uncontrolled result, the controlled dimensional error is minimized significantly and the out-of-roundness and finish are also reduced by half. The controlled finish, actually, is very close to the rms of e_t, the minimum that an optimal controller can achieve. The periodic disturbance is smeared by the stochastic disturbance as can be seen in the plots of the time response. The estimated parameters, therefore, do not reflect the dynamics of the sinusoidal disturbance any more. Instead, they constitute a suboptimal controller to minimize the variance and the bias of the output. Increase of the model order to four, full order of the simulated system, will slightly improve the geometrical accuracy. Nevertheless the true parameters of the system can still not be identified. This is the general characteristic of the implicit type of self-tuning control when the desired response is not spectrally rich enough. Besides, the insignificant improvement in accuracy by the full order means that the implicit type of controller is rather robust for a mode of lower order. For higher level of disturbance, Table 5.2 shows that the self-tuner maintains near optimal accuracy.

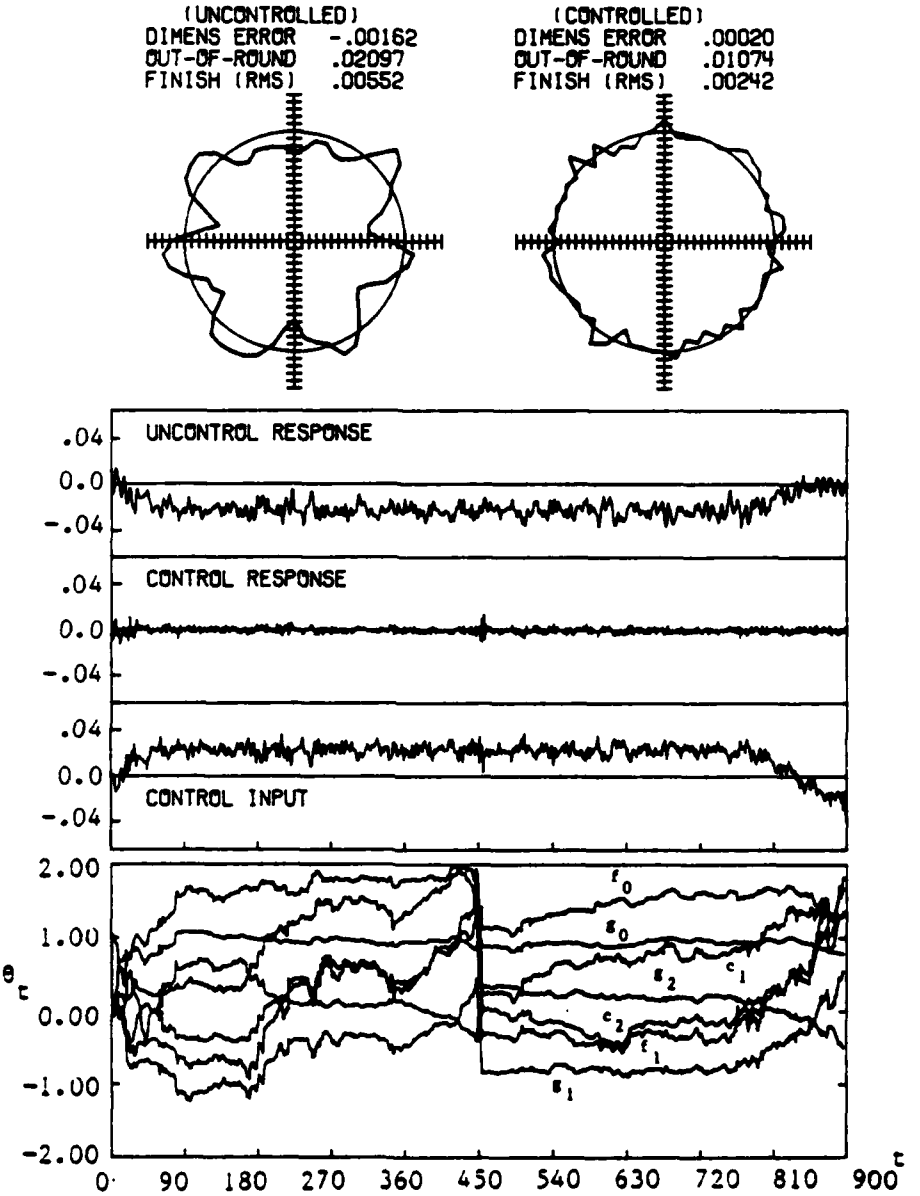

Figure 5.9 GAC System With Both Periodic and Stochastic Disturbances (Simulation I-7)

Table 5.2 Simulation Results of Different Disturbance Levels and System Delays

simulation condition	DIMENS ERROR	OUT-OF-ROUND	FINISH [RMS]
I-7	0.00020 (-.00162)	0.01074 (0.02097)	0.00242 (0.00552)
I-8*	0.00070 (-.00048)	0.02217 (0.04205)	0.00469 (0.00955)
I-9*	0.00226 (0.00360)	0.04411 (0.07682)	0.00879 (0.01801)
I-10**	0.00161 (-.00162)	0.02009 (0.02097)	0.00444 (0.00552)
I-11**	0.00122 (-.00162)	0.01877 (0.02097)	0.00469 (0.00552)

(data) - result of uncontrolled system
* - high level of disturbance (see Table 5.1)
** - large time delay (see Table 5.1)

When the system delay k is greater than one, as we have learned, perturbation in the last few revolutions of machining is necessary to alleviate the input changes and make the controller stable. This is particularly true in a stochastic system. Only with the perturbation, (5.3), we can obtain the geometrical accuracies as shown in Table 5.2 for k=2 and 3. The results, though quite poor compared with those for k=1, are still near optimal, because the theoretical rms for k=2 is 0.00448, which coincides with the simulated results. The change of the output variance due to the increase in time delay may not be so large as was obtained through simulation. It depends on the actual dynamics of the stochastic disturbance and the system in real operation. A good practice is to reduce the system delay for measurement as much as possible.

The important phenomenon of the machining process, chatter, can be simulated by increasing the stiffness ratio. It is found by simulation that the uncontrolled system begins to be unstable as the stiffness ratio increases to .15, which is close to the theoretical value 0.105. Fig. 5.10 shows that, when the ratio is 0.20, the uncontrolled system becomes more unstable and produces regenerative chatter. And, as the theory in Chapter 3 predicted, the chatter frequency is 10.8 Hz which is slightly larger than the natural frequency, 9.55 Hz. The controlled system, however, remains stable with accuracy as satisfactory as that shown in Fig. 5.9. The stiffness ratio can even be raised to 6.0, as shown in Fig. 5.11, and the controlled system maintains good geometrical accuracy. Therefore, the increase in stability is at least by a factor of 40

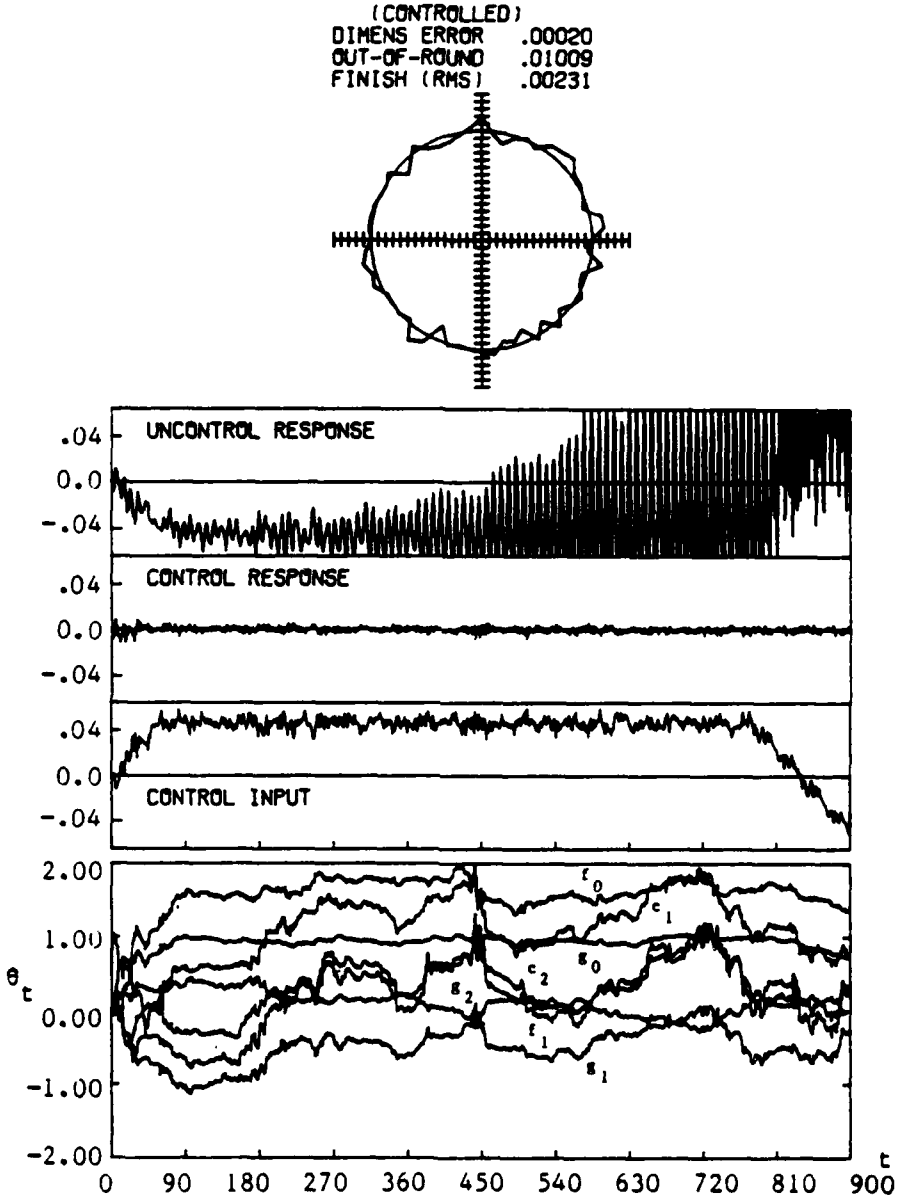

Figure 5.10 GAC System for Unstable Machining Process (Simulation I-12)

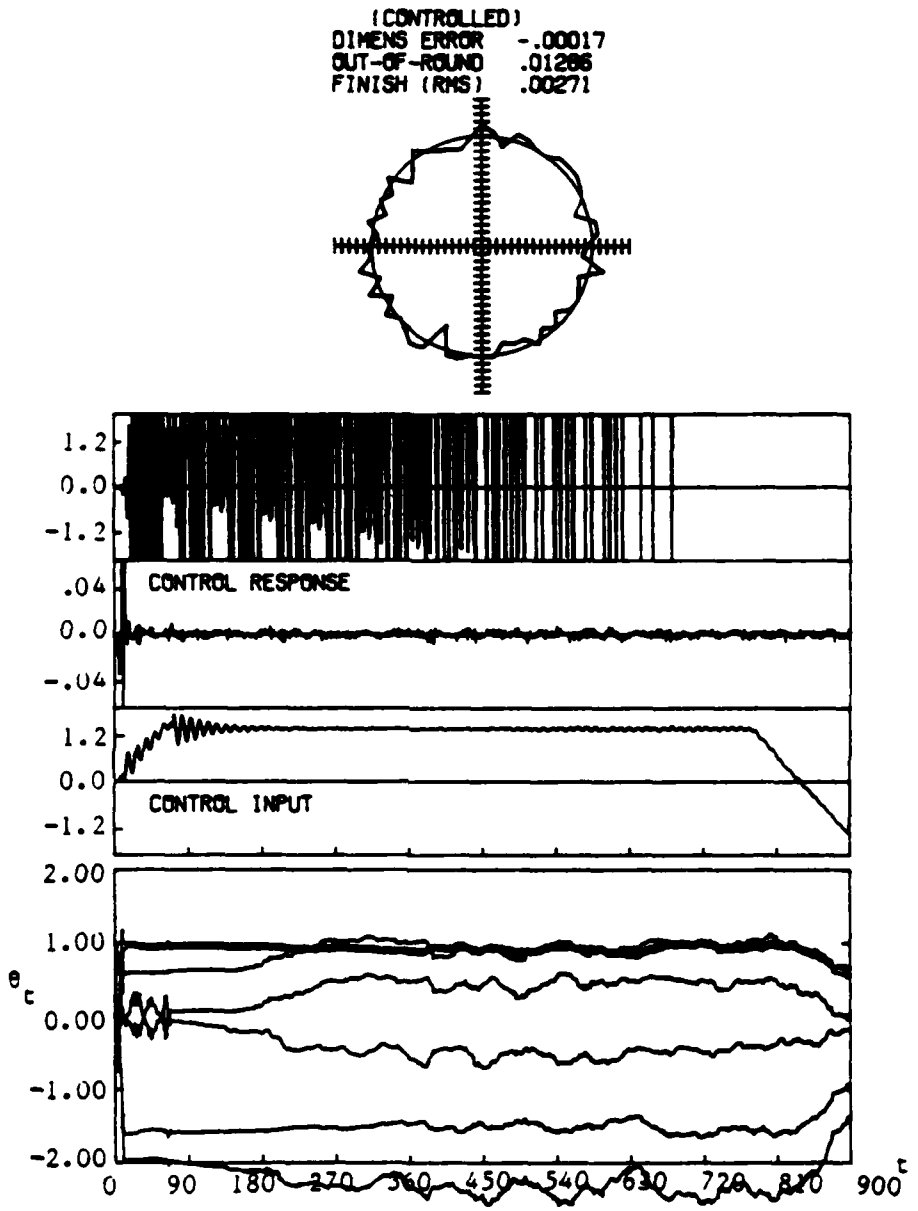

Figure 5.11 GAC System for More Unstable Machining Process (Simulation I-13)

(=6.0/0.15) in the simulation. It is comparable with the results of Comstock et al. [29] and of Nactigal and Maddux [76]. According to the analysis in Chapter 4, since the simulated system has a stable polynomial $B(z^{-1})$ in (4.1), the controlled system is stable no matter how large the stiffness ratio is. This is similar to what is claimed by Mitchell [66] that a factor of 1000 increase in stability is attainable. Experimentally, however, the stiffness ratio is found to be of the order of 0.5 to .02 and damping ratio to be about 0.25 to 0.01 [104]. Therefore, it is more appropriate to say that an accurate and chatter-free machining can be obtained by means of the self-tuning controller.

To see the necessity of incorporating the physical insight into the self-tuning model, the general model in Chapter 3 is tested and compared. A constant but unknown term is added in the model to account for the static deflection resulting from the cutting load. With the same order of model and other simulation conditions as those of Fig. 5.10, the general self-tuner also results in a stable system as shown in Fig. 5.12. The controlled accuracies, however, are much worse than those of Fig. 5.11, which uses the proposed model and operates in a more adverse condition, k_c/k_m=6.0. It is found that, as the stiffness goes higher, the controlled inaccuracies of the general self-tuner become unreasonably large and the system can be considered as being unstable. Hence, careful modeling of the process to be controlled is very important to enhance the effectiveness of self-tuning control.

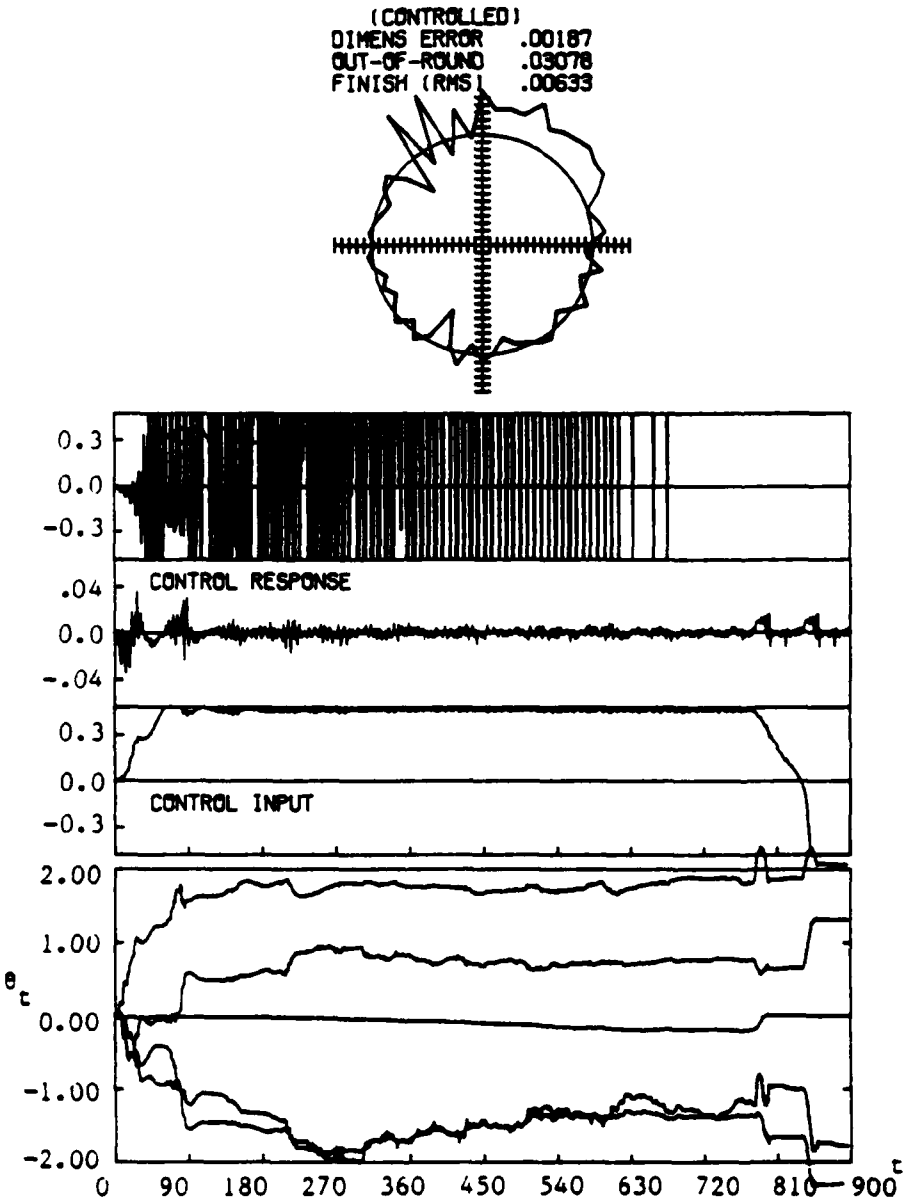

Figure 5.12 GAC Using General STC for Unstable System (Simulation I-14)

5.3 Simulation With Multiprobe Measurement

The second part of the simulation is to test the GAC system with multiprobe measurement. The interesting properties of the multiprobe measurement, as we have analyzed in Chapter 4, can be verified by simulation with deterministic disturbance only. Selecting proper value of the detuning factor is very important to achieve geometrical accuracies as good as those of the former simulation. With the stochastic disturbance added in, the performance of noise rejection and increase in stability can be evaluated.

5.3.1 Configuration of Probes for Simulation

The configuration of the multiprobe measurement, as shown in Fig. 4.3, is as follows:

$$\alpha = 90^{\circ}, \quad \beta = 30^{\circ}$$

and thus, (4.21) gives

$$P_d(z^{-1}) = \frac{2}{\sqrt{3}} - z^{-5} + \frac{1}{\sqrt{3}} z^{-20} \tag{5.4}$$

which has the following characteristic roots:

$0.933\, e^{j\theta}$, $\theta = \pm 25.55^{\circ}, \pm 46.45^{\circ}, \pm 97.55^{\circ},$

$\pm 118.45^{\circ}$, or $\pm 169.55^{\circ}$

$1.000\, e^{j\theta}$, $\theta = \pm 6^{\circ}, \pm 66^{\circ}, \pm 78^{\circ}, \pm 138^{\circ}$, or $\pm 150^{\circ}$

This arrangement is favorable for the self-tuning control because all the zeros of $P_d(z^{-1})$ lie inside or on the unit circle. However, from (4.30), it suppresses harmonics with frequencies $m^*\Omega$, where m^* equals to

$$m^* = \text{mod}[\frac{kp}{\gcd(m_\alpha, m_\beta)} \pm 1,\ p], \quad m_\alpha = 15,\ m_\beta = 5,\ p = 60$$

$$= \text{mod}[12k \pm 1,\ 60], \quad k = 0, 1, 2, \ldots$$

$$= 1, 11, 13, \ldots$$

We shall find what the controlled geometrical errors would be, if the periodic disturbance happens to be suppressed by the multiprobe measurement. Solutions will be made to overcome the control deficiency in this type of situation.

5.3.2 Test of Detuning Factor

As stated in Chapter 4, $p_d(z^{-1})$ has at least one zero on the unit circle; therefore, a detuning factor, $0 < \rho < 1$, is needed in (4.35) for computing the control input. Without using the detuning factor, i.e., $\rho=1$, Fig. 5.13 shows unsatisfactory control results under the same conditions of simulation as shown in Fig. 5.3. We see that the uncontrolled response is replaced by the controlled response which has compound sinusoidal wave behavior during cutting. This compound wave, through spectral analysis, consists of harmonics with frequencies Ω, 11Ω, and 13Ω, which are the components invisible to the multiprobe measurement. When the detuning factor is added in,

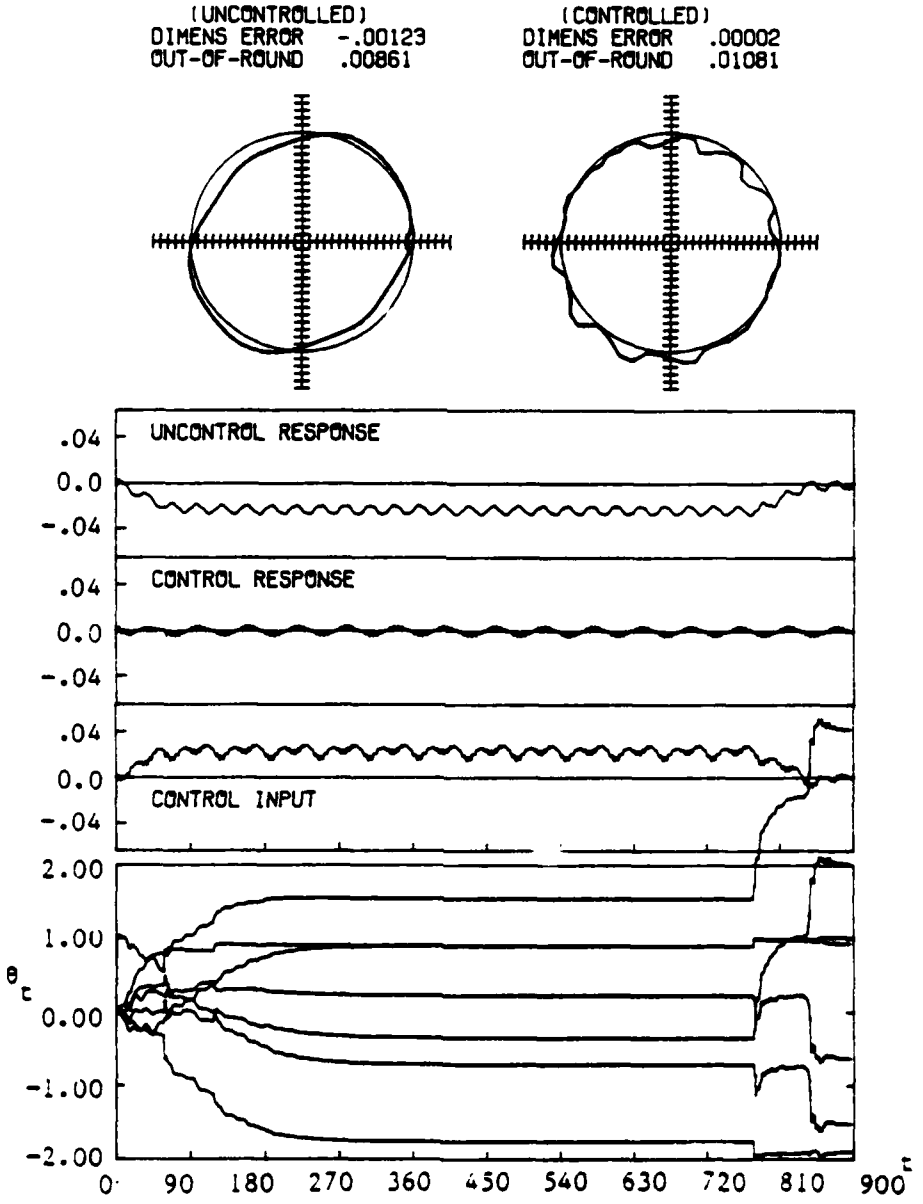

Figure 5.13 GAC System With Multiprobe Measurement and Periodic Disturbance (Simulation II-1)

ρ=.95, Fig. 5.14 shows that this compound wave dies out asymptotically, and satisfactory geometrical accuracy is obtained thereafter. The controlled response also shows that, due to the detuning factor, the controller acts less optimally. The specified infeed is not tracked as perfectly as that in Fig. 5.3 during the operation. Therefore, instead of retracting the tool, the tool is commanded to stay at the specified position in the last revolution of cutting. This gives the self-tuner more opportunities to reduce excess geometrical errors.

5.3.3 Test of Invisible Harmonics

For the case of suppression of harmonics in multiprobe measurement, Fig. 5.15 shows that the geometrical errors resulting from periodic disturbance with frequency Ω can not be removed from the GAC system. This result is quite understandable because the multiprobe measurement is unable to detect any errors having this frequency. The simulation, however, shows that the higher harmonics in the uncontrolled polar plot, which result from the nonlinearity of the system, can be compensated for by the controller. The geometry of the controlled machined part is a near perfect but eccentric circle. The indicated out-of-roundness actually represents twice the eccentricity of the machined part. For products whose roundness is much more critical than the eccentricity, the GAC system with multiprobe measurement is still very effective. Otherwise, the best way is to balance this periodic disturbance before the cutting operation takes place.

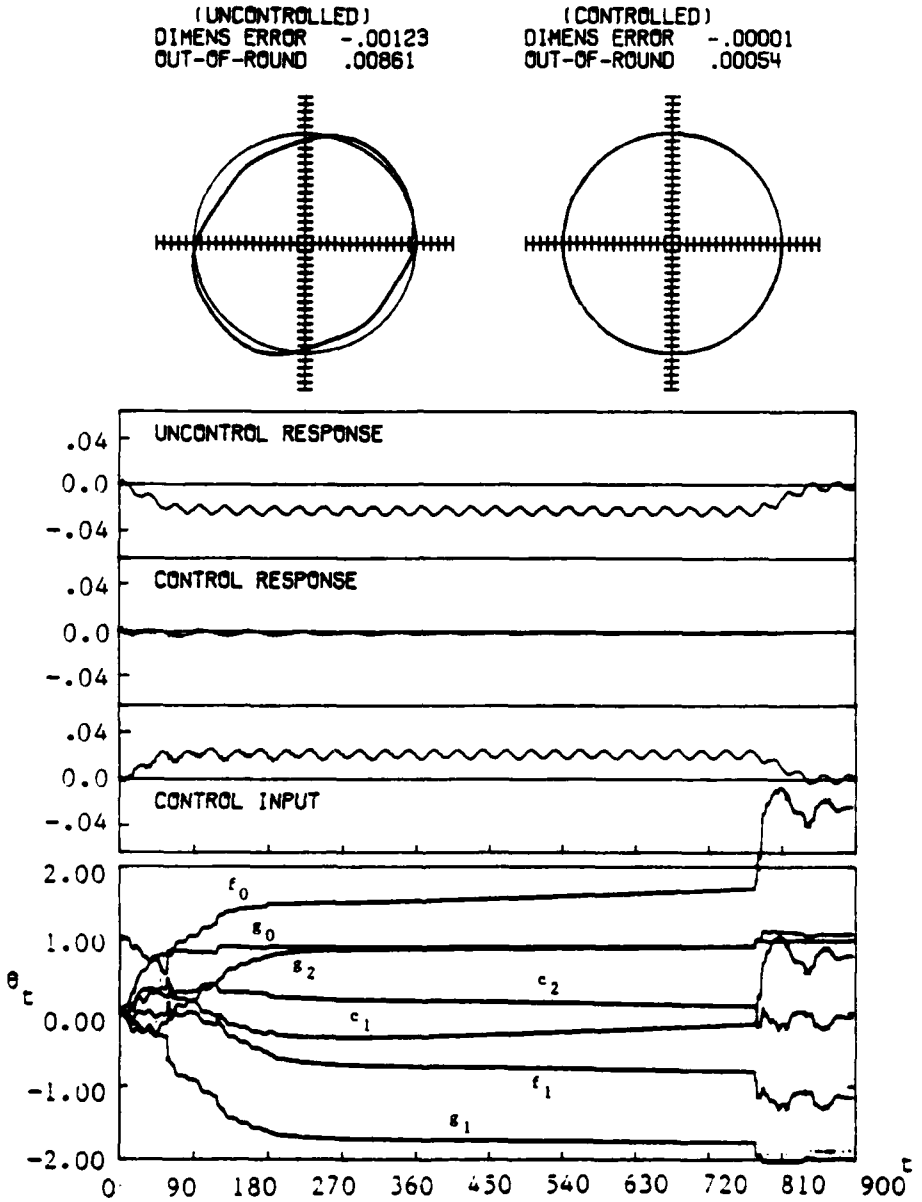

Figure 5.14 The Effect of Detuning Factor in GAC System With Multiprobe Measurement (Simulation II-2)

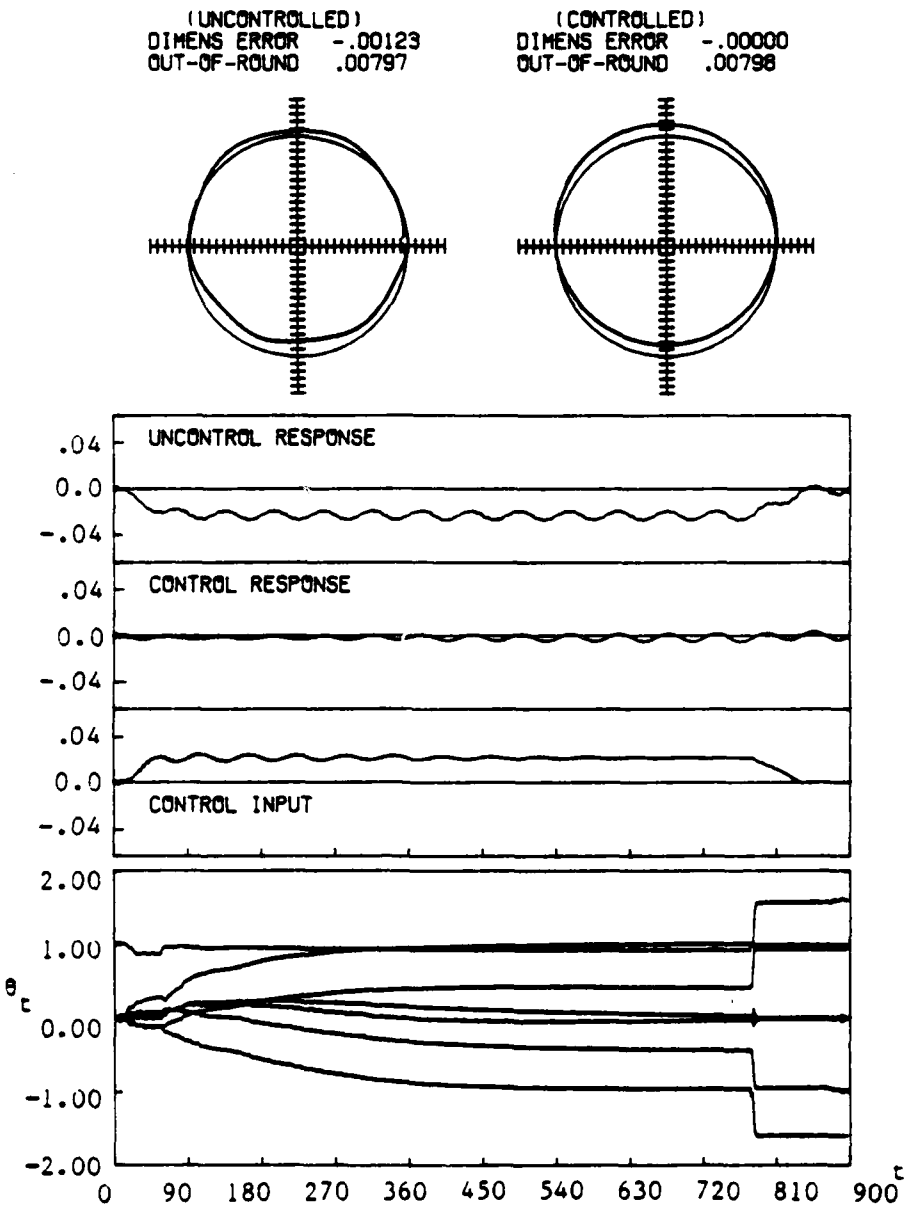

Figure 5.15 GAC System for Once-Per-Revolution Harmonic Invisible to Multiprobe Measurement (Simulation II-3)

The suppression of the fundamental harmonic is common to all configurations of the multiprobe measurement. The next higher suppressed harmonic of this particular configuration is of frequency 11Ω. Conceivably, Fig. 5.16 is obtained by showing that the reduction of the periodic disturbance is very small. To overcome this deficiency, the configuration is changed to

$$\alpha = 132^{\circ}, \quad \beta = 30^{\circ}$$

that is

$$P_d(z^{-1}) = 2.40487 - z^{-5} + 1.61803z^{-27}$$

which has unstable zeros

$$1.00288\, e^{\pm j140.43118^{\circ}}, \quad 1.00444\, e^{\pm j73.18414^{\circ}}$$

And, from (4.30), no harmonics are suppressed by this configuration except the fundamental one with frequency Ω.

Since some of the zeros of the new $P_d(z^{-1})$ lie outside the unit circle, lower detuning factor, ρ=.85, is required to stabilize the control system and result in satisfactory accuracies as shown in Fig. 5.17. However, the low detuning factor also detracts the performance somewhat. Other configurations can give similar results, too. It is found by simulation that the farther the unstable zeros of $P_d(z^{-1})$ are away from the unit circle, the lower the detuning factors needed is, and the less satisfactory the accuracy can be. The configuration with $\alpha = \beta$ has all zeros of $P_d(z^{-1})$ on the unit circle, but it is

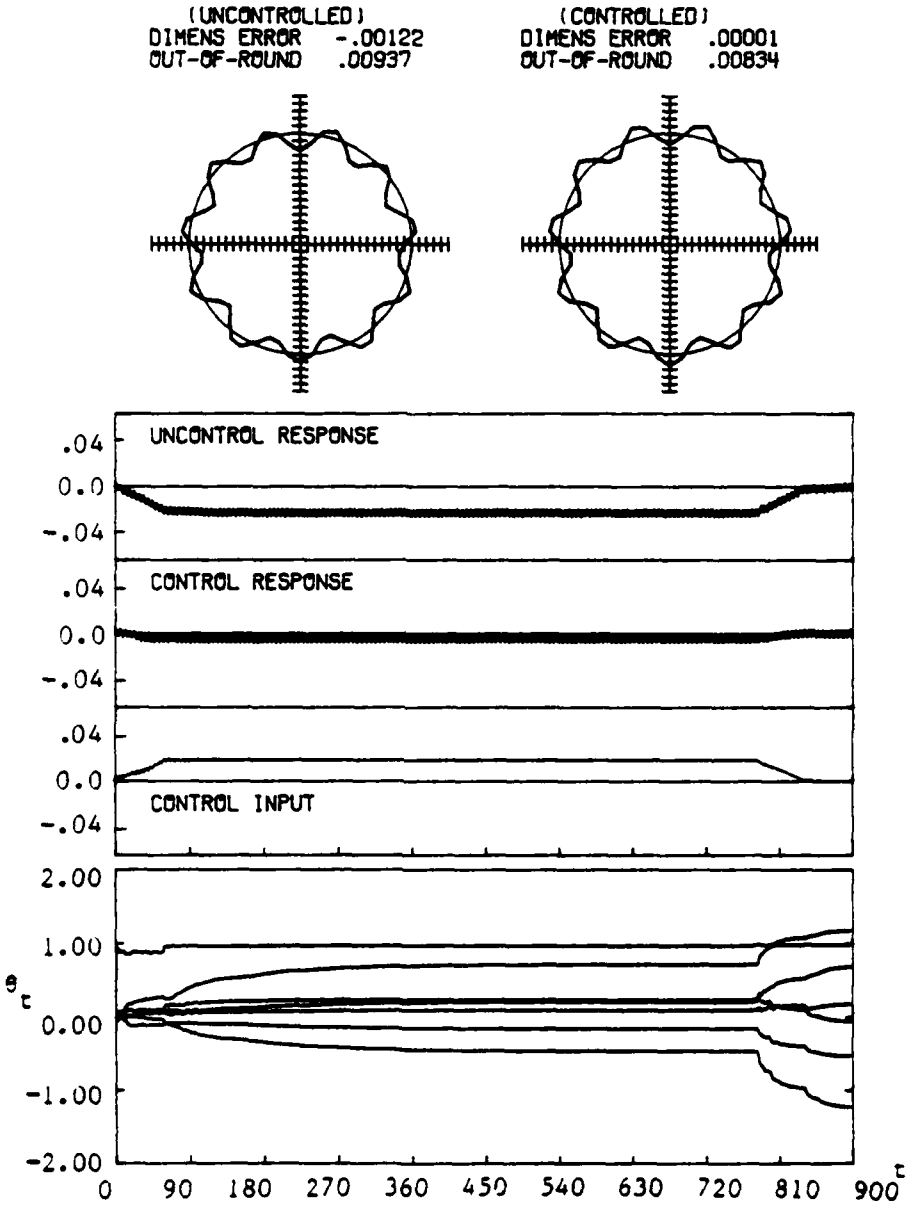

Figure 5.16 GAC System for Higher Harmonic Invisible to Multiprobe Measurement (SimulationII-4)

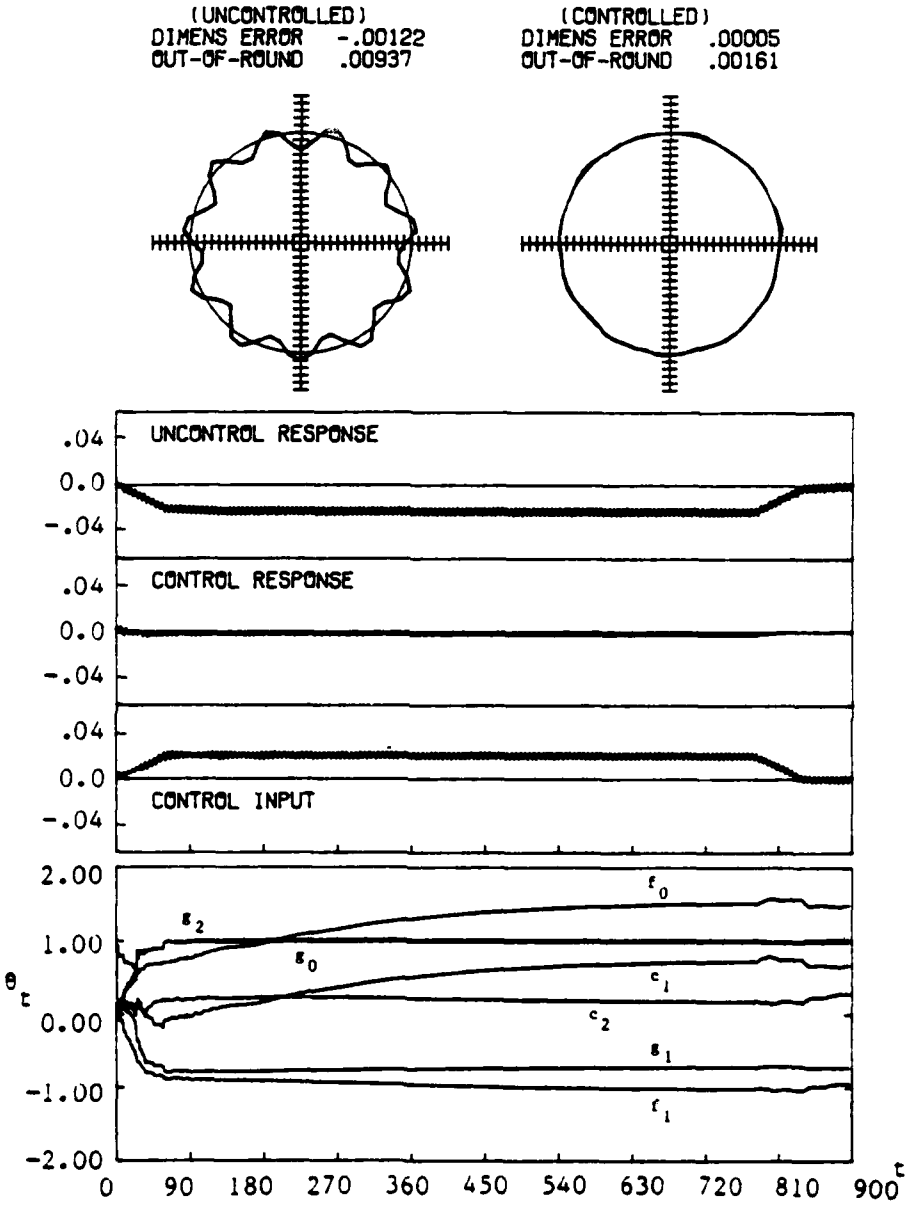

Figure 5.17 GAC System With Modified Configuration of Multiprobes (Simulation II-5)

very possible to miss the detection and the control of the disturbances having frequencies not equal to integral multiple of frequency Ω. The determination of the probe configuration depends on the convenience of the spatial arrangement of the probes, the prior knowledge of the disturbance frequencies, and the locations of the zeros of $P_d(z^{-1})$.

5.3.4 Test of Stochastic System and Stability

Here, we return to the original probe configuration corresponding to $\alpha=90^{\circ}$ and $\beta=30^{\circ}$. Under the same conditions of simulation as those used in Fig. 5.9, good control accuracies are obtained as shown in Fig. 5.18 in the presence of stochastic disturbance. The selected detuning factor, $\rho=0.88$, is smaller than that used in Fig. 5.14, equal to 0.95. In general, a stochastic control system requires a lower detuning factor than a deterministic system does. The forgetting factor, however, changes in the opposite direction because the self-tuning controller needs more data for variance reduction in the stochastic cases. Also, it is found by simulation that a large forgetting factor is good for a low detuning factor. Therefore, the forgetting factor

$$\lambda = 1.0 - .5 \; / \; t$$

is used in Figs. 5.17 and 5.18 and the following simulation.

As the stiffness ratio increases to 0.2, the controlled system remains stable and accurate, again. Comparing the controlled responses of Fig. 5.19 to those of Fig. 5.18, we see that, in the

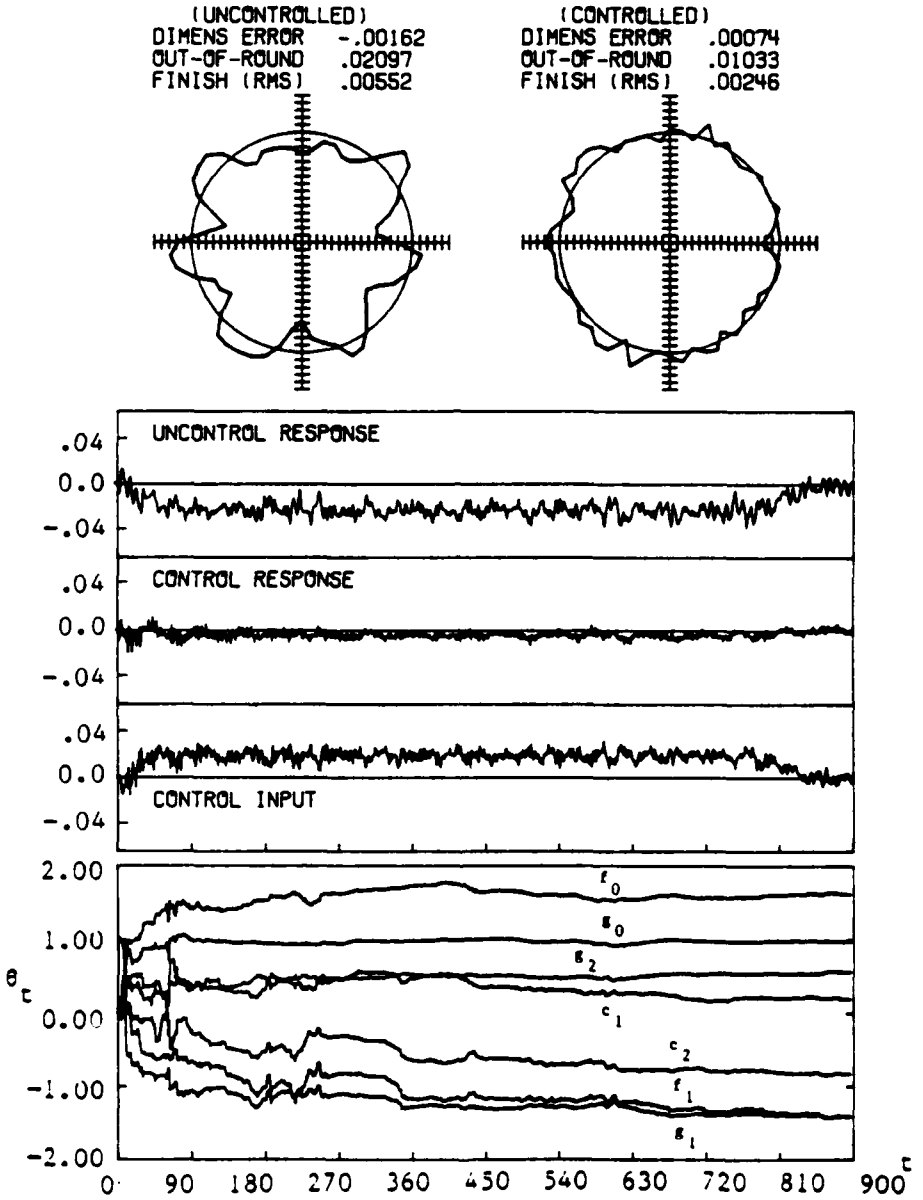

Figure 5.18 GAC System With Multiprobe Measurement, Periodic disturbance and Stochastic Disturbance (Simulation II-6)

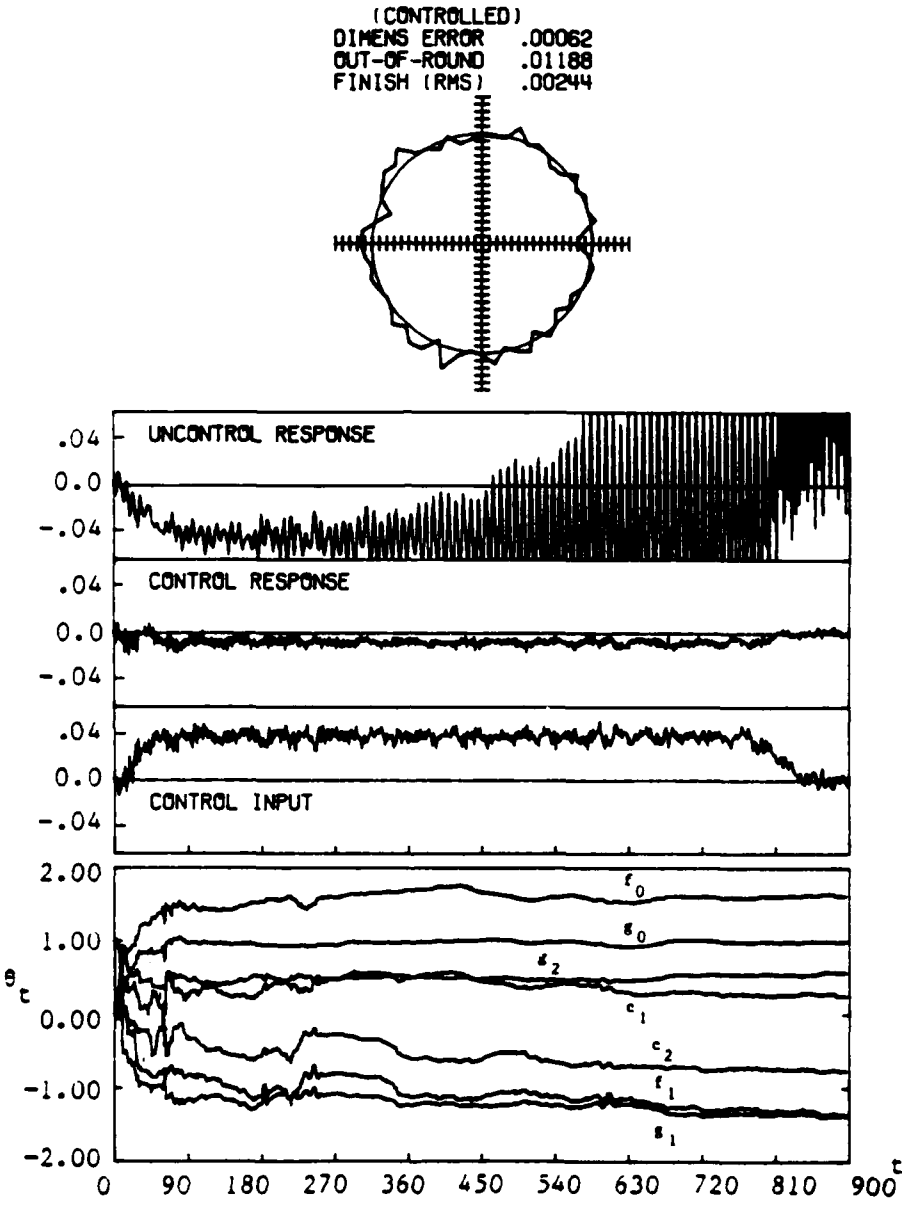

Figure 5.19 GAC System With Multiprobe Measurement for Unstable Machining Process (Simulations II-7)

middle of the operation, the static error in Fig. 5.19 is approximately twice that of Fig. 5.18 with the same detuning factor. And, as shown in Fig. 5.20, this static error increases proportionally when the stiffness ratio goes up to 2.0. The system is still stably controlled. However, in the stage of dwell cutting, the static error decreases more slowly than the specified depth-of-cut. Consequently, increase of the duration of dwell cutting will result in better geometrical accuracy. In Fig. 5.20, an extra revolution of dwell cutting is added and satisfactory accuracies are obtained as shown. The large dimensional excess suggests that another revolution of dwell cutting can be beneficial.

The increase in stability, found by simulation, is by about a factor of 20. The detuning factor is the main reason for the limited closed loop stability. However, the improvement in performance is quite significant.

5.4 Summary of Discussions

In the first part of the simulation, where the measurement problem is not considered, we observed the following:

(I.a) Deterministic disturbances can be fully compensated for by the self-tuning controller irrespective of the amplitudes, the frequency contents, and the types of the disturbances.

(I.b) A time varying forgetting factor is very usetul not only to speed up the convergence at the startup stage, but also to enhance the adaptability of the controller for the environmental changes or modeling errors.

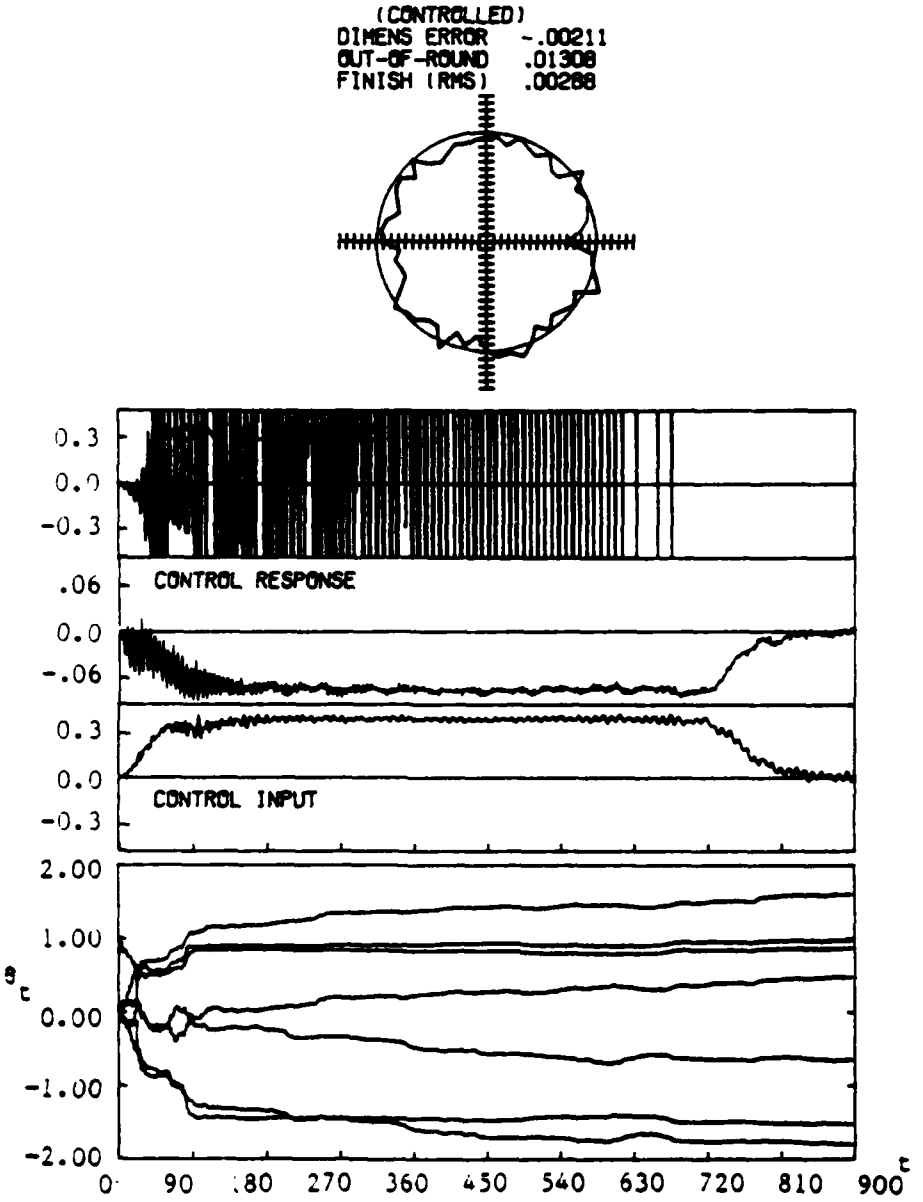

Figure 5.20 GAC System With Multiprobe Measurement for More Unstable Machining Process (Simulation II-8)

(I.c) Self-tuning controller gives perfect tracking during the operation. However, if the system time delay is greater than one, the controller may not be able to follow the input change as quickly toward the end of the cutting operation. Perturbation can be added before and during the input change. Transient response will thus be reduced.

(I.d) In the presence of various levels of deterministic disturbance and stochastic disturbance, the implicit type of self-tuning control is successful in accomplishing near optimal performance with lower order model. The controller we used is robust.

(I.e) The increase in stability can be by a factor of at least 40 for the self-tuning controller. In other words, the self-tuned system is chatter free.

(I.f) A self-tuning model derived with physical insight into the machining process can give much better performance than the general self-tuner.

In the second part, multiprobe is used to tackle the measurement problem of the GAC system. By simulation, we have the following important findings:

(II.a) A detuning factor is crucial for the success of the GAC system with multiprobe measurement. Normally, it has a positive value smaller than one.

(II.b) The multiprobe measurement always suppresses certain harmonics. Those disturbances, thus, cannot be reduced. For the disturbance with the same frequency as the spindle rotation, the GAC system can not do much except removing disturbance induced by the

nonlinearity of the system and generating a perfect round but eccentric part. For higher harmonics, the uncontrollability can be avoided by selecting the probe configuration properly.

(II.c) The probe configuration determines the zeros of $P_d(z^{-1})$. The farther the unstable zeros are away from the unit circle, the smaller the detuning factor used should be, and the less satisfactory the geometrical accuracies obtained are.

(II.d) Stochastic systems need a lower detuning factor than deterministic systems. The detuning factor can be adjusted together with the forgetting factor to get better performance. The detuning factor limits the increase in stability which the GAC system can get. However, the improvement is still very satisfactory.

CHAPTER 6

A COMPARISON OF STC AND FCC

As stated in Chapters 1 and 4, the stochastic properties of machining processes should be considered while modeling a GAC system for removing the nonrepeatable machining errors [47,48,77,78]. However, research engineers have just started to accomplish this actively in recent years. Rao and Wu [84] proposed "compensatory control" for roundness control in cylindrical grinding. Of late this technique was expanded and called "forecasting compensatory control" (FCC) [54,55,68,69].

Basically, FCC is a GAC method which uses in-process measurement. The machining process is modeled by a stochastic process, AR(m), in FCC. The compensation is obtained by giving an input which cancels the error predicted by the stochastic model. The modeling strategy of FCC ignores the relationship between the inputs and the outputs of the machining system. Also, it lacks a systematic approach for designing the compensatory controller. Thus, the performance of the compensated system can hardly be assured.

Realizing this, we propose the STC method in Chapter 4 for cylindrical machining processes. This technique adopts a more rigorous modeling and control strategy. The stochastic model is deduced from the machine tool dynamics which has been discussed in

Chapter 2. Therefore, the self-tuning controller can be designed and analyzed systematically for a better control performance.

The objective of this chapter is to compare the performance of these two control strategies by theoretical investigation, digital simulation, and analog test. In theoretical investigation, the theoretical control performances of both control techniques are examined in the aspects of command tracting and disturbance rejection. In digital simulation, a metal cutting process is simulated to test the machining accuracy and stability obtainable from both strategies. The analog test is to compare the control performances of both strategies which are subject to the constraints of finite word length and sampling in microprocessor based control systems.

6.1 Theoretical Investigation

For simplicity, a general single input single output (SISO) system, as shown in Fig. 6.1, is used for this comparison. All the variables and dynamics are presented in discrete time domain. The dynamics of the process, G_p, is assumed to have the following transfer function

$$G_p = B(z^{-1}) \; / \; A(z^{-1}) \tag{6.1}$$

where

$$A(z^{-1}) = 1 + a_1 z^{-1} + \ldots + a_n z^{-n}$$

$$B(z^{-1}) = z^{-k} B'(z^{-1})$$

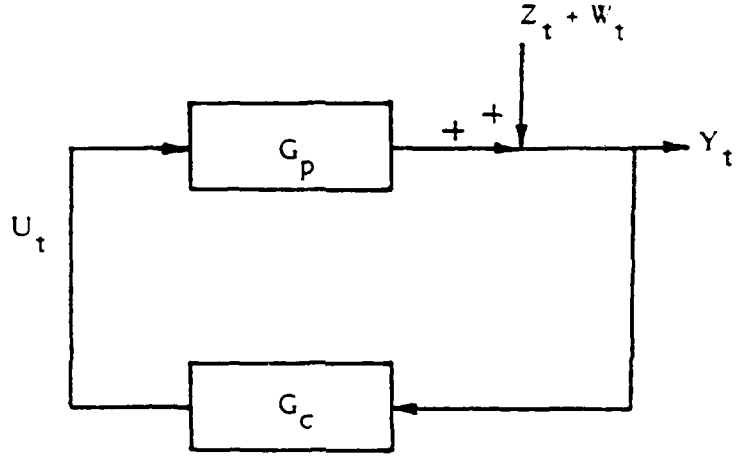

Figure 6.1 A SISO Control System

$$= z^{-k}(b_0 + b_1 z^{-1} + \ldots + b_n z^{-n})$$

and z^{-1} is a backward shift operator. The coefficients, a_i's and b_i's, are related to the dynamic characteristics of the process, and they are considered to be unknown in adaptive control. The order n and the time delay k are, however, assumed to be known here. The deterministic disturbance z_t and the stochastic disturbance w_t are unmeasurable, but bounded. The observed output y_t is fed to the controller G_c, where the control input u_t is generated by the specified control strategy or algorithm.

STC

The design of the STC controller is based on the certainty equivalent principle. Therefore, we shall first discuss the design of the optimal controller as a convenient way for investigating the theoretical control performance of the STC sysetem. A theorem for the STC controller, then, will be presented to substantiate the findings.

The output of the system as shown in Fig. 6.1 is governed by

$$y_t = G_p u_t + z_t + w_t \tag{6.2}$$

To simplify the comparison, the stochastic disturbance w_t can be omitted presently without loss of generality. Hence,

$$y_t = G_p u_t + z_t \tag{6.3}$$

Since most of the stationary deterministic disturbances are constant

or periodic in the time domain, one can always find an operator of the form

$$P(z^{-1}) = p_0 + p_1 z^{-1} + \ldots + p_s z^{-s}$$

such that

$$P(z^{-1}) z_t = 0 \tag{6.4}$$

By substituting (6.1) into (6.3), it gives

$$y_t = \frac{B'(z^{-1})}{A(z^{-1})} u_{t-k} + z_t \tag{6.5}$$

Suppose that the output y_{t+k} can be predicted by the linear combination of the observed outputs and inputs, that is,

$$y_{t+k} = F(z^{-1}) y_t + G(z^{-1}) u_t \tag{6.6}$$

where

$$F(z^{-1}) = f_0 + f_1 z^{-1} + \ldots$$

$$G(z^{-1}) = g_0 + g_1 z^{-1} + \ldots$$

Thus, for the desired output y^*_{t+k}, the control input should be

$$u_t = \frac{1}{G(z^{-1})} y^*_{t+k} - \frac{F(z^{-1})}{G(z^{-1})} y_t \tag{6.7}$$

Substituting (6.7) into (6.5) gives

$$y_{t+k} = \frac{B'}{AG + BF} y^{*}_{t+k} + \frac{AG}{AG + BF} z_{t+k} \tag{6.8}$$

where the operator z^{-1} is omitted for simplicity in the expression. In order to achieve $y_{t+k} = y^{*}_{t+k}$, F and G must satisfy

$$B' = AG + BF = AG + z^{-k}B'F \tag{6.9}$$

$$Gz_{t+k} = 0 \tag{6.10}$$

From (6.4), if P is a factor of G, the condition (6.10), cancellation of the deterministic disturbance, will be satisfied. Also, the condition (6.9) requires that there be a factor $B'(z^{-1})$ in $G(z^{-1})$. Therefore,

$$G = EB'P \tag{6.11}$$

where

$$E = e_0 + e_1 z^{-1} + \ldots$$

Substituting (6.11) into (6.9) gives

$$1 = APE + z^{-k}F \tag{6.12}$$

There exists a unique solution for E and F in (6.12), if the order of E equals to k-1, and the order of F equals to n+s-1.

The above derivations demonstrate that the system can be optimally controlled, $y_t = y^{*}_t$, if the controller (6.7), with F and G satisfying (6.11) and (6.12), is used. In STC, where the polynomials

F and G have to be estimated through a certain adaption mechanism, the same optimality can also be achieved. This can be seen from the following theorem [39]:

Theorem: If the system (6.5) satisfies

(i) all the zeros of BP lie inside or on the unit circle.

(ii) all the zeros of transfer function B/A lie strictly inside the unit circle.

(iii) the zeros of the polynomial BP on the unit circle have a Jordon block of size one.

the self-tuning controller

$$y^*_{t+k} = \hat{F}y_t + \hat{G}u_t \tag{6.13}$$

$$\hat{\theta}_t = \hat{\theta}_{t-1} + S_{t-1}\phi_{t-k}(y_t - \phi^T_{t-k}\hat{\theta}_{t-1}) \tag{6.14}$$

$$S_{t-1} = S_{t-2} - \frac{S_{t-2}\phi_{t-k}\phi^T_{t-k}S_{t-2}}{1 + \phi^T_{t-k}S_{t-2}\phi_{t-k}} \tag{6.15}$$

where

$$\hat{\theta}_t = [\hat{f}_0, \hat{f}_1, \ldots, \hat{g}_0, \hat{g}_1, \ldots]^T$$

$$\phi_t = [y_t, y_{t-1}, \ldots, u_t, u_{t-1}]^T$$

will lead to a stable closed loop system, and the output will converge to y^*_t asymptotically.

The inclusion of the polynomial P in the above assumptions, which results from the existence of the deterministic disturbance z_t,

can be taken away if P has no multiple roots on the unit circle. For the system having the stochastic disturbance in addition to the deterministic disturbance, the above self-tuning controller can be extended by incorporating extra parameters in θ_t to account for the dynamics of the stochastic disturbance. Again, the disturbances can be reduced and the specified output will be tracked [39].

An important point of the theorem is that the estimated polynomials $\bar{F}$ and G are not necessary to satisfy the relationship as (6.12) for the optimal performance of the output. This usually happens in the applications of STC, particularly for the above type of self-tuning controller which estimates directly the parameters of the controller rather than those of the process to be controlled. The STC system will find its own parameters to satisfy the control objective. This can be seen from the simulation results in the next section.

FCC

In FCC, it is assumed that the output of an uncontrolled machining system, y_t, can be fitted by an autoregressive model, AR(m) [83]

$$\Phi' y_t = e_t$$

$$\Phi' = 1 - \phi_1' z^{-1} - \ldots - \phi_m' z^{-m}$$

This model can be derived from (6.2) by letting $u_t = 0$ and converting the disturbances into an autoregressive process with white noise e_t.

By the following factorization

$$1 = \Phi' E + z^{-k}\Phi$$

$$E = e_0 + e_1 z^{-1} + \ldots + e_{k-1} z^{-k+1}$$

$$\Phi = \phi_0 + \phi_1 z^{-1} + \ldots + \phi_{m-1} z^{-m+1}$$

the output y_{t+k} can be predicted by the linear combination of its previous outputs at time t, t-1,..., t-m, that is,

$$y_{t+k} = \hat{y}_{t+k} + Ee_{t+k}$$

$$\hat{y}_{t+k} = \Phi y_t \tag{6.16}$$

For the desired output y^*_{t+k}, the control input of FCC is [84,54,55, 68,69]

$$u_t = y^*_{t+k} - y_{t+k} = y^*_{t+k} - \Phi y_t \tag{6.17}$$

For the system with deterministic disturbance only, substituting (6.17) into (6.5) gives

$$y_{t+k} = \frac{B'}{A + B'} y^*_{t+k} + \frac{A}{A + B'} z_{t+k} \tag{6.18}$$

Equation (6.18) shows that it is not possible to realize $y_{t+k} = y^*_{t+k}$ or to cancel z_{t+k}, provided that the control law (6.17) is used. The reason for the inability to fully track the specified output or eliminate the disturbance is that FCC does not consider the dynamic

relationship between the system output and the compensation input. This is not the case for the in-process control of the machining system.

When $y^{*}_{t+k}=0$, from (6.18), it gives

$$y_{t+k} = \frac{A}{A + B'} z_{t+k} \tag{6.19}$$

The above closed loop system is the same as a conventional control system with a unit negative feedback. The simulation in the next section will show this characteristic.

6.2 Digital Simulation

In digital simulation, the plunge cutting process described in Chapters 4 and 5 is simulated and both techniques are tested on a CDC 6000 computer system.

The model used in STC, from (4.1), is

$$A(y_t - y_{t-p} + \delta_t) = B(u_{t-k} - y_{t-p} + \delta_t) + Ce_t \tag{6.20}$$

where

$$A = 1 + a_1 z^{-1} + \ldots + a_n z^{-n}$$

$$B = b_0 + b_1 z^{-1} + \ldots + b_n z^{-n}$$

$$C = 1 + c_1 z^{-1} + \ldots + c_n z^{-n}$$

The STC algorithm, from (4.11) and (4.12), is to update the

parameters of F,G, and C in the following model

$$y_t = F(y_{t-k} - y_{t-p-k} + \delta_{t-k}) + G(u_{t-k} - y_{t-p} + \delta_t) +$$

$$C(y_{t-p} - \delta_t) + \varepsilon_t \tag{6.21}$$

and to generate the control input by the following control law

$$u_t = (-1/\hat{g}_0)[F(y_t - y_{t-p} + \delta_t) + (G - \hat{g}_0)(u_t - y_{t-p+k} + \delta_{t+k})$$

$$+ C(y_{t-p+k} - \delta_{t+k})] + y_{t-p+k} - \delta_{t+k} \tag{6.22}$$

In designing the FCC controller, the model for parameter estimation is

$$y_t = \hat{\phi}_0 y_{t-k} + \hat{\phi}_1 y_{t-k-1} + \ldots + \hat{\phi}_{m-1} y_{t-k-m+1} + \hat{\phi}_m + \varepsilon_t \tag{6.23}$$

where the estimate $\hat{\phi}_m$ is added to account for the nonzero value which may exist in y_t. And the control law is

$$u_t = -\hat{\phi}_0 y_t - \hat{\phi}_1 y_{t-1} - \ldots - \hat{\phi}_{m-1} y_{t-m+1} - \hat{\phi}_m \tag{6.24}$$

Recursive least squares method is used for updating the parameters of both control techniques. Because of the existence of the deterministic disturbance the order of the model in (6.20) is not less than four. However, to test the robustness of the STC system for the reduced order of the model, n=2 is assumed. Hence, there are seven parameters to be estimated in (6.21) - $\hat{f}_0, \hat{f}_1, \hat{g}_0, \hat{g}_1, \hat{g}_2, \hat{c}_1$, and $\hat{c}_2$. For the same complexity in parameter estimation, therefore, the order m in (6.23) is assumed to be six.

The simulation results depicted in Fig. 6.2, where the stochastic disturbance is set to zero, demonstrate that the originally unstable cutting system, $k_c/k_m=0.2$, can be stabilized by the self-tuning controller, and the machining error can be nearly eliminated. The polar plot represents the final geometrical error of the machined part. The control input shows that the self-tuning controller automatically compensates for the unknown deterministic disturbance and the structural deflection resulting from the nominal cutting force. The estimates $\hat{g}_0$, $\hat{g}_1$ and $\hat{g}_2$, which are related to the control input, satisfy (6.4). It shows how the self-tuning controller adjusts its parameters to counter the deterministic disturbance.

For the stochastic machining system as shown in Fig. 6.3, STC, again, stabilizes the system and produces good accuracy. The error left on the machined part has the root-mean-squares (rms) value approximating to that of e_t in Chapter 5, 0.002, which is the minimum value we can get.

When the structural compliance is doubled, $k_c/k_m=0.4$, the uncontrolled cutting system becomes more unstable as shown in Fig. 6.4. The STC system still shows good stability and accuracy.

As mentioned in the theoretical investigation, the STC algorithm used in the above simulations belongs to the direct or implicit type of adaptive control [39], which tends to update the estimates for minimizing the output error rather than for matching the true parameters. Hence, we can get the optimal or nearly optimal output

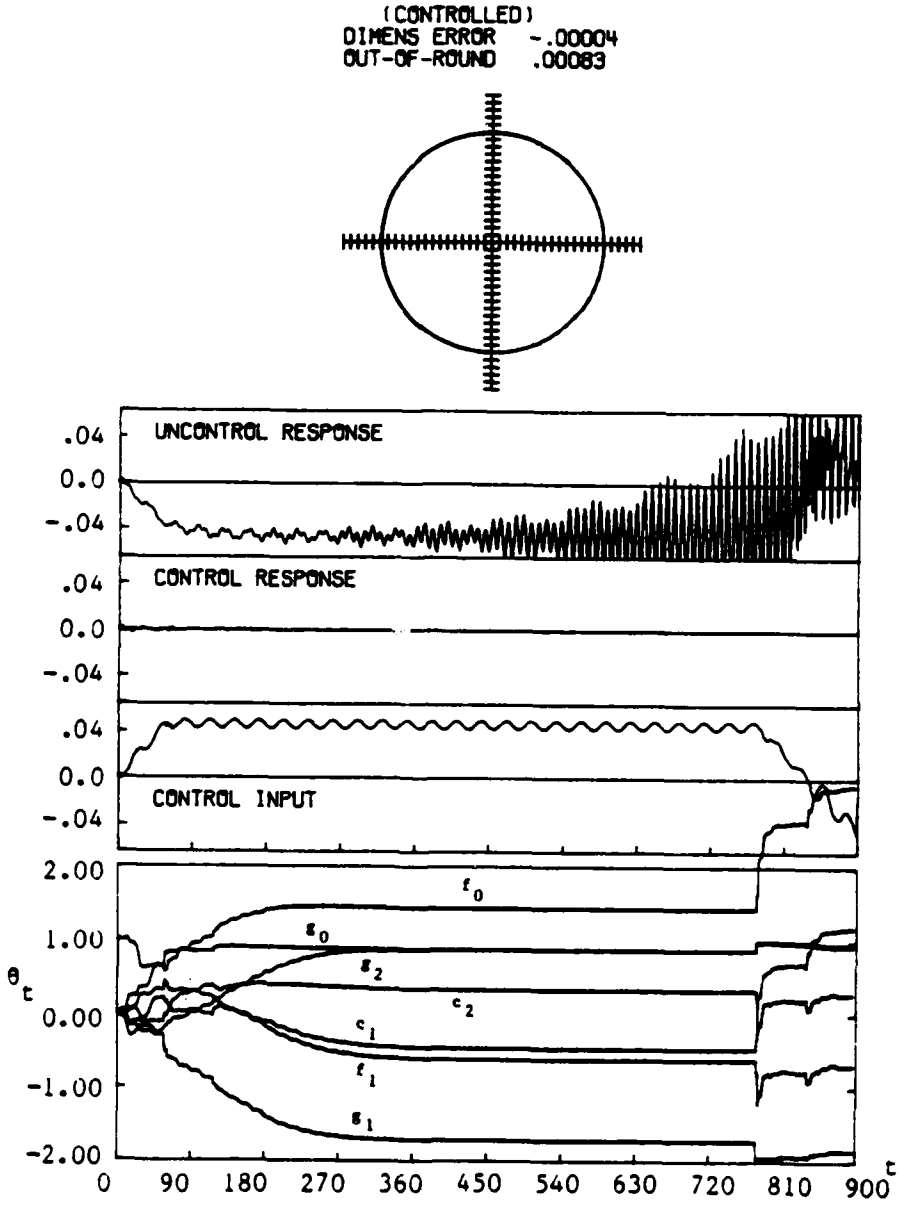

Figure 6.2 STC for Machining Process With Deterministic Disturbance Only

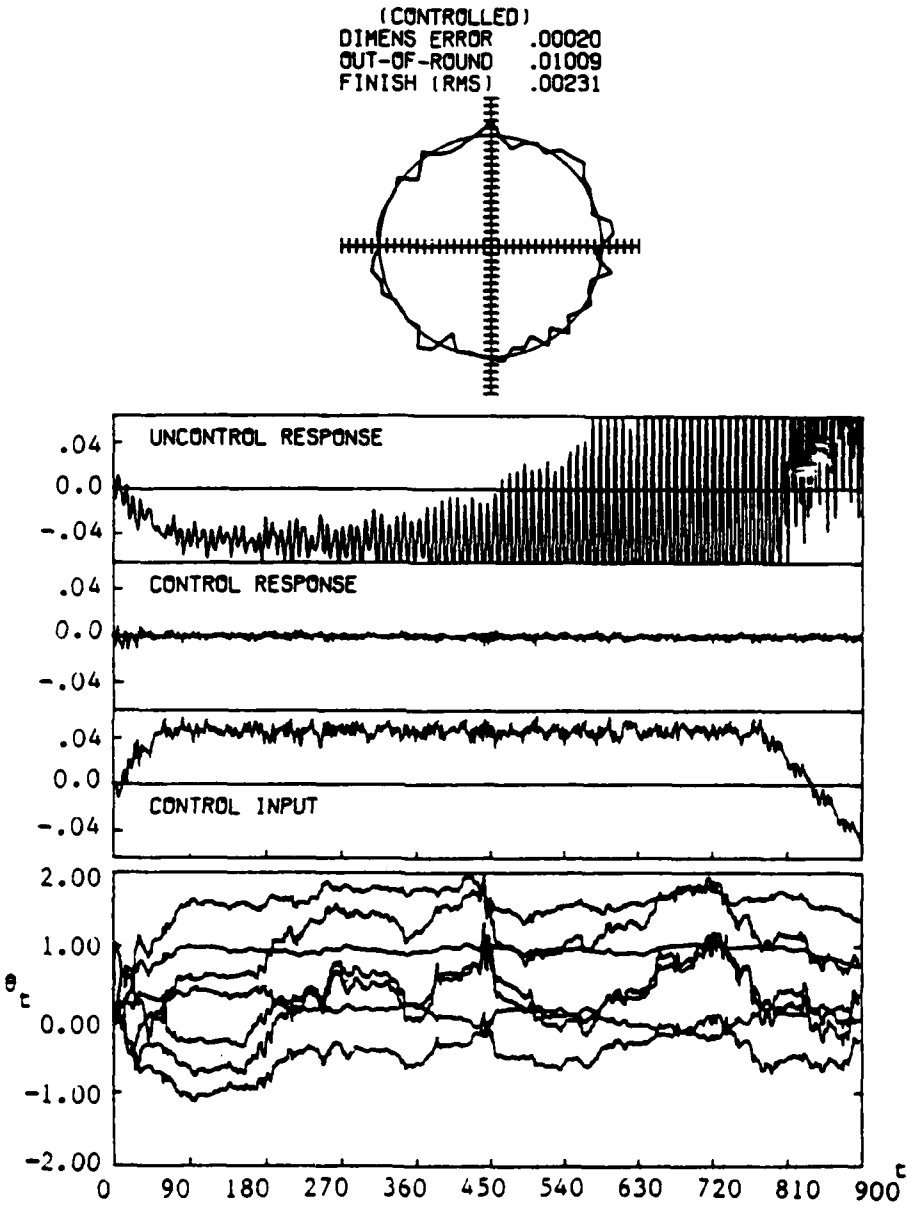

Figure 6.3 STC for Machining Process With Both Deterministic and Stochastic Disturbances

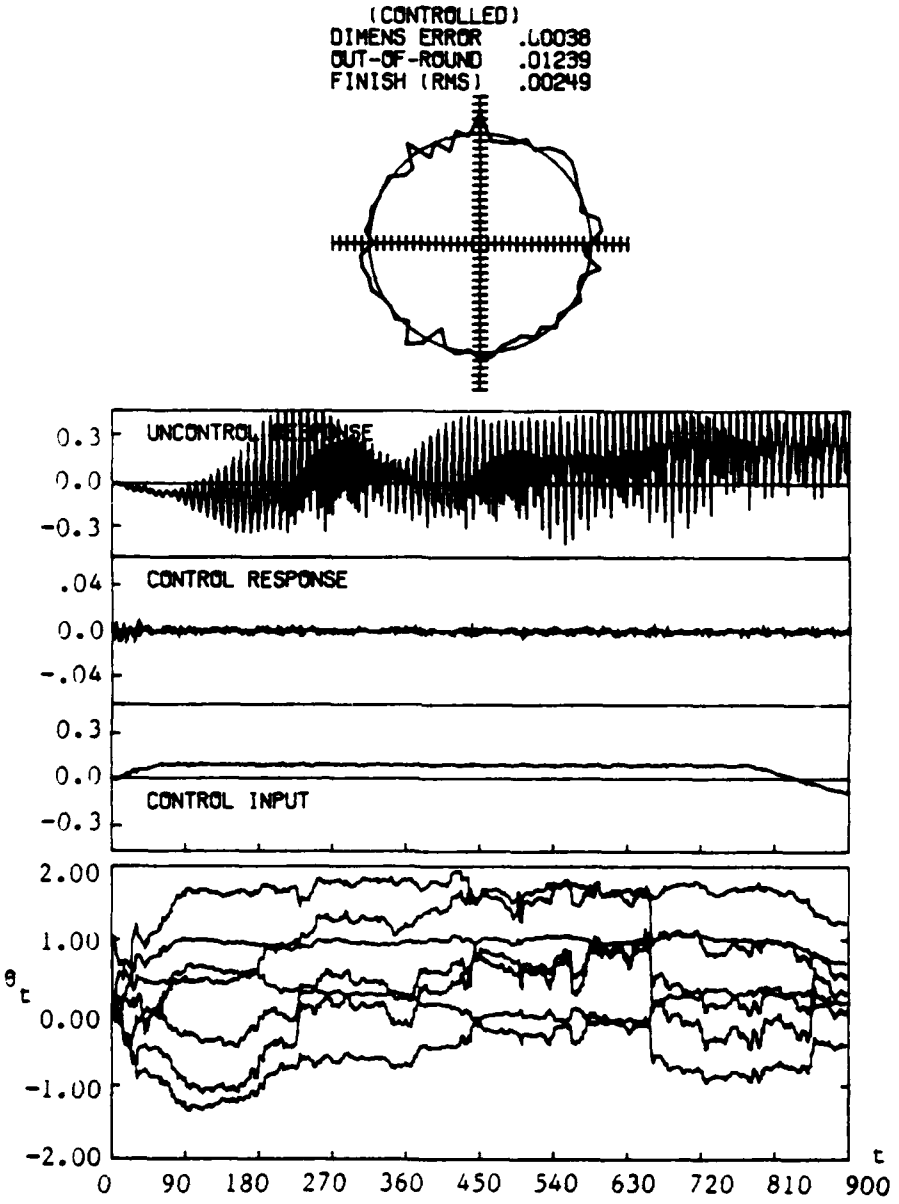

Figure 6.4 STC for Machining Process With Less Rigid Structure

despite the nonconvergence of the estimates. Furthermore, the linear and reduced-order controller provides a certain degree of robustness by showing satisfactory stability and accuracy in the simulated system which has a more complicated structure.

Figs. 6.5 and 6.6 show the simulation results from FCC with the simulation conditions corresponding to those of Figs. 6.2 and 6.3 respectively. Although the systems are stabilized by the forecasting compensator, the accuracies of the parts are much worse than those generated by the STC system. The out-of-roundness shown in Fig. 6.5 is about four times that shown in Fig. 6.2. The control response and the control input show that the structural deflection during the machining operation is only partly compensated for. It confirms the conclusion from the theoretical investigation that the forecasting compensator is essentially a unit feedback controller.

By considering the confidence interval of the parameter estimation, the estimates of Fig. 6.6 reveal that the FCC machining system, when k = 1, can be modeled as a random walk process

$$y_t = y_{t-1} + e_t \tag{6.25}$$

Consequently, the control input is

$$u_t = - y_t \tag{6.26}$$

which is the simple compensatory control (SCC) by one step delay [54]. The control inputs and the system outputs in Figs. 6.5 and 6.6 satisfy approximately the relationship given by (6.26). The same

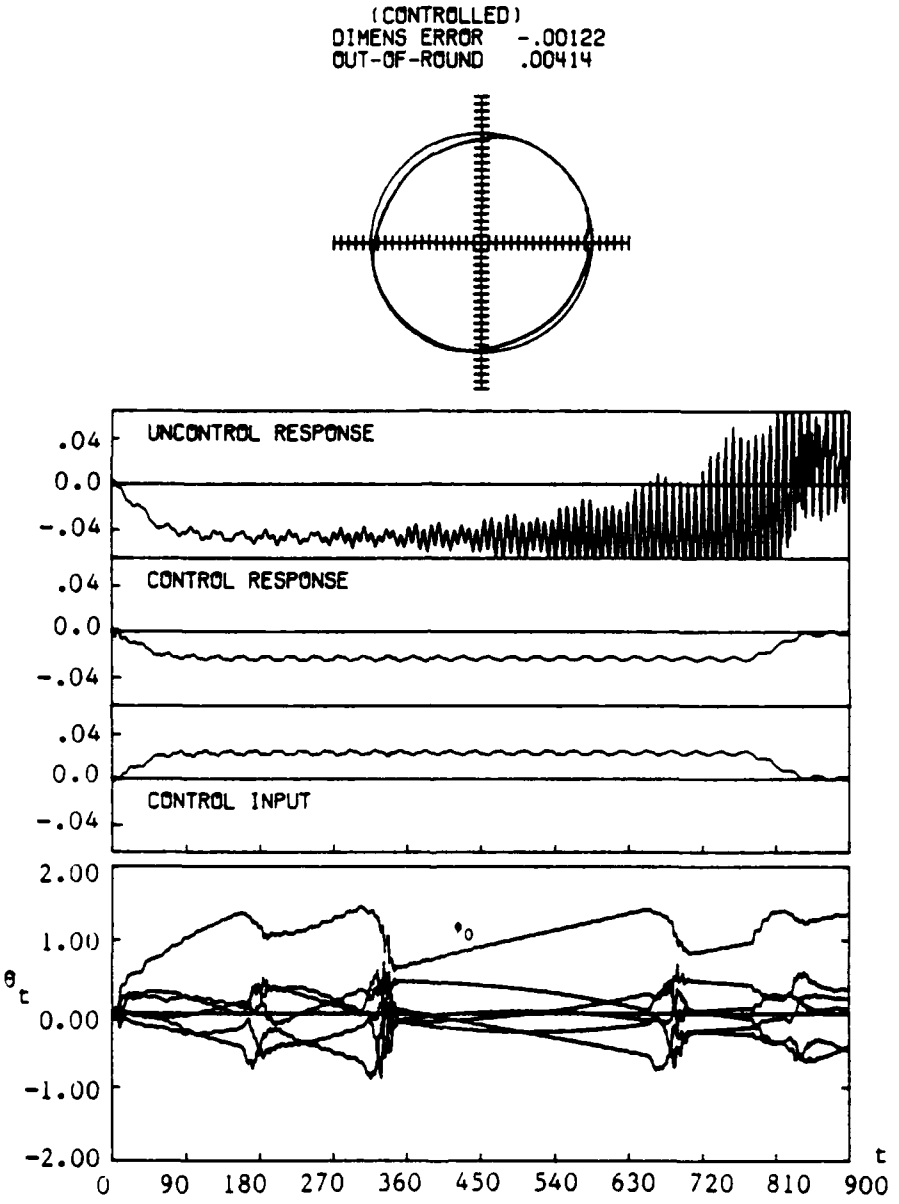

Figure 6.5 FCC for Machining Process With Deterministic Disturbance Only

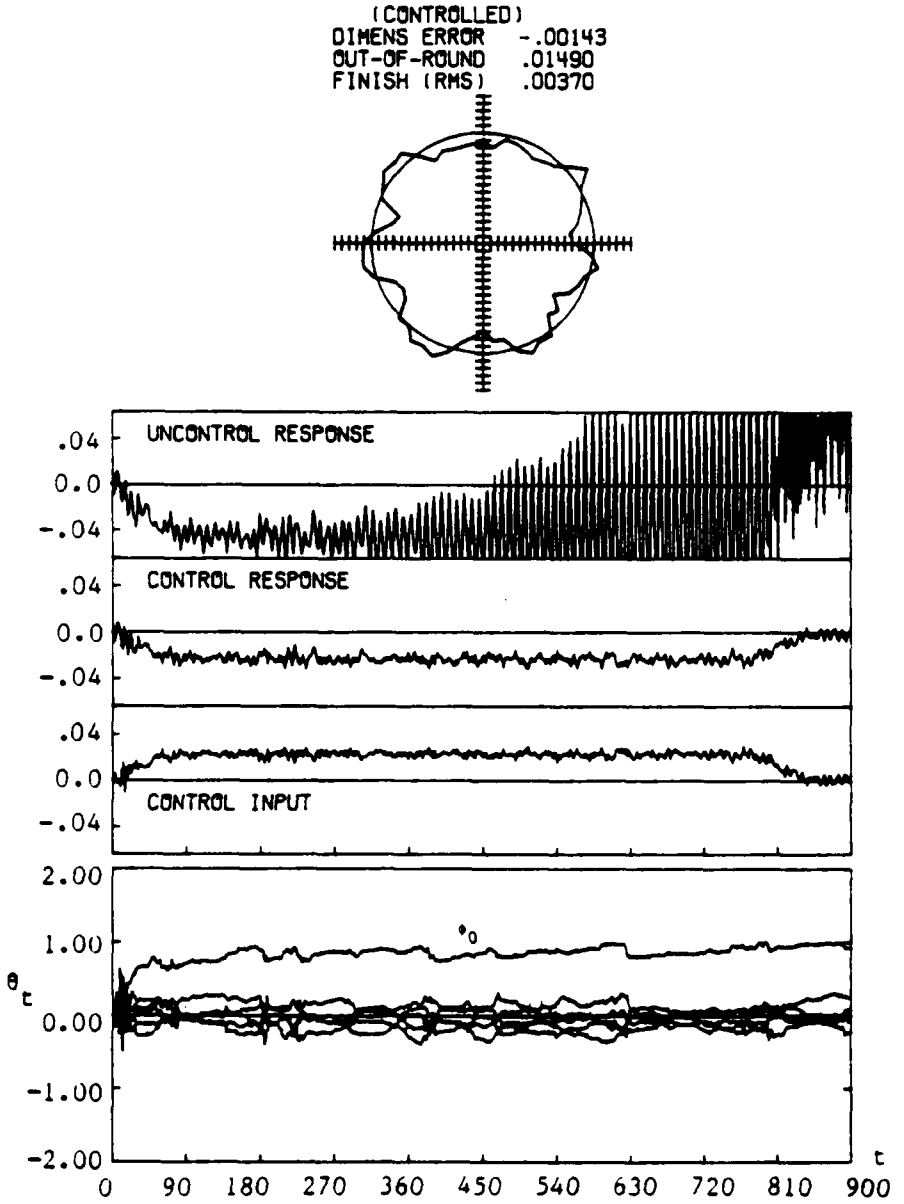

Figure 6.6 FCC for Machining Process With Both Deterministic and Stochastic Disturbances

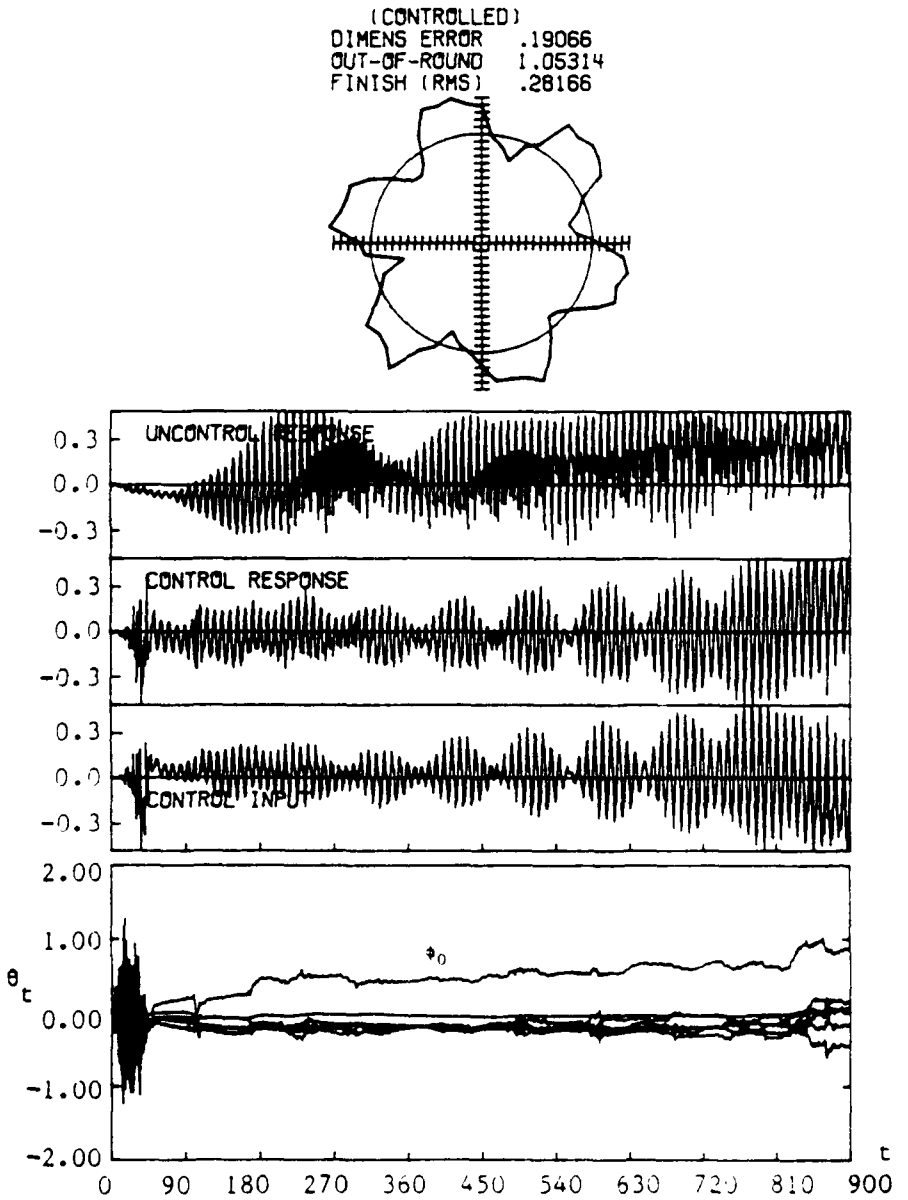

Figure 6.7 FCC for Machining process With Less Rigid Structure

results can be seen in the cutting test conducted by Moon et al. [69].

For the less rigid system as that simulated in Fig. 6.4, FCC is unable to stabilize the system any more, as shown in Fig. 6.7. Further simulation show that the increase in stability gained by STC can be five times that by FCC.

6.3 Analog Test

In the above simulation, we have compared the control performance of the two control techniques by using the machining model of chatter control and the experimental machining properties. Therefore, similar control performance may be expected in the control of the real machining operation. However, some considerations in real implementation still need to be tested for assuring the actual performance. The analog test is to examine the control performance of the two control strategies subject to finite word-length and sampling rate of the microprocessor controller. The system setup is shown in Fig. 6.8.

The electronic circuit for the test is an RLC low pass filter representing a second order dynamic system as shown in Fig. 6.9. The input disturbance z_t is a sinusoidal signal generated by a function generator. Without the control loop, Fig. 6.10 shows the output of the uncontrolled system. The large sinusoidal wave in the figure results from the deterministic disturbance generated by the function generator. Since the circuit is not accurately made, a small wave with higher frequency is superimposed to the large wave in the

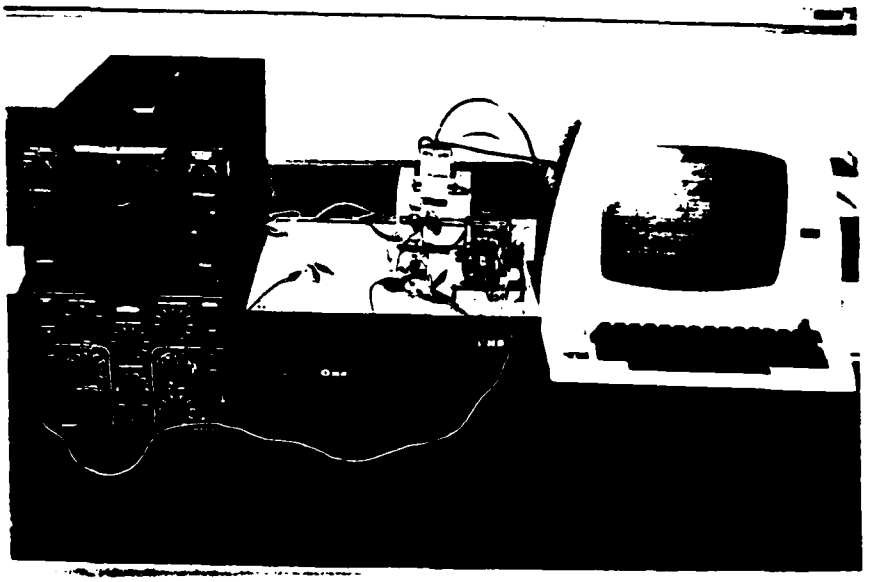

Figure 6.8 Experimental Setup for Analog Test

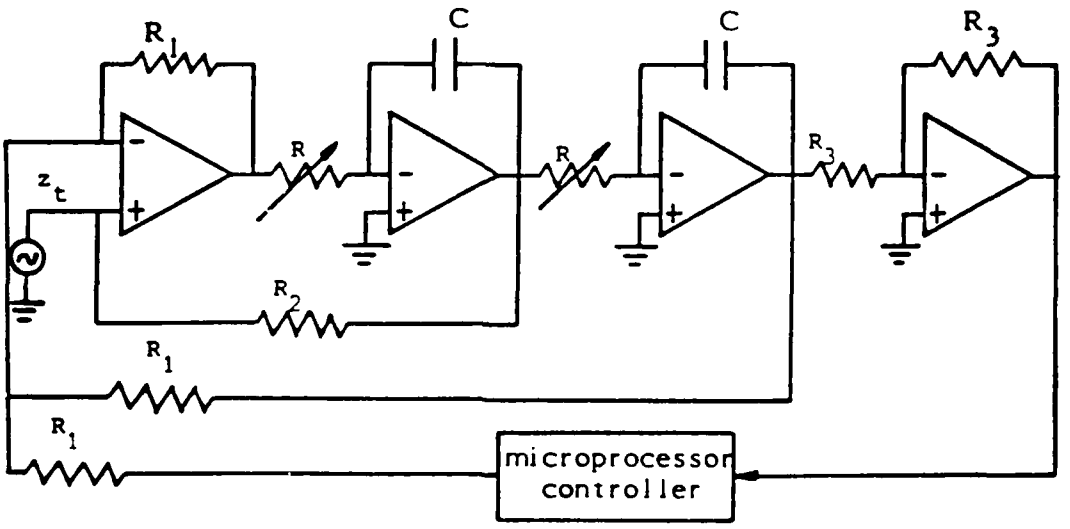

Figure 6.9 Electronic Circuit for Analog Test

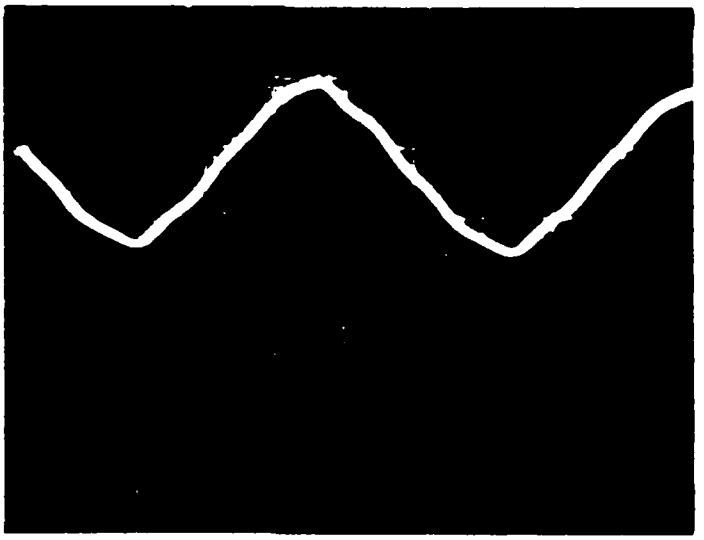

Figure 6.10 Output of Uncontrolled System

figure. This unforeseen nonlinearity is also a good source to test the robustness of the control algorithms. The objective of the control function is to compensate for the effect of the deterministic disturbance and to get the minimum output.

An M68000-based data acquisition and control system was devised to test both control techniques on the electronic circuit. The digital controller has a 12-bit analog to digital converter (ADC) and a 12-bit digital to analog converter (DAC). In numerical computation, each 16-bit data word is fixed-point formatted. The higher byte represents the integer part of the data and the lower byte stands for the fraction part of the data. The finite word-length of the processor and the converters limit the maximum amplitude of the control action. The maximum sampling speed of the digital controller mainly depends on the number of parameters to be estimated. About one millisecond is needed for the control with five parameters.

Only the output signal y_t is needed by the microprocessor controller. The exact frequency and the amplitude of the disturbance are unknown to the controller. However, the approximate range of the frequency is necessary in order to make sure that the sampling rate of the controller is sufficiently high for avoiding the aliasing problem. In this test, the frequency of the disturbance is about 10 Hz, and the sampling rate is 100 Hz.

By using the STC algorithm as shown in equations (6.13-15) with n=2 and k=1, Fig. 6.11 shows that the variance of the output is

nearly eliminated, and the disturbance is countered by the discrete control input having the same frequency. The output of the FCC system, however, is only slightly improved as shown in Fig. 6.12. The forecasting compensator, obviously, is much less effective than the self-tuning controller. Again, from Fig. 6.12, the forecasting compensator behaves like a unit feedback controller.

6.4 Summary

In this chapter, we have theoretically shown that STC can achieve the optimal control performance despite the unidentified deterministic and stochastic disturbances. And, FCC, which works like a unit feedback controller, is less effective than STC in command tracking and disturbance rejection.

The digital simulation shows that the STC technique can not only achieve the optimal response, but also stabilize the uncontrolled machining system. The FCC technique, on the other hand, produces less satisfactory output as found in the theoretical investigation. And it has less capability of stabilizing the uncontrolled system. The simulation also shows that the FCC system behaves as a random walk process. Since the experimental machining properties are used in the simulation, similar results may be expected in the control of the real machining system.

In the analog test, the two control techniques are tested and compared by an electronic circuit with a microprocessor controller. The results show that STC is still more effective than FCC even with the constraints of the finite word-length and sampling rate.

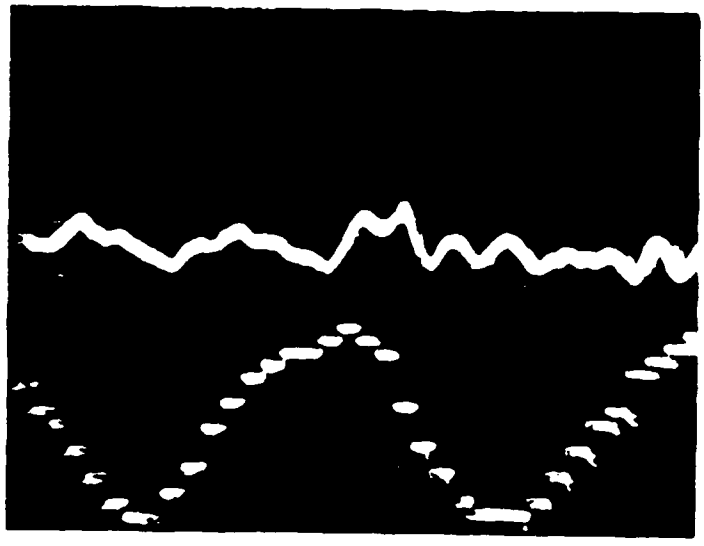

Figure 6.11 Output of STC System

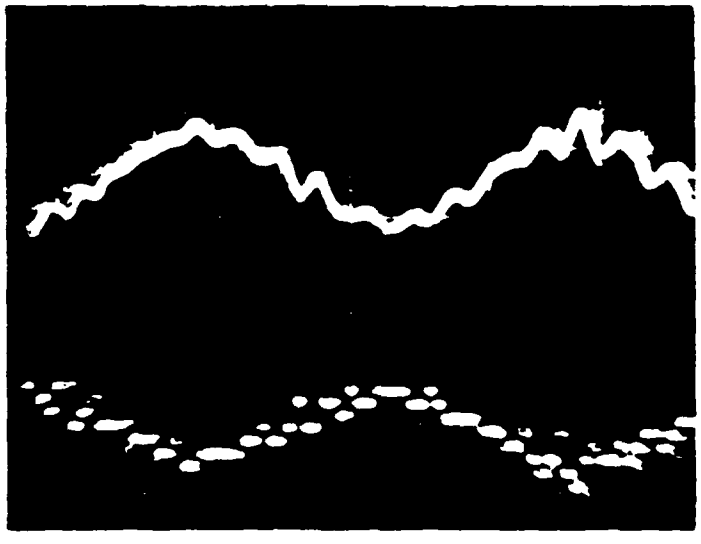

Figure 6.12 Output of FCC System

CHAPTER 7

CONCLUSIONS AND RECOMMENDATIONS

7.1 Conclusions

A new GAC system is proposed and formulated for improving the geometrical accuracies of cylindrical machined parts. The development is accomplished by tackling the three major problems in GAC: measurement, modeling, and adaptive control.

In measurement, we use Whitehouse's multiprobe measurement to solve the separation problem in in-process measurement of geometrical error. New formulations are derived and analyzed for incorporating the multiprobe measurement into the digital adaptive controller. This is the first time that multiprobe measurement is used for control purpose.

In modeling, the interaction of regenerative cutting dynamics and structural dynamics is identified to be the most prominent physics governing the dynamic behavior of cylindrical machining processes. From this we derive a stochastic model in a discrete form for the plunge cutting process. Both the stochastic and the deterministic disturbances are incorporated in the model. This model is, though linear, very usefull for designing a digital GAC system.

In adaptive control, the self-tuning control theory is used to generate an adaptive control algorithm for the model we derived. Theoretical properties of the algorithm are analyzed to assess the performance of the GAC system in practical application and to suggest the ways for improvement. Also derived is a modified algorithm for the GAC system with multiprobe measurement. A detuning factor is introduced for stabilizing the GAC system with multiprobe measurement.

Simulations are carried out to evaluate the performance of the developed algorithms. The results show that the proposed GAC system not only improves the accuracies considerably but also improves the stability of the machining system by a factor of more than forty. The GAC system with multiprobe has similar performance, except, as the theoretical analysis predicted, that certain harmonic disturbances may not be controllable for some specific space configurations of the probes. This problem can be overcome by changing the configuration slightly and selecting an appropriate value for the detuning factor. The increase in stability through the detuning factor is at the expense of geometrical accuracies normally. The simulation also show that the self-tuning control algorithms are robust to nonlinearities and low model orders.

A comparison of STC and FCC shows that the strategies of modeling and control we used can result in better performance than other existing strategies. Also the comparison in the analog test shows that the algorithm of STC does work well, as we have predicted, in a microprocessor based control system.

7.2 Recommendations

To enhance the applicability of this new GAC system, the following subjects are recommended for future work:

(1) A cutting test will further substantiate this work. As we have shown in Chapter 6 that the microprocessor controller is simple to implement, the major work will be the setting up of sensors and actuators. For internal grinding or turning processes, the accessibility of the sensors become more critical.

(2) In traverse cutting we need a reliable method for determining the overlap factor before the operation of GAC. In-process estimation of the overlap factor is not practical because it makes the estimation process nonlinear.

(3) The strategies of modeling and control can be modified and applied to other machining processes, such as milling [102], centerless grinding [13,85], EDM, ECM, and laser machining.

(4) Other sensors, such as force transducers and accelerometers can be used in addition to the displacement sensor to help the measurement problem and to ensure the optimal performance.

(5) The parameters estimated on-line can be used for monitoring the conditions of the machining system during machining, such as tool wear or breakage, defective spindle bearings, and other malfunctions of the machine tool.

BIBLIOGRAPHY

BIBLIOGRAPHY

[1] ANSI Standard, Measurement of Out-of-Roundness, B89.3.1, 1972.

[2] Albrecht, P., "Dynamics of the Metal Cutting Process," ASME paper 64-WA/PROD-16, 1976.

[3] Allidina, A. Y. and Hughes, F. M., "Generalized Self-tuning Controller With Pole Assignment," IEE proceedings, Vol. 127, Pt. D, No. 1, Jan. 1980, pp. 13-18.

[4] Arnold, R. N., "The Mechanism of Tool Vibration in the Cutting of Steel," Proceedings Institution of Mechanical Engineers, 1946, pp. 261-284.

[5] Astrom, K. J., "Self-tuning Regulators - design principles and applications," In K. S. Narendra and R. V. Monopoli (Eds.), Application of Adaptive Control, Academic Press, New York, 1980, pp. 1-68.

[6] Astrom, K. J. (Ed.), "Self-tuning Control," special issue of Optimal Control Application & Methods, Vol. 3, 1982.

[7] Astrom, K. J., "Theory and Applications of Adaptive Control - A Survey," Automatica, Vol. 19, No. 5, 1983, pp. 471-186.

[8] Astrom, K. J., Hagander, P., and Sternby, J., "Zeros of Sampled Systems," Automatica, Vol. 20, No. 1, 1984, pp. 31-38.

[9] Astrom, K. J. and Wittenmark, B., "Problems of Identification and Control", J. of Math. Analysis and Applications, Vol. 34,, 1971, pp. 90-113.

[10] Astrom, K. J. and Wittenmark, B., "On Self Tuning Regulators", Automatica, Vol. 9,, 1973, pp. 185-199.

[11] Astrom, K. J. and Wittenmark, B., "Self-tuning Controllers Based on Pole-Zero Placement," IEE Proceedings, Vol 127, Pt. D, No. 3, May 1980, pp. 120-130.

[12] Astrom, K. J. and Wittenmark, B., Computer-Controlled Systems, Prentice-Hall, N. J., 1984.

[13] Bhateja, C. P., "Current State of the Art of Workpiece Roundness Control in Precision Centerless Grinding," Annals of the CIRP, Vol. 33, No. 1, 1984, pp. 199-203.

[14] Bierman, G. J., Factorization Methods for Discrete Sequential Estimation, Academic Press 1977.

[15] Blaedel, K. L., "Error Reduction," Proceedings of the Machine Tool Task Force Conference, Vol. 5, 1980, pp. 61-72.

[16] Bollinger, J. G., "Machine-tool Vibration," Shock and Vibration Handbook, McGraw-Hill, 1979.

[17] British Standard, Assessment of Departures From Roundness, B.S. 3730:1964.

[18] Bryan, H., "Tolerance - Economic Sense," Annals of the CIRP, Vol. 19, 1971, pp. 115-120.

[19] Bryan, J., Brooks, H., and Clouser, R., "Piezoelectric-Supported Thrust Bearing for the Tool Slide of a Diamond Turning Machine," Annals of the CIRP, Vol. 24, No. 1, 1975, pp. 355-356.

[20] Bryan, J. B. and Vanherck, P., "Unification of Terminology Concerning the Error Motion of Axes of Rotation," Annals of the CIRP, Vol. 24, 1975, pp. 555-562.

[21] Bryant, M. D. and Reeves, R. B., "Precise Positioning Problems Using Piezoelectric Actuators With Force Transmission Through Mechanical Contact," Precision Engineering, Vol. 6, NO. 3, July 1984, pp. 129-134.

[22] Chetwynd, D. G., "Roundness Measurement Using Limacons," Precision Engineering, 1979, pp. 137-141.

[23] Clarke, D. W., "Introduction to Self-Tuning Controllers," In C. J. Harris and S. A. Billings, Self-Tuning and Adaptive Control: theory and application, Peter Peregrinus, 1981, pp. 37-71.

[24] Clarke, D. W., "Self-tuning Control of Nonminimum-phase Systems," Automatica, Vol. 20, No. 5, 1984, pp. 499-500.

[25] Clarke, D. W. and Gawthrop, P. J., "Self-tuning Controller," IEE Proceedings, Vol. 122, No. 9, Sept. 1975, pp. 929-934.

[26] Clarke, D. W. and Gawthrop, P. J., "Self-tuning Control," IEE Proceedings, Vol. 126, No. 6, June 1979, pp. 633-640.

[27] Clarke, D. W. and Gawthrop, P. J., "Implementation and Application of Microprocessor-Based Self-tuners," The 5th Symposium on Identification and System Parameter Estimation, Darmstadt, 1979, pp. 197-208.

[28] Clarke, D. W. and Gawthrop, P. J., "Implementation and Application of Microprocessor Self-tuners," Automatica, Vol. 17, 1980, pp. 233-244.

[29] Comstock, T. R., Tse, F. S., and Lemon, J. R., "Application of Controlled Mechanical Impedance for Reducing Machine Tool Vibrations," Trans. ASME, J. of Engineering for Industry, Vol. 91, No.4, Nov. 1969, pp. 1057-1062.

[30] Cook, N. H., "Self-excited Vibration in Metal Cutting," Trans. ASME, J. of Engineering for Industry, Vol. 81, May 1959, pp. 183-186.

[31] DeGarmo, E. P., Materials and Processes in Manufacturing, 5th ed., Macmillan, New York, 1979.

[32] Donaldson, R. R.,"A Simple Method for Separating Spindle Error from Test Ball Roundness Error," Annals of the CIRP, Vol. 21, 1972, pp. 125-126.

[33] Eykhoff, P., System Identification - parameter and state estimation, John Wiley, London, 1974.

[34] Farago, F. T., Handbook of Dimensional Measurement, Industrial Press, 1982.

[35] Feldbaun, A. A., "Dual-Control Theory I-IV", Auto. Remote Control Vol. 21, 1961, pp. 874-880, pp. 1033-1039; Vol. 22, 1962, pp. 1-12, pp. 109-121.

[36] Fortescue, T. R., Kershenbaum, L. S., and Ydstie, B. E., "Implementation of Self-tuning Regulators With Variable Forgetting Factors," Automatica, Vol. 17, No. 6, 1981, pp. 831-835.

[37] Franklin, G. F. and Powell, J. D., Digital Control of Dynamic systems, 11. Addison-Wesley 1980.

[38] Gawthrop, P. J., "Some Interpretations of the Self-tuning Controller," IEE Proceedings, Vol. 124, No. 10, Oct. 1977, pp. 889-894.

[39] Goodwin, G. C. and Sin, K. S., Adaptive Filtering, Prediction, and Control, Prentice-Hall, N. J., 1984.

[40] Hahn, R. S., "Metal-cutting Chatter and Its Elimination," Trans. ASME, Vol. 75, 1953, pp. 1073-1080.

[41] Harris, C. J. and Billings, S. A. (Eds.), Self-tuning and Adaptive Control: theory and application, Peter Peregrinus, 1981.

[42] Hocken, R. J., Machine Tool Accuracy, Proceedings of the Machine Tool Task Force Conference, Vol. 5, 1980.

[43] Hoshi, T., "Types of Machining Vibration," Machine Tool Task Force Conference, Vol. 3, 1980

[44] Hume, K. J., A History of Engineering Metrology, Mechanical Engineering Pub. Ltd., 1980.

[45] Isermann, R., Digital Control Systems, Springer, New York, 1981.

[46] Isermann, R., "Parameter Adaptive Control Algorithms - a tutorial," Automatica, Vol. 18, No. 5, 1982, pp. 513-528.

[47] Jona, M. G., "Contribution to the Development of Geometrical Adaptive Control in Turning," 11th Int. J. of MTDR, Conf., Birmingham, 1970, pp. 429-445.

[48] Jona, M. G., "Scope and Possibilities of Geometrical Adaptive Control in Turning," Annals of the CIRP, Vol. 19, 1971, pp. 305-309.

[49] Kakino, Y., Yamamoto, Y., and Ishii, N., "New Measuring Method of Rotating Accuracy of Spindle," Annals of the CIRP, Vol. 26, 1977, pp. 241-244.

[50] Kaliszer, H., Mishina, O., and Webster, J., "Adaptively Controlled Surface Roughness and Roundness During Grinding," Proceedings of the 20th MTDR, Birmingham, 1979, pp. 471-478.

[51] Kalman, R. E., "Design of a Self-optimizing Control System," Trans. ASME, Feb. 1958, pp. 468-478.

[52] Kato, S. and Marui, E., "On the Cause of Regenerative Chatter Due to Workpiece Deflection," Trans. ASME, J. of Engineering for Industry, Vol. 96, Feb. 1974, pp. 179-186.

[53] Kegg, R., "Industrial Problems in Grindings," Annals of the CIRP, Vol. 32, 1983, pp. 559-561.

[54] Kim, K. H., Forecasting Compensatory Control of Roundness, Ph.D. thesis, University of Wisconsin-Madison, 1983.

[55] Kim, K. H., Eman, K. F., and Wu, S. M., "Forecasting Compensatory Control of Spindle Error Motion in Cylindrical Grinding," ASME Winter Annual Meeting on Statistics in Manufacturing, 1983, pp. 75-81.

[56] Lam, K. P., "Implicit and Explicit Self-tuning Controllers," D. Phil. Thesis, Oxford University, 1980.

[57] Lee, D. T. L., Friedlander, B., and Morf, M., "Recursive Ladder Algorithms for ARMA Modeling," IEEE Trans. on Aut. Control, Vol. AC-27, No. 4, 1982, pp. 753-764.

[58] Ljung, L., "On Positive Real Transfer Functions and the Convergence of Some Recursive Schemes," IEEE Trans. on Auto. Control, Vol. AC-22, No. 4, Aug. 1977, pp. 529-550.

[59] Ljung, L. and Soderstrom, T., Theory and Practice of Recursive Identification, MIT Press, 1983.

[60] Maddux, K. and Nachtigal, C. L., "Wideband Active Chatter Control Scheme," ASME paper 72-WA/Aut-10.

[61] Makila, P. M., "Self-tuning Control With Linear Input Constraints," Optim. Control Appl. Methods, Vol. 3, 1982, pp. 337-353.

[62] Makila, P. M., Westerland, T., and Toivonen, H. T., "Constrained Linear Quadratic Gaussian Control With Process Applications," Automatica, Vol. 20, No. 1, 1984, pp. 15-29.

[63] McCool, J. I., "Systematic and Random Errors in Least Squares Estimation for Circular Contours," Precision Engineering, 1979, pp. 215-220.

[64] Merchant, M. E.,"Basics Mechanics of the Metal Cutting Process," Trans. ASME, Vol. 66, 1944, pp. A168-A175.

[65] Merritt, H. E., "Theory of Self-excited Machine-tool Chatter," Trans. ASME, J. of Engineering for Industry, Vol. 87, No. 4, Nov. 1965, pp. 447-454.

[66] Mitchell, E. E., "A Survey of Active Machine Tool Control," JACC Conference, 1977, pp. 512-520.

[67] Mitchell, E. E. and Harrison, E., "Design of a Hardware Observer for Active Machine Tool Control," JACC Conference, 1976, pp. 260-266.

[68] Moon, E. J., Eman, K. F., and Wu, S. M., "Simulation Study of Forecasting Compensatory Control of Machining Straightness," ASME Winter Annual Meeting on Controls in Manufacturing, 1983, pp. 47-63.

[69] Moon, E. J., Eman, K. F., and Wu, S. M., "Implementation of Forecasting Compensatory Control for Machining Straightness," ASME Winter Annual Meeting on Computer Integrated Manufacturing and Robotics, 1984, pp. 231-241.

[70] Moore, W. R., Foundations of Mechanical Accuracy, The Moore Special Tool Company, Connecticut, 1970.

[71] Morf, M., Vieira, A., and Lee, D. T., "Ladder Forms for Identification and Speed Processing," IEEE Conference on Decision and Control, 1977, pp. 1074-1078.

[72] Murthy, T. S. R. and Abdin, S. Z., "Minimum Zone Evaluation of Surfaces," Int. J. MTDR, Vol. 20, 1980, pp. 123-136.

[73] Murthy, T. S. R., Mallanna, C., and Visveswaran, M. E., "New Methods of Evaluating Axis of Rotation Error", Ann. CIRP, 1978, pp. 365-369.

[74] Nachtigal, C., "Design of a Force Feedback Chatter Control System", Trans. ASME J. of Dyn. Sys., Meas., and Control, 1972, pp. 5-10.

[75] Nachtigal, C. L. and Cook, N. H., "Active Control of Machine Tool Chatter," Trans. ASME, J. of Basic Engineering, Vol. 92, Ser. D, NO. 2, Jun 1970, pp. 238-244.

[76] Nachtigal, C. L. and Maddux, K. C., "An Adaptive Active Chatter Control Scheme," ASME paper 72-WA/Aut-10.

[77] Peklenik, J., "Geometrical Adaptive Control of Manufacturing Systems," Annals of the CIRP, Vol. 18, 1970, pp. 265-272.

[78] Peklenik, J. and Kwiatkowski, A. W., "Random Processes in Manufacturing Systems," Annals of the CIRP, Vol. 15, 1967, pp. 67-74.

[79] Peterka, V., "Adaptive Digital Regulation of Noisy Systems," IFAC Symposium on Parameter Identification, 1970.

[80] Peters, J., "Metrology in Design and Manufacturing - Facts and Trends," Annals of the CIRP, Vol. 26, 1977, pp. 415-421.

[81] Rahman, M. and Ito, Y., "Machining Accuracy of a Cylindrical Workpiece Held by a Three-Jaw Chuck," Bull. Japan Soc. of Precision Engineering, Vol. 13, No. 1, Mar. 1979, pp. 7-12.

[82] Rao, S. B., Compensatory Control of Form Errors in Machining, Ph.D. thesis, University of Wisconsin, Madison 1980.

[83] Rao, S. B., Collins, J. F., and Wu, S. M., "A Quantitative Analysis of Roundness Error in Cylindrical Chuck Grinding", Int. J. of MTDR, 1981, pp. 41-48.

[84] Rao, S. B. and Wu, S. M., "Compensatory Control of Roundness Error in Cylindrical Chuck Grinding," Trans. ASME, J. of Engineering for Industry, Vol. 104, 1982, pp. 23-28.

[85] Rowe, W. B., "Research into the Mechanics of Centerless Grinding," Precision Engineering, 1979, pp. 75-84.

[86] Sawabe, M. and Fujimuma, N., "Influence of Radial Motion on Form Error of Workpiece in Turning," Annals of The CIRP, Vol. 27, 1978, pp. 505-509.

[87] Shiraishi, M.,"Geometrical Adaptive Control in NC Turning Operation," Trans. ASME, J. of Engineering for Industry, Vol. 106, 1984, pp. 75-80.

[88] Sin, K. S. and Goodwin, G. C., "Stochastic Adaptive Control Using a Modified Least Squares Algorithm," Automatica, Vol. 18, No. 3, 1982, pp. 315-321.

[89] Sisson, T. R. and Kegg, R. L., "An Explanation of Low-speed Chatter Effects," Trans. ASME, J. of Engineering for Industry, Vol. 91, No. 4, Nov. 1969, pp. 951-958.

[90] Sonozake, S. and Fujiwara, H., "A Finishing Method for Higher Roundness of Cylinder," Bull. Japan Soc. of Precision Engineering, Vol. 11, No. 1, Mar. 1977, pp. 43-44.

[91] Srinivasan, K. and Nachtigal, C. L., "Investigation of the Cutting Process Dynamics in Turning Operations," Trans. ASME, J. of Engineering for Industry, Vol. 100, Aug. 1978, pp. 323-331.

[92] Strejc, V., "Least Squares Parameter Estimation," Automatica, Vol. 16, pp. 535-550.

[93] Taniguchi, N., "Current Status in, and Future Trend of, Ultraprecision Machining and Ultrafine Materials Processing," Annals of the CIRP, Vol. 32, 1983, pp. 573-582.

[94] Taylor, F. W., "On the Art of Cutting Metals," Trans. ASME, 1907, p. 30.

[95] Thomas, G. G., Engineering Metrology, John Wiley & Sons, 1974.

[96] Thornton, C. L. and Bierman, G. J., "Filtering and Error Analysis via the UDU Covariance Factorization," IEEE Trans. on Aut. Control, Vol. AC-23, No. 5, 1978, pp. 901-907.

[97] Tlusty, J., "Analysis of the State of Research in Cutting Dynamics," Annals of the CIRP, Vol. 27, 1978, pp. 583-589.

[98] Tobias, S. A., Machine Tool Vibration, Wiley, New York 1965.

[99] Ulsoy, A. G., Koren, Y., and Rasmussen, F., "Principal Developments in the Adaptive Control of Machine Tools," Trans. ASME, J. of Dyn. Sys., Meas., and Control, Vol. 105, June 1983, pp. 107-112.

[100] Unbehauen, H. (Ed.), Methods and Applications in Adaptive Control, Springer-Verlag, 1980.

[101] Unification Document Me: Axes of Rotation, Annals of the CIRP, Vol 25, 1976, pp. 545-564.

[102] Watanabe, T. and Iwai, S., "A Geometric Adaptive Control System to Improve the Accuracy of Finished Surfaces Generated by Milling Operations.," Symposium on Measurement and Control of Batch Manufacturing, ASME Winter Annual Meeting, 1982, pp. 121-134.

[103] Weck, M., Verhaag, E., and Gather, M., "Adaptive Control for Face-milling Operations With Strategies for Avoiding Chatter-vibrations and for Automatic Cut Distribution," Annals of the CIRP, Vol 24, No. 1, 1975, pp. 405-409.

[104] Welbourn, D. B. and Smith, J. D., Machine-tool Dynamics, An Introduction, Cambridge University Press, 1970.

[105] Wellstead, P. E., "Self-tuning Digital Control Systems," In S. Bennett and D. A. Linkens (Eds.), Computer Control of Industrial Processes, Peter Peregrinus, 1982.

[106] Wellstead, P. E., Edmunds, J. M., Prager, D., and Zanker, P., "Self-tuning Pole/Zero Assignment Regulators," Int. J. Control, Vol. 30, No. 1, 1979, pp. 1-26.

[107] Wellstead, P. E., Prager, D., and Zanker, P., "Pole Assignment Self-tuning Regulator," IEE Proceedings, Vol. 126, No. 8, Aug. 1979, pp. 781-787.

[108] Wellstead, P. E. and Sanoff, S. P., "Extended Self-tuning Algorithm," Int. J. of Control, Vol. 34, 1981, pp. 433-455.

[109] Wellstead, P. E. and Zanker, P., "Techniques of Self-tuning," Optim. Control Appl. Methods, Vol. 3, 1982, pp. 305-322.

[110] Whitehouse, D. J., "A Best Fit Reference Line for Use in Partial Axes", J. Phys. E: Sci. Inst., 1973, pp. 921-924.

[111] Whitehouse, D. J., "Some Theoretical Aspects of Error Separation Techniques in Surface Metrology," J. Phys. E: Sci. Inst., 1976, pp. 531-536.

[112] Wittenmark, B., "Stochastic Adaptive Control Methods: A Survey," Int. J. of Control, Vol. 21, 1975, pp. 705-730.

[113] Wittenmark, B. and Astrom, K. J., "Practical Issues in the Implementation of Self-tuning Control," Automatica, Vol. 20, No. 5, 1984, pp. 595-605.

[114] Wu, D-J. W., A Mathematical Model of Machining Chatter, Ph.D. thesis, Purdue University, 1982.

APPENDICES

Appendix 1

Derivation of (4.1)

The continuous transfer function of the tool-workpiece structure can be represented by:

$$MT(s) = \frac{1}{k_m} \frac{\omega_n^2}{s^2 + 2\zeta\omega_n s + \omega_n^2}$$

ω_n = natural frequency of the structure

ζ = damping ratio of the structure

k_m = stiffness of the structure

By taking the Z-transformation with a zero-order-hold [37], the discrete transfer function is derived as follows:

$$MT = (1 - z^{-1})Z\{\frac{MT(s)}{s}\}$$

$$= \frac{1}{k_m} \frac{\beta_1 z^{-1} + \beta_2 z^{-2}}{1 + \alpha_1 z^{-1} + \alpha_2 z^{-2}}$$

or more generally [23],

$$MT = \frac{1}{k_m} \frac{\beta_0 + \beta_1 z^{-1} + \beta_2 z^{-2}}{1 + \alpha_1 z^{-1} + \alpha_2 z^{-2}}$$

where

$$\alpha_1 = -2e^{-aT} \cos bT, \qquad \alpha_2 = e^{-2aT}$$

$$\beta_1 = 1 - e^{-aT} \cos bT - \frac{a}{b} e^{-aT} \sin bT$$

$$\beta_2 = e^{-2aT} + \frac{a}{b} e^{-aT} \sin bT - e^{-aT} \cos bT$$

$$a = \zeta\omega_n$$

$$b = \omega_n \sqrt{1 - \zeta^2}$$

and T is the unit sampling time interval.

The discrete form of the regenerative process in Chapter 2 is

$$Z\{\frac{1 - \mu e^{-s\tau}}{s}\}$$

or

$$1 - \mu z^{-p}$$

where the regenerative delay p is equal to τ/T or $1/(\Omega T)$. The overlap factor is

$$0 \leq \mu \leq 1$$

The cutting process CP can be represented by the cutting stiffness, i.e., $CP = k_c$. The stochastic and the deterministic disturbances of Fig. 4.2 are given as

$$W_t = (1 + c_1' z^{-1} + c_2' z^{-2})\xi_t$$

$$Z_t = d_0 + d_1 t + \Sigma r_i \sin(2\pi i \Omega t + \phi_i)$$

respectively, where ξ_t is an uncorrelated random process with zero mean and variance σ_ξ^2.

The GAC system is, thus, governed by the following equations

$$Y_t = W_t + Z_t + Y_s(t) - X_t + u_{t-k} \tag{A.1}$$

$$X_t = \frac{k_c}{k_m} \frac{\beta_0 + \beta_1 z^{-1} + \beta_2 z^{-2}}{1 + \alpha_1 z^{-1} + \alpha_2 z^{-2}} (Y_t - \mu Y_{t-p}) \tag{A.2}$$

By substituting (A.2) into (A.1) and using the following two definitions

$$y_t = Y_t - Y_s(t)$$

$$\delta_t = Y_s(t) - \mu Y_s(t-p)$$

we can have the following equation

$$y_t = W_t + Z_t - \frac{\beta_0^* + \beta_1^* z^{-1} + \beta_2^* z^{-2}}{1 + \alpha_1 z^{-1} + \alpha_2 z^{-2}} (y_t - \mu y_{t-p} + \delta_t) + u_{t-k}$$

or

$$(1 + a_1' z^{-1} + a_2' z^{-2})(y_t - \mu y_{t-p} + \delta_t)$$

$$= (b_0' + b_1'z^{-1} + b_2'z^{-2})(u_{t-k} - \mu y_{t-p} + \delta_t)$$

$$+ (b_0' + b_1'z^{-1} + b_2'z^{-2})(W_t + Z_t) \qquad (A.3)$$

where

$$\beta_i^* = \beta_i k_c/k_m, \quad i = 0,1,2$$

$$a_i' = (\alpha_i + \beta_i^*)/(1 + \beta_0^*), \quad i = 1,2$$

$$b_i' = \alpha_i/(1 + \beta_0^*), \quad i = 0,1,2 \text{ and } \alpha_0 = 1$$

For the deterministic disturbance Z_t we can find such a polynomial

$$P(z^{-1}) = (1 - z^{-1})^j \prod_i (1 - 2(\cos 2\pi i\Omega)z^{-1} + z^{-2}), \quad j \geq 0$$

so that

$$P(z^{-1})Z_t = 0$$

Thus, multiplying (A.3) by $P(z^{-1})$ gives the following model

$$A(z^{-1})(y_t - \mu y_{t-p} + \delta_t) = B(z^{-1})(u_{t-k} - \mu y_{t-p} + \delta_t) + C(z^{-1})\xi_t$$

where

$$A(z^{-1}) = A'(z^{-1})P(z^{-1}) = 1 + a_1z^{-1} + \ldots + a_nz^{-n}$$

$$B(z^{-1}) = B'(z^{-1})P(z^{-1}) = b_0 + b_1z^{-1} + \ldots + b_nz^{-n}$$

$$C(z^{-1}) = C'(z^{-1})B'(z^{-1})P(z^{-1}) = 1 + c_1 z^{-1} + \ldots + c_n z^{-n}$$

and n is an appropriate positive integer which represents the model order. The polynomials of A, B and C may have common zeros on the unit circle because of the periodic disturbances.

The model is linear only if overlap factor μ is known analytically or experimentally. A special case is the plunge cutting process which has $\mu = 1$.

Appendix 2

STC With Weighted Minimum Variance Criterion

The control criterion of weighted minimum variance

$$\text{Min } E[y_{t+k}^2 + \beta' u_t^2 | t], \quad \beta' > 0$$

gives the following control law for (4.1)

$$y_{t+k|t} + \beta u_t = 0, \quad \beta = \beta'/g_0$$

The self-tuning algorithm is thus [39],

(i) choose appropriate β

(ii) estimate the model parameters

$$\theta_t = \theta_{t-1} + K_t \varepsilon_t$$

$$K_t = \frac{P_{t-1} z_t}{\lambda^2 + z_t^T P_{t-1} z_t}, \quad \lambda^2 = \text{forgetting factor } (\leq 1)$$

$$P_t = (I - K_t z_t^T) P_{t-1} / \lambda^2$$

$$z_t = [(y_{t-k} - y_{t-p-k} + \delta_{t-k}), (y_{t-k-1} - y_{t-p-k-1} + \delta_{t-k-1}), \ldots,$$

$$(u_{t-k} - y_{t-p} + \delta_t), (u_{t-k-1} - y_{t-p-1} + \delta_{t-1}), \ldots,$$

$$\eta(y_{t-p-1} - \delta_{t-1}), \eta(y_{t-p-2} - \delta_{t-2}), \ldots]^T, \quad \eta = 1 + \beta$$

$$\hat{\theta}_t = [\hat{f}_0, \hat{f}_1, \ldots, \hat{g}_0, \hat{g}_1, \ldots, \hat{c}_1, \hat{c}_2, \ldots]^T$$

$$\varepsilon_t = (y_t + \beta u_{t-k}) - z_t^T \hat{\theta}_{t-1}$$

(iii) u_t can be obtained from

$$z_{t+k}^T \hat{\theta}_t = 0$$

Notice that when $\beta = 0$, the above algorithm becomes minimum variance STC.

Appendix 3

The FORTRAN Program for Digital Simulation

In this Appendix we give the FORTRAN program which is used for the digital simulation in Chapters 5 and 6. The program is written for the proposed GAC system with multiprobe measurement, (4.33-35). By modifying the program so that the probe function

$$P_d(z^{-1}) = 1$$

and the detuning factor

$$\rho = 1$$

the program can also be run for the GAC system without multiprobe measurement, (4.11) and (4.12).

Subroutine SIML is the simulated plunge cutting process as described in Chapter 5. The adaption mechanism is programmed according to the minimum variance criterion as shown in Appendix 2. Subroutine SQRTES is a recursive least squares routine with square root factorization [41]. Three types of the varying forgetting factors are programmed in subroutine VFORG. The third type, which is proposed by Fortescue et al. [36], needs

F1 = Σ_0 (constant chosen for appropriate adaption speed)

F2 = $1 + z_t^T P_{t-1} z_t$

F3 = ϵ_t

```
      PROGRAM PLGMLP(INPUT,OUTPUT,PLOT,TAPE5=INPUT,TAPE6=OUTPUT)
C ***************************************************************
C                 ADAPTIVE ROUNDNESS CONTROL
C
C     THIS IS A TECHNIQUE OF ADAPTIVE CONTROL WITH MULTIPROBE
C     MEASUREMENT.  IT HAS TWO MAJOR PARTS:
C     1. RECURSIVE PARAM EST
C     2. IMPLICIT MIN VAR CONTROL
C     REF: ASTROM & WITTENMARK (1973)
C          CLARKE (1981)
C          WHITEHOUSE(1976)
C          PH.D. THESIS BY YHU-TIN LIN, AUG., 1985, PURDUE UNIV.
C     GEN LIB: IMSL
C***************************************************************
C
      COMMON RNS,FREQ,PHASE,AMPL,ALPH,BETA,GAMA,JF,JG
      COMMON Y(1000),U(1000),E(1000),X(20),YS(1000),FEED,F(1000)
      DIMENSION A(10),B(10),C(10),YP(1000)
      DIMENSION Z(20),THETA(20),THETB(20),S(120),ZY(20),ZU(20),ZD(20)
C
      READ 200,IP,IPRINT,IFEED,K,N,NA,NEEDPLT,NT
C
      K1=K+1
      L=N+K+1
      LK=L+K
      LK1=L+K+1
      LN1=L+N+1
      N1=N+1
      NC=NA+1
      NK=N+K
      NPAR=N+L+N
      NTO=NT-1
      NTK=NT+K
      NTP=NT-IP*2
C
C ***** SETUP OF MULTIPROBE CONFIG.
C
      READ 200,JF,JG
      DPI=2.*3.1415926
      ALPH=SIN(DPI*(JG-JF)/IP)/SIN(DPI*JG/IP)
      BETA=-1.0
      GAMA=SIN(DPI*JF/IP)/SIN(DPI*JG/IP)
C
C ***** SETUP OF SIMULATION CONDITIONS
C
      READ 210, AMPL,FEED,PHASE,PSQR,RNS,STIFF
      FREQ=2.*(2.*3.141592654/IP)
      READ 220,(A(J),J=1,NA),(B(J),J=1,NA),(C(J),J=1,NC)
      PRINT 230,RNS,FREQ,AMPL,JF,JG,ALPH,BETA,GAMA
      PRINT 240,NT,N,K,IP,NPAR,IFEED,FEED,STIFF,PSQR
C
```

```
C ***** SELECT FORGETTING FACTOR AND DETUNING FACTOR
C
C        JFORG=1      F1-F2/I
C              2      F1*FORGET+F2
C              3      FORTESCUE(1981)
      READ 250,JFORG,F1,F2,F3,DTUNE
      PRINT 270,JFORG,F1,F2,F3,DTUNE
C
C ***** INITIALIZATION OF PLOT
C
C       NEEDPLT=0    NO PLOT
C               1    TWO POLAR PLOTS
C               2    ALL PLOTS
C               3    CONTROLLED POLAR & TIME SERIES (UNSTABLE SYSTEM)
C               4    ONLY TIME SERIES
C
      IF (NEEDPLT.EQ.0) GO TO 30
      CALL PLOTS
      CALL FACTOR(.4)
      SFPOLA=40.
      XC=0.
      YC=12.5
      YXL=4.
      CALL PLOT(12.5,0.,3)
      CALL PLOT(12.5,16.,3)
      IF (NEEDPLT.EQ.1) GO TO 30
C
      SFPARA=1.
      SFTIME=15.
      XINI=0.
      XLEN=10.
      YINI=4.2
      YLEN=2.
      THERO=2.
      THMIN=-THERO/SFPARA
      CALL LABEL(NT,XINI,XLEN,YINI,YLEN,THMIN)
      DT=XLEN/NT
      T=XINI
      T0=XINI
      UZERO=YINI+1.
      YZERO=YINI+3.
      YZERU=YINI+5.
      DO 20 J=1,NPAR
   20 THETB(J)=0.
C
C ***** TEST UNCONTROLLED SYSTEM
C IFEED = 0, NO RETRACTION; =1, WITH RETRACTION
C
   30 CONTINUE
      DO 40 J=1,NA
      B(J)=B(J)*STIFF
   40 X(J)=0.
      YS0=0.
```

```
      DO 50 I=1,NTK
      YS(I)=FEED*I
      IF (I.GT.NTP) YS(I)=YS(NTP)
      IAP=I-IP
      IF (IAP.LE.0) GO TO 50
      IF (IFEED.EQ.0) YS0=YS(IAP)
      IF (IFEED.EQ.0) YS0=FEED*IAP
   50 F(I)=YS(I)-YS0
      ICTL=0
      CALL SIML(A,B,C,NT,NA,IP,ICTL)
      IL=NT
      DO 60 I=1,NT
      F(IL)=PROBE(F,IL)
      IL=IL-1
   60 YP(I)=Y(I)-YS(I)
      NTR=NT-IP
      IF (NEEDPLT.NE.1.AND.NEEDPLT.NE.2) GO TO 65
      NTR=NT-IP
      XC=XC+2.5
      IFCON=0
      CALL RONDPLT(YP,XC,YC,YXL,NTR,IP,RNS,IFCON,SFPOLA)
   65 IF (NEEDPLT.LE.1) GO TO 70
      CALL SPLOT(YP,NT,YZERU,T0,DT,SFTIME)
      CALL PLOT(XINI,THERO,3)
C
C ***** INITIALIZATION FOR PARAM EST
   70 PRINT 280
      ICTL=1
C -----------------------------------------------------------------
      READ 220,(THETA(J),J=1,NPAR)
      THETA(N1)=1.
      DO 80 J=1,NA
   80 X(J)=0.
      DO 90 I=2,LK1
   90 CALL SIML(A,B,C,I,NA,IP,ICTL)
      CALL INIT(YP,ZY,ZU,ZD,S,N,K,IP,PSQR)
C
C ***** RECURSIVE EST BY SQUARE ROOT METHOD W. FORGET FACTOR
C
      ZDK=ZU(1)-PROBE(U,LK)
      DO 110 I=LK1,NT0
      CALL VFORG(FORGET,JFORG,I,F1,F2,F3)
      IY=I-K
      YP(I)=Y(IY)-YS(IY)
      CALL MOVE(ZY,K1,Z,1,N)
      CALL MOVE(ZU,K1,Z,N1,L)
      CALL MOVE(ZD,K1,Z,LN1,N)
      ZZ=ZDK
      IF (K.NE.0) ZZ=-ZD(K)
      PHI=PROBE(YP,I)+ZZ
      CALL SQRTES(PHI,Z,S,THETA,NPAR,ERR,FORGET)
C ***** DATA UPDATE & CONTROL
      CALL UPDAT(ZY,PHI,NK)
```

```
      CALL UPDAT(ZU,0.,LK)
      CALL UPDAT(ZD,-ZDK,NK)
      SUM=SCAPRD(ZY,THETA,1,1,N)+SCAPRD(ZU,THETA,1,N1,L)+
     &  SCAPRD(ZD,THETA,1,LN1,N)
      I1=I+1
      IK1=I1+K
      IKP=IK1-IP
      ZDK=F(IK1)
      IF (IKP.GT.0) ZDK=ZDK-PROBE(YP,IKP)
      ZU(1)=(ZDK-SUM)/THETA(N1)
      U(I)=(ZU(1)-ZDK-PROBE(U,I))/ALPH*DTUNE
      ZU(1)=PROBE(U,I)+ZDK
C -----------------------------------------------------------------
      IY0=IY-1
      IF (I.GT.IPRINT) PRINT 260,YP(I),U(IY0),ERR,(THETA(J),J=1,NPAR)
      IF (NEEDPLT.LE.1) GO TO 100
      CALL CPLOT(THETA,THETB,NPAR,T,DT,THERO,SFPARA)
C ***** COMPUTE SYSTEM OUTPUT
  100 CALL SIML(A,B,C,I1,NA,IP,ICTL)
  110 CONTINUE
C
C ***** PLOT CONTROL INPUT & OUTPUT
C
      DO 120 I=NT,NTK
      IY=I-K
      IY0=IY-1
      YP(I)=Y(IY)-YS(IY)
  120 PRINT 260,YP(I),U(IY0)
      IF (NEEDPLT.EQ.0.OR.NEEDPLT.EQ.4) GO TO 130
      NTKP=NTK-IP
      XC=XC+5.
      IFCON=1
      CALL RONDPLT(YP,XC,YC,YXL,NTKP,IP,RNS,IFCON,SFPOLA)
  130 IF (NEEDPLT.LE.1) GO TO 150
C
      DO 140 I=1,NT
      IK=I+K
  140 YP(I)=YP(IK)
      CALL SPLOT(YP,NT,YZERO,T0,DT,SFTIME)
      CALL SPLOT(U,NT,UZERO,T0,DT,SFTIME)
  150 CONTINUE
      CALL PLOT(0.,0.,999)
      STOP
  200 FORMAT(10I5)
  210 FORMAT(8F10.0)
  220 FORMAT(5F10.0)
  230 FORMAT(1X,'RNS=',F5.4,' FREQ=',F10.8,' AMPL=',F5.4,' JF=',
     & I2,' JG=',I2,' ALPH=',F10.6,' BETA=',F10.6,' GAMA=',F10.6)
  240 FORMAT(1X,'NT=',I4,' N=',I2,' K=',I2,' IP=',I2,' NPAR=',I2,
     & ' IFEED=',I2,' FEED=',F5.4,' STIFF=',F5.2,' PSQR=',F5.1)
  250 FORMAT(I5,4F10.0)
  260 FORMAT(1X,16F8.5)
  270 FORMAT(1X,'TYPE OF FORGET:',I2,' F1=',F8.5,' F2=',F8.5,' F3=',
```

```
     &    F8.5,' DETUNE=',F8.5)
  280 FORMAT(1X,80('-')/7X,'Y=',6X,'U=',4X,'ERR=',2X,'THETA=')
      END
      SUBROUTINE INIT(YP,ZY,ZU,ZD,S,N,K,IP,PSQR)
C *****************************************************************
C     INITIALIZATION OF VARIABLES
C *****************************************************************
C
      COMMON RNS,FREQ,PHASE,AMPL,ALPH,BETA,GAMA,JF,JG
      COMMON Y(1000),U(1000),E(1000),X(20),YS(1000),FEED,F(1000)
      DIMENSION YP(1000),ZK(20),ZY(20),ZU(20),ZD(20),S(120)
      L=N+K+1
      NK=N+K
      K1=K+1
      LK=L+K
      DO 2210 I=1,LK
      YP(I)=0.
      IK=I-K
 2210 IF (IK.GT.0) YP(I)=Y(IK)-FEED*IK
C
      LKK1=LK+K+1
      DO 2220 J=1,LK
      LKP=LKK1-IP
      ZK(J)=F(LKK1)
      IF (LKP.GT.0) ZK(J)=ZK(J)-PROBE(YP,LKP)
 2220 LKK1=LKK1-1
C
C *** INIT Z(.) & X(.)
C
      JY=LK
      DO 2230 J=1,NK
      JU=K1+J
      ZY(J)=PROBE(YP,JY)+ZK(JU)
 2230 JY=JY-1
C
      DO 2240 J=1,LK
      ZU(J)=PROBE(U,JU)+ZK(J)
 2240 JU=JU-1
C
      DO 2245 J=1,NK
      J1=J+1
 2245 ZD(J)=-ZK(J1)
C
C *** INIT S(.)TRANSPOSE- UPPER TRIANGLE, IN ROW-WISE
C
      NPAR=N+L+N
      JI=1
      DO 2250 J=1,NPAR
      DO 2250 I=J,NPAR
      S(JI)=0.
      IF (I.EQ.J) S(JI)=PSQR
 2250 JI=JI+1
      RETURN
```

```
      END
      SUBROUTINE SIML(A,B,C,IT,N,IP,ICTL)
C ***************************************************************
C     SIMULATED PLUNGE CUTTING PROCESS
C      ICTL=0   (UNCONTROL)
C      ICTL=1   (CONTROL)
C ***************************************************************
C
      COMMON RNS,FREQ,PHASE,AMPL,ALPH,BETA,GAMA,JF,JG
      COMMON Y(1000),U(1000),E(1000),X(20),YS(1000),FEED
      DIMENSION A(20),B(20),C(20)
      I1=IT
      I2=IT
      N1=N+1
      IF (ICTL.NE.0) GO TO 2120
      I1=2
      SEED=12347.D0
      CALL GGNML(SEED,IT,E)
      RU=.001
      SEED=127.D0
      CALL GGNML(SEED,IT,U)
      DO 2110 I=1,IT
      U(I)=U(I)*RU
      IF (I.GT.N1) U(I)=0.
 2110 E(I)=E(I)*RNS
      Y(1)=E(1)+YS(1)+AMPL*SIN(FREQ+PHASE)
C
 2120 CONTINUE
      DO 2150 I=I1,I2
      E1=E(I)
      IN1=I-N1
      IF (IN1.GT.0) E1=E1+C(N1)*E(IN1)
      X(N1)=0.
      DO 2140 J=1,N
      IJ=I-J
      IF (IJ.LE.0) GO TO 2130
      E1=E1+C(J)*E(IJ)
      Y1=Y(IJ)
      IJP=IJ-IP
      IF (IJP.GT.0) Y1=Y1-Y(IJP)
      X(N1)=X(N1)+B(J)*Y1
 2130 JN=N1-J
      X(N1)=X(N1)-A(JN)*X(J)
      J1=J+1
 2140 X(J)=X(J1)
      Y(I)=E1-X(N1)+YS(I)+AMPL*SIN(FREQ*I+PHASE)
      I0=I-1
      Y(I)=Y(I)+U(I0)
      IBP=I-IP
      IF (IBP.LE.0) GO TO 2150
      YB=Y(I)-Y(IBP)
      IF (YB.LT.0.) YB=0.
      Y(I)=YB+Y(IBP)
```

```
 2150 CONTINUE
      RETURN
      END
      SUBROUTINE VFORG(FORGET,JFORG,I,F1,F2,F3)
C ***********************************************************************
C     COMPUTE TIME VARYING FORGET
C ***********************************************************************
C
      IF (JFORG.EQ.1) FORGET=F1-F2/I
      IF (JFORG.EQ.2) FORGET=F1*FORGET+F2
      IF (JFORG.NE.3) RETURN
      FORGET=1.-F3*F3/(F1*F2)
      RETURN
      END
      SUBROUTINE SQRTES(PHI,Z,S,THETA,N,E,FORGET)
C ***************************************************************
C          RECURSIVE PARAM ESTIMATION OF SISO SYSTEM
C          BY SQUARE ROOT METHOD
C          REF: CLARKE (1981)
C
C ***************************************************************
C
      DIMENSION S(120),Z(20),GK(20),G(20),THETA(20)
C
C *** CAL PRED ERROR
C
      E=PHI-SCAPRD(Z,THETA,1,1,N)
C
C *** CAL SCALAR DIVISOR-SIGSQ AND KALMAN GAIN
C
      SIGSQ=FORGET*FORGET
      K=N
      JI=1
      DO 3090 J=1,N
 3090 GK(J)=0.0
C
      DO 3100 J=1,N
      FJ=SCAPRD(S,Z,JI,J,K)
      K=K-1
      SIGSQ=SIGSQ+FJ*FJ
      DO 3100 I=J,N
      GK(I)=GK(I)+FJ*S(JI)
 3100 JI=JI+1
C
C
      SIG=SQRT(SIGSQ)
      DO 3110 I=1,N
 3110 G(I)=GK(I)/SIG
C
C *** RECURSIVE ALGORITHM ON S(.)
C
      K=1
      DO 3130 J=1,N
```

```
      A=SQRT(S(K)*S(K)-G(J)*G(J))
      U=S(K)/A
      V=-G(J)/A
      S(K)=A/FORGET
      IF(J.EQ.N)GO TO 3130
      K1=K+1
      J1=J+1
      DO 3120 I=J1,N
      B=S(K1)
      S(K1)=(U*S(K1)+V*G(I))/FORGET
      G(I)=U*G(I)+V*B
 3120 K1=K1+1
      K=K1
 3130 CONTINUE
C
C *** CAL NEW PARAMETERS
C
      A=E/SIGSQ
      DO 3140 I=1,N
 3140 THETA(I)=THETA(I)+GK(I)*A
      RETURN
      END
      FUNCTION SCAPRD(A1,A2,I1,I2,L)
C ***************************************************************
C     CAL. SCALAR PRODUCT OF TWO COLUMN MATRICES
C ***************************************************************
C
      DIMENSION A1(100),A2(100)
      SCAPRD=0.0
      J1=I1
      J2=I2
      DO 2410 I=1,L
      SCAPRD=SCAPRD+A1(J1)*A2(J2)
      J1=J1+1
 2410 J2=J2+1
      RETURN
      END
      SUBROUTINE MOVE(A,IA,B,IB,LEN)
C ***********************************************************
C     MOVE A TO B
C ***********************************************************
C
      DIMENSION A(50),B(50)
      JA=IA
      JB=IB
      DO 2510 I=1,LEN
      B(JB)=A(JA)
      JA=JA+1
 2510 JB=JB+1
      RETURN
      END
      SUBROUTINE UPDAT(Z,Y,NPAR)
C ***************************************************************
```

```
C     SHIFT I/O  DATA (FIFO)
C ***************************************************************
C
      DIMENSION Z(20)
      J=NPAR
      DO 2310 I=2,NPAR
      J1=J-1
      Z(J)=Z(J1)
 2310 J=J1
      Z(1)=Y
      RETURN
      END
      FUNCTION PROBE(Y,I)
C ***************************************************************
C     FILTERED OUTPUT OF THREE PROBES
C ***************************************************************
C
      COMMON RNS,FREQ,PHASE,AMPL,A,B,C,JF,JG
      DIMENSION Y(1000)
      IJF=I-JF
      IJG=I-JG
      PROBE=Y(I)*A
      IF (IJF.GT.0) PROBE=PROBE+Y(IJF)*B
      IF (IJG.GT.0) PROBE=PROBE+Y(IJG)*C
      RETURN
      END
      SUBROUTINE ACCUR(Y,I,N,DIMERR,OUTRND,FINISH)
C ***************************************************************
C     EVAL. ACCURACY OF MACHINED PART
C ***************************************************************
C
      DIMENSION Y(1000)
      SUM=0.
      SUMSQ=0.
      YMAX=0.
      YMIN=0.
      K1=I+1
      K2=I+N
      DO 2520 K=K1,K2
      IF (Y(K).GT.YMAX) YMAX=Y(K)
      IF (Y(K).LT.YMIN) YMIN=Y(K)
      SUM=SUM+Y(K)
 2520 SUMSQ=SUMSQ+Y(K)*Y(K)
      DIMERR=SUM/N
      FINISH=SQRT(SUMSQ/N-DIMERR*DIMERR)
      OUTRND=YMAX-YMIN
      PRINT *,'OUTRND',OUTRND,' FINISH',FINISH,' DIMERR',DIMERR
      RETURN
      END
      SUBROUTINE CPLOT(THETA,THETB,NPAR,T,DT,OFFSET,SF)
C ***************************************************************
C     PLOT OF PARAMETERS
C ***************************************************************
```

```
C
      DIMENSION THETA(20),THETB(20)
      T1=T
      T=T+DT
      THETB(1)=THETA(1)
      DO 4110 J=1,NPAR
      CALL PLOT(T,OFFSET+THETA(J)*SF,2)
      J1=J+1
      IF(J1.LE.NPAR) GO TO 4100
      J1=1
      T1=T
 4100 CALL PLOT(T1,OFFSET+THETB(J1)*SF,3)
 4110 THETB(J1)=THETA(J1)
      RETURN
      END
      SUBROUTINE SPLOT(Y,NT,ZERO,T0,DT,SF)
C ***************************************************************
C     PLOT OF SINGLE TIME SERIES
C ***************************************************************
C
      DIMENSION Y(2000)
      CALL PLOT(T0,ZERO,3)
      T=T0
      DO 4115 I=1,NT
      T=T+DT
      Y(I)=Y(I)*SF
      IF(ABS(Y(I)).GT.1.0)Y(I)=SIGN(1.,Y(I))
 4115 CALL PLOT(T,Y(I)+ZERO,2)
      RETURN
      END
      SUBROUTINE RONDPLT(Y,XC,YC,YXL,I,N,RNS,IFCON,SF)
C ***************************************************************
C     POLAR PLOT OF FORM GEOM. AND EVAL. OUT-OF-ROUNDNESS
C ***************************************************************
C
      DIMENSION Y(1000)
      CALL AXISX(XC,YC-YXL/2,' ',1,YXL,90.,0.,.1,.1,31)
      CALL AXISX(XC-YXL/2,YC,' ',1,YXL,0.0,0.,.1,.1,31)
      R=1.5
      DANG=2.*3.1415926/N
      CALL PLOT(XC,YC,-3)
      CALL CIRCLE(R,DANG,N)
      CALL NEWPEN(2)
C
      A=Y(I)*SF+R
      CALL PLOT(A,0.,3)
      I1=I+1
      I2=I+N-1
      DO 3500 K=I1,I2
      R1=R+Y(K)*SF
      ANG=DANG*(K-I)
      X1=R1*COS(ANG)
      Y1=R1*SIN(ANG)
```

```
 3500 CALL PLOT(X1,Y1,2)
      CALL PLOT(A,0.,2)
      CALL NEWPEN(1)
      CALL ACCUR(Y,I,N,DIMERR,OUTRND,FINISH)
      HIGH=.2
      XS=-2.
      XN=.5
      YSN=3.0
      IF (IFCON.EQ.0) CALL SYMBOL(XS,YSN,HIGH,'   (UNCONTROLLED)',0.,17)
      IF (IFCON.EQ.1) CALL SYMBOL(XS,YSN,HIGH,'   (CONTROLLED)',0.,17)
      YSN=YSN-HIGH*1.5
      CALL SYMBOL(XS,YSN,HIGH,'DIMENS ERROR:',0.,12)
      CALL NUMBER(XN,YSN,HIGH,DIMERR,0.,5)
      YSN=YSN-HIGH*1.5
      CALL SYMBOL(XS,YSN,HIGH,'OUT-OF-ROUND:',0.,12)
      CALL NUMBER(XN,YSN,HIGH,OUTRND,0.,5)
      IF (RNS.EQ.0) GO TO 3550
      YSN=YSN-HIGH*1.5
      CALL SYMBOL(XS,YSN,HIGH,'FINISH (RMS):',0.,12)
      CALL NUMBER(XN,YSN,HIGH,FINISH,0.,5)
 3550 CALL PLOT(0.,0.,3)
      CALL PLOT(-XC,-YC,-3)
      RETURN
      END
      SUBROUTINE CIRCLE(R,DANG,N)
      CALL PLOT(R,0.,3)
      DO  3600 I=1,N
      ANG=DANG*I
      X=R*COS(ANG)
      Y=R*SIN(ANG)
 3600 CALL PLOT(X,Y,2)
      RETURN
      END
      SUBROUTINE LABEL(NT,XIO,XLO,YIO,YLO,THMIN)
C ***************************************************************
C     PLOT OF LABELING AND COORDINATE FRAME
C ***************************************************************
C
      DX=NT/XLO
      XI=XIO
      XL=XLO
      YI=YIO
      YL=YLO
      Y=YI
      CALL AXIS(XI,YI,' ',-1,XL,0.,0.,DX,20)
      DO 4220 J=1,3
      CALL AXIS(XL,Y,' ',1,YL,90.,0.,1.,16)
      CALL AXIS(XI,Y,' ',-1,YL,90.,0.,1.,16)
      DO 4220 K=1,2
      Y=Y+1.
      CALL PLOT(XI,Y,3)
      CALL PLOT(XL,Y,2)
 4220 CONTINUE
```

```
      YI=0.
      YL=4.
      DY=-THMIN*2./YL
      CALL PLOT(XI,YL,3)
      CALL PLOT(XL,YL,2)
      CALL AXIS(XI,YI,' ',-1,XL,0.,0.,DX,4)
      CALL AXIS(XL,YI,' ',1,YL,90.,0.,1.,16)
      CALL AXIS(XI,YI,'THETA',5,YL,90.,THMIN,DY,7)
      XS=.50
      YS=Y-.4
      XN=-.3
      YN=Y-1.
      HIGH=.2
      CALL SYMBOL(XS,YS,HIGH,'UNCONTROL RESPONSE',0.,18)
      CALL NUMBER(XN,YN,HIGH,0.,0.,0)
      YS=YS-2.
      YN=YN-2.
      CALL SYMBOL(XS,YS,HIGH,'CONTROL RESPONSE',0.,16)
      CALL NUMBER(XN,YN,HIGH,0.,0.,0)
      YS=YS-3.
      YN=YN-2.
      CALL SYMBOL(XS,YS,HIGH,'CONTROL INPUT',0.,13)
      CALL NUMBER(XN,YN,HIGH,0.,0.,0)
      RETURN
      END
#EOR
   60  880    0    0    2    2    0  900
    5   20
      .004      .004         0       50.      .002        .1
-1.602708 .94176453 .17093188 .16812465 2.0
1.31      .28       0.        0.
    1      .995        .5         0       .98
#EOR
```

APPENDIX 4

Project Staff in 1983–1984

Faculty

M. M. Barash, Ransburg Professor of Manufacturing and Professor of Industrial Engineering.....	Principal Investigator & Project Director
C. R. Liu, Professor of Industrial Engineering.....	Principal Investigator
K. S. Fu, Goss Distinguished Professor of Engineering (Elec.Eng.).....	Faculty Associate
J. Modrey, Professor of Mechanical Engineering.....	Co–Principal Investigator
A. L. Sweet, Professor of Industrial Engineering.....	Co–Principal Investigator
W. Stevenson, Professor of Mechanical Engineering.....	Faculty Associate
J. J. Talavage, Professor of Industrial Engineering.....	Faculty Associate
R. Hannam*, Visiting Associate Professor of Industrial Engineering.....	Faculty Associate
W. Johnson**, Visiting Professor of Industrial Engineering.....	Faculty Associate
A. Shumsherrudint, Visiting Associate Professor of Industrial Engineering.....	Faculty Associate

(*University of Manchester Institute of Science and Technology, England
**University of Cambridge, England
†Cranfield Institute of Technology, England)

AD-A163 003 THE SCIENCE OF AND ADVANCED TECHNOLOGY FOR COST-EFFECTIVE MANUFACTURE OF (U) PURDUE UNIV LAFAYETTE IN SCHOOL OF INDUSTRIAL ENGINEERING

UNCLASSIFIED Y LIN ET AL SEP 85 N00014-83-K-0385 F/G 13/8 NL

3/3

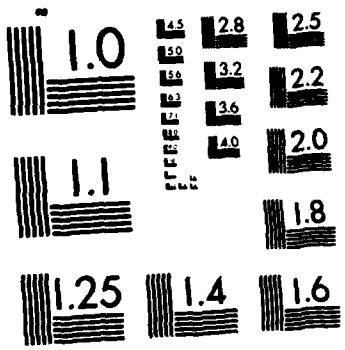

MICROCOPY RESOLUTION TEST CHART
NATIONAL BUREAU OF STANDARDS-1963-A

Graduate Research Assistants

P. Chen
Y.C. Chou
P. Ferreira
R. Khanna
S.K. Lee
G.R. Liang
Y.T. Lin
J. Lopez
D. Noller
Y.S. Ouyang
U. Roy
S. Shodhan
R. Srinivasan
S. Venkatramen
R. Venugopal
M.C. Wu
J. York

END

FILMED

2-86

DTIC